Biomass and Bioenergy 217 (2027) 109859

Contents lists available at ScienceDirect

Biomass and Bioenergy

journal homepage: www.elsevier.com/locate/biombioe

Integrated valorization of oil palm empty fruit bunch (OPEFB) by deep eutectic solvent pretreatment: Glucose production enhancement and lignin-CMC composite for sustainable packaging

Candra Wijaya [a,b], Andika Prastika [a], Olivia Izzati Atiqa [a], Tabina Raissa Apol [a], Urania Noor Lintang Pertiwi [a], Lieke Riadi [b], Maktum Muharja [a], Arief Widjaja [a,*]

[a] Department of Chemical Engineering, Institut Teknologi Sepuluh Nopember, Kampus ITS Sukolilo, Surabaya, 60111, Indonesia
[b] Department of Chemical Engineering, Universitas Surabaya (UBAYA), Jalan Raya Kalirungkut (Tenggilis), Surabaya, 60293, Indonesia

ARTICLE INFO

Keywords:
Oil palm empty fruit bunch
Deep eutectic solvent
Fractionation
Enzymatic hydrolysis
CMC-lignin film
Modified severity factor

ABSTRACT

Oil palm empty fruit bunch (OPEFB) is an abundant lignocellulosic residue with potential for integrated biorefinery applications, but its recalcitrant structure limits direct enzymatic conversion and lignin utilization. This study investigated the integrated valorization of OPEFB through deep eutectic solvent (DES) pretreatment using choline chloride–lactic acid (ChCl:LA) and choline chloride–glycerol–$FeCl_3$ (ChCl:Gly:$FeCl_3$) systems for glucose production, lignin recovery, and CMC–lignin composite film development. Modified severity descriptors, namely combined delignification factor (CDF) and combined hydrolysis factor (CHF), were applied to describe severity-dependent lignin removal and xylan hydrolysis. The CDF and CHF models successfully described the severity-dependent fractionation behavior of OPEFB during DES pretreatment. ChCl:LA promoted stronger lignin solubilization and higher lignin recovery, while ChCl:Gly:$FeCl_3$ enhanced hemicellulose removal and enzymatic digestibility through Lewis acid-assisted deconstruction. The highest enzymatic hydrolysis yields reached 75.8% for ChCl:LA and 93.8% for ChCl:Gly:$FeCl_3$. On a 100 g raw OPEFB basis, ChCl:LA pretreatment at 140 °C for 6 h produced 21.6 g glucose and 24.7 g recovered lignin, whereas ChCl:Gly:$FeCl_3$ pretreatment at 140 °C for 3 h produced 21.7 g glucose and 23.1 g recovered lignin. The recovered DES lignins showed high purity and were successfully incorporated into CMC-based films. ChCl:LA lignin improved water resistance and reduced WVTR, while ChCl:Gly:$FeCl_3$ lignin provided stronger antioxidant activity and tensile reinforcement. These findings demonstrate that DES pretreatment enables the dual valorization of OPEFB into fermentable glucose and functional lignin-derived packaging materials, supporting a multiproduct biorefinery pathway for sustainable biomass utilization.

1. Introduction

The transition from fossil-based resources to renewable carbon feedstocks has become increasingly important for the development of sustainable fuels, chemicals, and materials [1,2]. Lignocellulosic biomass is one of the most promising renewable resources because it is abundant, renewable, and composed of carbohydrate and aromatic fractions that can be converted into multiple value-added products [3–5]. However, the efficient utilization of lignocellulosic biomass remains restricted by its naturally recalcitrant structure. Cellulose microfibrils are embedded within hemicellulose and lignin, while lignin–carbohydrate complexes provide additional resistance against chemical and enzymatic deconstruction [6,7]. As a result, pretreatment is required to disrupt the biomass matrix, improve cellulose accessibility, and enable the selective recovery of lignin for further valorization [8,9].

Oil palm empty fruit bunch (OPEFB) is an abundant lignocellulosic residue generated from the palm oil industry, particularly in tropical countries such as Indonesia and Malaysia [10]. OPEFB contains cellulose, hemicellulose, and lignin as its major structural components, making it a promising feedstock for biorefinery applications [11]. The cellulose-rich fraction can be hydrolyzed into glucose and further converted into biofuels or biochemicals, while the lignin fraction can serve as a renewable aromatic polymer for material applications [12,13].

* Corresponding author.
E-mail address: arief.widjaja@its.ac.id (A. Widjaja).

https://doi.org/10.1016/j.biombioe.2026.109859
Received 25 May 2026; Received in revised form 16 July 2026; Accepted 16 July 2026
Available online 20 July 2026

Nevertheless, the compact fiber structure and relatively high lignin content of OPEFB limit its direct enzymatic digestibility. Without suitable pretreatment, lignin can act as a physical barrier and induce non-productive enzyme adsorption, thereby reducing hydrolysis efficiency [7]. Therefore, an effective OPEFB fractionation strategy should not only enhance glucose production but also recover lignin in a form suitable for downstream utilization.

Several pretreatment methods have been reported for lignocellulosic biomass, including dilute acid, alkaline, hydrothermal, organosolv, and ionic liquid-based processes [14–17]. Although these methods can improve enzymatic hydrolysis, they may involve limitations such as high chemical loading, corrosion, severe operating conditions, inhibitor formation, or limited selectivity toward lignin recovery [18,19]. In this context, DESs have emerged as promising green solvents for lignocellulosic biomass fractionation. DESs are commonly formed through hydrogen-bond interactions between a hydrogen-bond acceptor and a hydrogen-bond donor, producing solvent systems with low volatility, tunable acidity, and strong lignin solubilization capacity [20,21]. Choline chloride-based DESs are particularly attractive because they can be combined with various hydrogen-bond donors, including organic acids and polyols, to tailor pretreatment performance [22].

Among acidic DES systems, choline chloride–lactic acid (ChCl:LA) was selected as a representative Brønsted-acidic DES because lactic acid-based DESs have been widely reported to promote lignin dissolution, xylan elimination, and enzymatic digestibility enhancement in lignocellulosic biomass [23–26]. The acidic nature of lactic acid can facilitate the cleavage of ether and ester linkages in lignin and lignin–carbohydrate complexes, while choline chloride contributes hydrogen-bonding and ionic interactions that assist lignin solubilization and cell wall deconstruction [22,27,28]. Therefore, ChCl:LA was chosen to represent a delignification-oriented DES route in which lignin recovery is expected to be a major output. In contrast, choline chloride–glycerol (ChCl:Gly) represents a milder polyol-based DES matrix, but its deconstruction ability can be strengthened by incorporating $FeCl_3$ as a Lewis acid catalyst. Fe^{3+} species can coordinate with oxygen-containing bonds and facilitate the cleavage of glycosidic and ether linkages, thereby enhancing hemicellulose disruption, biomass deconstruction, cellulose accessibility, and subsequent enzymatic hydrolysis [29–32]. Previous studies on metal chloride-assisted pretreatment have also shown that Fe^{3+}-based systems can intensify xylan depolymerization and improve enzymatic digestibility, supporting the use of $FeCl_3$-containing DESs for hydrolysis-oriented fractionation [33–35]. Thus, ChCl:Gly:$FeCl_3$ was selected as a Lewis-acid-assisted DES system to represent a hemicellulose-disruption-oriented route. The comparison between ChCl:LA and ChCl:Gly:$FeCl_3$ was therefore designed not as a random solvent screening, but as a mechanistic comparison between two choline chloride-based DES systems with different dominant catalytic environments, Brønsted-acid-driven delignification and Lewis-acid-assisted hemicellulose deconstruction. This comparison is relevant for determining whether OPEFB valorization should be directed toward higher lignin recovery, higher glucose production, or a balanced dual-product biorefinery strategy.

In addition to experimental evaluation, severity-based parameters can provide a useful framework for interpreting lignocellulosic fractionation. Conventional severity factors generally combine temperature and reaction time, but they do not fully account for solvent acidity, catalyst contribution, or DES composition [9,36]. Therefore, modified severity descriptors such as the combined delignification factor (CDF) and combined hydrolysis factor (CHF) have been proposed to better describe selective lignin removal and carbohydrate hydrolysis under chemically assisted pretreatment systems [13,37]. CDF is particularly relevant for evaluating the collective influence of pretreatment temperature, time, and solvent or catalyst contribution on lignin removal. Meanwhile, CHF can be used to describe the severity-dependent behavior of carbohydrate hydrolysis or enzymatic glucose production. In DES pretreatment, these descriptors may help connect operating conditions with two key outcomes: delignification efficiency and glucose release from the cellulose-rich solid fraction. This is important because excessive pretreatment severity may enhance lignin removal but may also reduce carbohydrate recovery, alter lignin structure, or affect the suitability of recovered lignin for material applications.

Most DES pretreatment studies have primarily focused on improving enzymatic hydrolysis or maximizing lignin removal [38,39]. However, a more complete biorefinery approach requires the valorization of both the carbohydrate-rich solid and the recovered lignin fraction. Lignin is often regarded as a low-value by-product, even though its aromatic structure, phenolic hydroxyl groups, hydrophobicity, antioxidant activity, and ultraviolet-blocking ability make it suitable for functional material applications [40,41]. Previous OPEFB–DES work has demonstrated that DES pretreatment can enhance lignin removal, preserve cellulose, improve enzymatic hydrolysis, and recover lignin as a potential product stream, supporting its relevance for multiproduct biomass utilization [42–44]. However, the direct conversion of recovered DES lignin into functional packaging materials remains less explored, particularly when combined with severity-based interpretation of glucose production and lignin recovery.

Carboxymethyl cellulose (CMC) is a biodegradable cellulose derivative with good film-forming ability, transparency, and compatibility with water-based processing [45]. However, neat CMC films commonly suffer from high water sensitivity, limited moisture barrier properties, and insufficient mechanical stability for broader packaging applications [40]. The incorporation of lignin into CMC films can address some of these limitations by increasing hydrophobic interactions, introducing aromatic UV-absorbing domains, and enhancing antioxidant functionality [46,47]. In this regard, lignin recovered from DES pretreatment may provide additional value beyond its role as a fractionation by-product. Instead, it can be directly utilized as a functional component in lignin-CMC composite films, supporting the development of biodegradable and biomass-derived packaging materials.

Nevertheless, the integration of DES pretreatment, glucose production, lignin recovery, severity-based analysis, and lignin-based composite film fabrication remains insufficiently explored. A pretreatment condition that enhances enzymatic hydrolysis does not always generate lignin with suitable properties for material applications. Conversely, conditions that favor lignin recovery may influence cellulose preservation and glucose release. Therefore, an integrated assessment is needed to determine whether DES pretreatment can simultaneously improve enzymatic glucose production and provide recovered lignin suitable for CMC-based packaging films. Such an approach is important for advancing OPEFB utilization from a single-product sugar platform toward a multiproduct biorefinery system.

This study investigates the integrated valorization of OPEFB through DES pretreatment for glucose production enhancement and lignin-CMC composite film development. Two DES systems, ChCl:LA and ChCl:Gly:$FeCl_3$, were evaluated to determine their effects on biomass fractionation, component removal, CDF- and CHF-related pretreatment behavior, enzymatic glucose release, lignin recovery, and the functional performance of lignin-CMC films. The pretreated solid fractions were subjected to enzymatic hydrolysis to assess glucose production, while the recovered lignin was incorporated into CMC films and evaluated for its physical, mechanical, surface, and barrier-related properties. Unlike previous studies that mainly focused on DES-assisted delignification or enzymatic saccharification, this work integrates severity-based fractionation analysis, carbohydrate conversion, and lignin-derived material development within a single OPEFB valorization pathway. This strategy demonstrates the dual role of OPEFB as a glucose platform and renewable source of functional lignin for sustainable packaging applications.

2. Materials and methods

2.1. Materials

The OPEFB was supplied by PT. Sawit Arum Madani (Blitar, Indonesia). The biomass was washed, dried, and prepared according to the National Renewable Energy Laboratory (NREL) protocol [48], and then ground to a particle size of 40–60 mesh. Lactic acid, glycerol, and ferric chloride hexahydrate ($FeCl_3 \cdot 6H_2O$), all of analytical grade, were purchased from Merck (Germany). Choline chloride and cellulase derived from *Trichoderma reesei* were obtained from Sigma-Aldrich (USA). Unless otherwise specified, all other analytical-grade reagents used in this work were also supplied by Sigma-Aldrich.

2.2. Experimental diagram

A schematic representation of the experimental workflow is presented in Fig. 1. The diagram summarizes the main stages of the study, namely OPEFB preparation, deep eutectic solvent (DES) preparation, DES pretreatment, separation of the pretreated solid and filtrate fractions, lignin regeneration, enzymatic hydrolysis of the solid residue, and the preparation and characterization of CMC–lignin films. For lignin characterization and film fabrication, the lignin sample obtained under the pretreatment condition giving the highest lignin yield was used.

2.3. DES pretreatment and lignin recovery

The experimental procedure was adapted from prior research [49]. The ChCl:LA deep eutectic solvent (DES) was prepared by mixing choline chloride (ChCl) and lactic acid (LA) at a molar ratio of 1:2. Meanwhile, the ChCl:Gly:$FeCl_3$ DES was prepared by mixing ChCl and glycerol (Gly) at a molar ratio of 1:2, followed by the addition of $FeCl_3$ at a concentration of 0.01 mol/L. The $FeCl_3$ concentration was fixed at 0.01 mol/L based on previous Lewis acid-mediated ChCl:Gly DES studies, in which the same catalyst loading was used to intensify lignocellulose fractionation while maintaining a controlled DES formulation [29,50]. In the present work, only one $FeCl_3$ concentration was used because the main objective was not to optimize catalyst loading, but to compare two different DES fractionation mechanisms under controlled formulation conditions: Brønsted-acidic ChCl:LA and Lewis-acid-assisted ChCl:Gly:$FeCl_3$. Maintaining a constant $FeCl_3$ concentration allowed the effects of DES chemistry, temperature, and residence time to be evaluated without additional variation in Lewis acid loading, acidity, ionic strength, viscosity, and mass-transfer behavior. This approach is also consistent with previous studies on Lewis-acid-containing DES systems, where metal chlorides such as $FeCl_3$, $AlCl_3$, $CuCl_2$, and $ZnCl_2$ were evaluated as acid-site contributors to DES-mediated lignocellulose fractionation before further optimization of specific solvent composition or catalyst loading [29].

The mixtures were heated in a closed round-bottom flask at 70 °C under continuous stirring until clear and homogeneous liquids were formed. The mixture was then cooled to room temperature prior to use [51]. For the pretreatment, 4 g of OPEFB was mixed with 60 g of DES in a 250 mL three-neck round-bottom flask and heated at certain temperature and time [52]. The pretreatment variables were temperature, ranging from 100 to 140 °C, and residence time, ranging from 3 to 6 h, for each DES system. The pretreatment temperature and residence-time ranges were selected to evaluate a moderate DES pretreatment window that is commonly used to promote lignocellulosic fractionation while limiting excessive carbohydrate degradation and unnecessary energy input [23,26,52,53]. Temperatures above 140 °C were not included in this study because increasing acidic pretreatment severity may enhance component removal but can also accelerate sugar degradation, lignin condensation, pseudo-lignin formation, and solvent recovery burden, which may reduce the overall benefit of the process [6,27,54]. Therefore, the conditions identified in this study should be interpreted as the best-performing conditions within the investigated range, rather than as globally optimized pretreatment conditions. In addition, the $FeCl_3$ concentration in the ChCl:Gly:$FeCl_3$ system was fixed at 0.01 mol/L to focus the comparison on the effects of DES chemistry, temperature, and

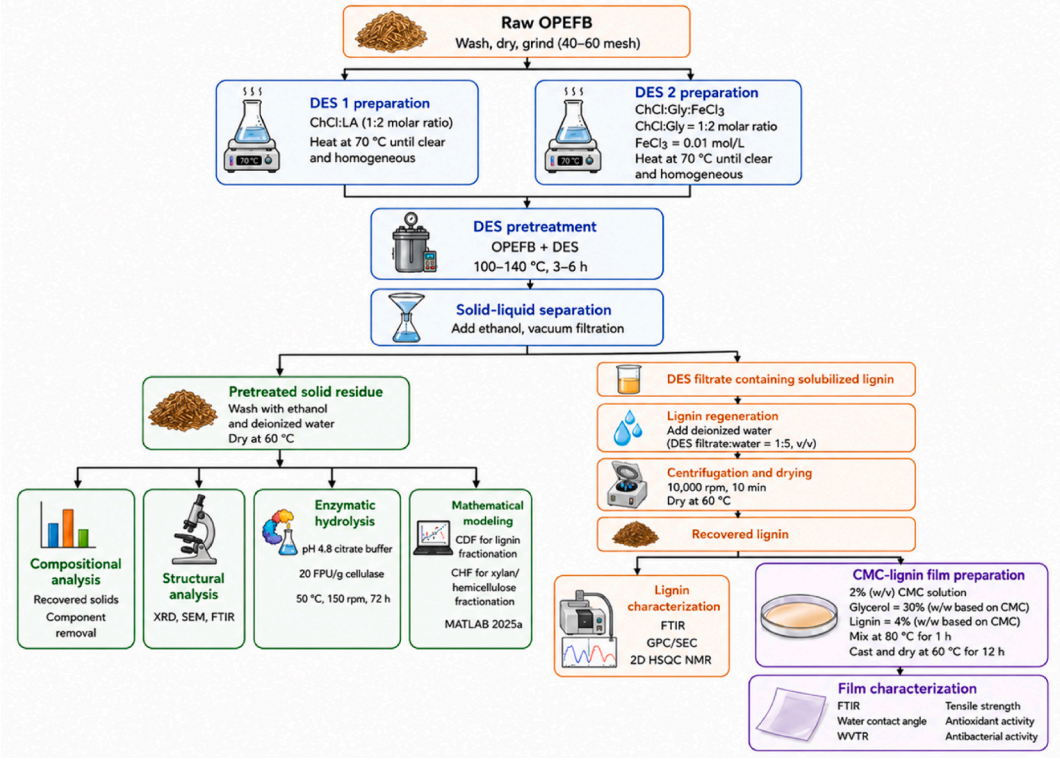

Fig. 1. Experimental workflow for OPEFB fractionation, lignin recovery, and CMC–lignin film fabrication.

residence time under a constant Lewis-acid catalyst loading. The influence of $FeCl_3$ concentration gradient was not evaluated in the present work and should be addressed in future optimization studies.

After pretreatment, 50 mL of ethanol was added to the slurry, and the mixture was vacuum-filtered. The solid residue was sequentially washed with 150 mL of ethanol and 150 mL of deionized water, then dried at 60 °C in an oven prior to further analysis. The DES phase containing solubilized lignin was subjected to lignin regeneration following the method of [51]. Briefly, deionized water was added to the DES filtrate at a ratio of 1:5 (v/v), allowing lignin to precipitate. The precipitate was recovered by centrifugation (HERMLE Z306 universal centrifuge, 10, 000 rpm, 10 min) and subsequently dried at 60 °C before characterization and preparation of lignin composite film. All pretreatment experiments were performed in triplicate to ensure reproducibility.

2.4. Mathematical reaction model

The fractionation behavior of lignocellulosic biomass during deep eutectic solvent pretreatment was modeled using response-specific combined severity factors. Since DES pretreatment simultaneously promotes lignin solubilization and hemicellulose disruption, two separate kinetic descriptors were used: the combined delignification factor (CDF) for lignin fractionation and the combined hydrolysis factor (CHF) for xylan/hemicellulose fractionation. The model was developed to integrate the effects of reaction temperature, pretreatment time, and the concentration of the dominant acidic or catalytic component in each DES system [55–57].

In this study, two DES systems were considered, namely ChCl:LA and ChCl:Gly:$FeCl_3$. For ChCl:LA, lactic acid was assigned as the active acidic component, while for ChCl:Gly:$FeCl_3$, $FeCl_3$ was assigned as the dominant Lewis-acidic catalytic component. Glycerol was considered part of the DES solvent matrix and was not included as an independent kinetic concentration term because the ChCl:Gly ratio was kept constant.

2.4.1. Lignin fractionation model

The removal of lignin from the solid fraction was assumed to follow an apparent pseudo-first-order kinetic model with respect to the residual lignin content. The active acidic or catalytic component of the DES was incorporated as a concentration-dependent term. The rate of lignin removal was expressed as Eq (1).

$$\frac{dL_{res}}{dt} = -k_L(T, C, \ldots)CL_{res} \tag{1}$$

where L_{res} represents the residual lignin fraction remaining in the pretreated solid, T is the reaction temperature (K), C is the concentration of the dominant active component in the DES system, and $k_L(T, C, \ldots)$ is the apparent delignification rate coefficient.

For the ChCl:LA system:

$$C = C_{LA} \tag{2}$$

where C_{LA} represents the lactic acid concentration.

For the ChCl:Gly:$FeCl_3$ system:

$$C = C_{Fe} \tag{3}$$

where C_{Fe} represents the $FeCl_3$ concentration.

The apparent delignification rate coefficient was described using an Arrhenius-type empirical relationship.

$$k_L = exp\left(\alpha_L - \frac{E_{a,L}}{RT} + \beta_L C\right) \tag{4}$$

Where $E_{a,L}$ is the apparent activation energy for lignin removal, R is the universal gas constant, and α_L and β_L are empirical fitted parameters. The term $\beta_L C$ represents the contribution of the active acidic or catalytic component to lignin fractionation [55,56,58].

Accordingly, the combined delignification factor was defined as Eq. (5)

$$CDF = \exp\left(\alpha_L - \frac{E_{a,L}}{RT} + \beta_L C\right)Ct \tag{5}$$

where t is the pretreatment time.

To account for the heterogeneous structure of lignin in the biomass matrix, lignin was divided into two fractions: a fast-removing lignin fraction and a slow-removing lignin fraction [58,59]. The corresponding rate equations were written as:

$$\frac{dL_f}{dt} = -k_L CL_f \tag{6}$$

$$\frac{dL_s}{dt} = -f_L k_L CL_s \tag{7}$$

where L_f and L_s represent the fast- and slow-removing lignin fractions, respectively. The parameter f_L is the relative rate constant of the slow-removing lignin fraction compared with the fast-removing fraction. The initial proportion of slow-removing lignin is denoted as θ_L, while $1 - \theta_L$ represents the fast-removing lignin fraction.

By solving the differential equations, the residual lignin fraction can be expressed as a function of CDF:

$$L_{res} = (1 - \theta_L)\exp(-CDF) + \theta_L \exp(-f_L CDF) \tag{8}$$

For the two DES systems, the CDF can be written separately as:

$$CDF_{LA} = \exp\left(\alpha_{L,LA} - \frac{E_{a,L,LA}}{RT} + \beta_{L,LA}C_{LA}\right)C_{LA}t \tag{9}$$

$$CDF_{Fe} = \exp\left(\alpha_{L,Fe} - \frac{E_{a,L,Fe}}{RT} + \beta_{L,Fe}C_{Fe}\right)C_{Fe}t \tag{10}$$

where CDF_{LA} and CDF_{Fe} represent the combined delignification factors for ChCl:LA and ChCl:Gly:$FeCl_3$ pretreatment, respectively.

The objective function for lignin fractionation was defined as the sum of squared errors between the modeled and experimental residual lignin values.

$$F_L = \sum_{i=1}^{N}\left(L_{res,i}^{model} - L_{res,i}^{exp}\right)^2 \tag{11}$$

where N is the number of experimental data points, while $L_{res,i}^{model}$ and $L_{res,i}^{exp}$ are the predicted and experimentally measured residual lignin fractions, respectively.

2.4.2. Hemicellulose/xylan fractionation model

The fractionation of hemicellulose was modeled based on the removal of xylan from the solid fraction. Similar to lignin removal, xylan solubilization was described using an apparent pseudo-first-order kinetic expression with respect to the residual xylan content [37,60]:

$$\frac{dX_{res}}{dt} = -k_X(T, C, \ldots)CX_{res} \tag{12}$$

where X_{res} represents the residual xylan fraction remaining in the pretreated solid, and $k_X(T, C, \ldots)$ is the apparent xylan hydrolysis or solubilization rate coefficient.

The apparent rate coefficient for xylan fractionation was expressed as:

$$k_X = \exp\left(\alpha_X - \frac{E_{a,X}}{RT} + \beta_X C\right) \tag{13}$$

where $E_{a,X}$ is the apparent activation energy for xylan removal, and α_X and β_X are empirical fitted parameters.

The combined hydrolysis factor was therefore defined as:

$$CHF = \exp\left(\alpha_X - \frac{E_{a,X}}{RT} + \beta_X C\right) Ct \tag{14}$$

In the context of this study, CHF was used to describe the extent of hemicellulose/xylan fractionation during DES pretreatment, rather than enzymatic hydrolysis.

Xylan was also assumed to consist of fast- and slow-removing fractions. The kinetic expressions for these fractions were written as:

$$\frac{dX_f}{dt} = -k_X C X_f \tag{15}$$

$$\frac{dX_s}{dt} = -f_X k_X C X_s \tag{16}$$

where X_f and X_s represent the fast- and slow-removing xylan fractions, respectively. The parameter f_X represents the relative rate constant of the slow-removing xylan fraction compared with the fast-removing fraction. The initial proportion of slow-removing xylan is denoted as θ_X [60,61].

By solving the corresponding differential equations, the residual xylan fraction can be expressed as:

$$X_{res} = (1-\theta_X)\exp(-CHF) + \theta_X \exp(-f_X CHF) \tag{17}$$

For the two DES systems, the CHF can be written separately as:

$$CHF_{LA} = \exp\left(\alpha_{X,LA} - \frac{E_{a,X,LA}}{RT} + \beta_{X,LA} C_{LA}\right) C_{LA} t \tag{18}$$

$$CHF_{Fe} = \exp\left(\alpha_{X,Fe} - \frac{E_{a,X,Fe}}{RT} + \beta_{X,Fe} C_{Fe}\right) C_{Fe} t \tag{19}$$

where CHF_{LA} and CHF_{Fe} represent the combined hydrolysis factors for ChCl:LA and ChCl:Gly:$FeCl_3$ pretreatment, respectively.

The objective function for xylan fractionation was defined as:

$$F_X = \sum_{i=1}^{N} \left(X_{res,i}^{model} - X_{res,i}^{exp}\right)^2 \tag{20}$$

where $X_{res,i}^{model}$ and $X_{res,i}^{exp}$ are the predicted and experimentally measured residual xylan fractions, respectively.

For clarity, the concentration term C_i used in the CDF and CHF equations refers to the molar concentration of the dominant active acidic or catalytic component in the prepared DES formulation, expressed in mol/L. For the ChCl:LA system, C_i corresponds to the effective lactic acid concentration, C_{LA}, calculated from the ChCl:LA molar ratio of 1:2 in the DES mixture. For the ChCl:Gly:$FeCl_3$ system, C_i corresponds to the $FeCl_3$ concentration, C_{FeCl_3}, which was fixed at 0.01 mol/L. Since the active component concentration was fixed within each DES system, C_i was used as a formulation-specific acid/catalyst contribution term, while temperature and residence time represented the varied operating conditions. The coefficient β_i has units of L/mol so that the product $\beta_i C_i$ is dimensionless in the exponential term. Therefore, the CDF and CHF values should be interpreted as empirical response-specific severity descriptors rather than independent optimization parameters for acid or catalyst concentration. All the objective functions were solved by using MATLAB 2025a.

2.5. Enzymatic hydrolysis

The enzymatic hydrolysis of OPEFB was performed using cellulase enzyme according to the procedure adapted from Huo et al. [23]. Briefly, 0.5 g of raw or pretreated solid residue was suspended in a citric acid–sodium citrate buffer solution at pH 4.8. Cellulase was then added at an enzyme loading of 20 FPU/g dry substrate, calculated based on the dry mass of raw or DES-pretreated OPEFB solid. The hydrolysis reaction was conducted in a shaker incubator at 50 °C and 150 rpm for 72 h. The enzymatic hydrolysis yield was calculated using Eq. (21), as described by Ref. [62].

$$\%Y_{EH} = \frac{released\ glucose \times 0.9(g)}{cellulose\ in\ substrate(g)} \times 100\% \tag{21}$$

where $\%Y_{EH}\%$ represents the enzymatic hydrolysis yield obtained from the hydrolysate.

To evaluate the relationship between pretreatment severity and enzymatic digestibility, Y_{EH} was correlated with both the CHF and CDF. CHF represents the severity of xylan or hemicellulose hydrolysis, while CDF represents the severity of lignin removal during DES pretreatment. These two descriptors were selected because enzymatic hydrolysis is affected by both hemicellulose removal and delignification[58,63]. Hemicellulose removal could improve cellulose accessibility by opening the polysaccharide matrix, whereas lignin removal can reduce physical shielding and non-productive enzyme adsorption.

The relationship between enzymatic hydrolysis yield and the modified severity factor was described using an empirical exponential model, as shown in Eq. (22):

$$\%Y_{EH} = a \cdot exp\ (b \cdot CHF) + c \tag{22}$$

where Y_{EH} is the enzymatic hydrolysis yield, *SF* represents either CHF or CDF, and *a*, *b*, and *c* are fitted parameters. In this model, *c* represents the asymptotic hydrolysis yield approached at higher pretreatment severity, *a* describes the difference between the initial and limiting hydrolysis yield, and *b* represents the sensitivity of enzymatic hydrolysis yield to increasing pretreatment severity. For each DES system, separate correlations were developed between Y_{EH} and CHF, and between Y_{EH} and CDF. The $CHF - Y_{EH}$ correlation was used to evaluate the contribution of hemicellulose/xylan removal to enzymatic digestibility, whereas the $CDF - Y_{EH}$ correlation was used to evaluate the contribution of delignification. The fitting quality was evaluated using the coefficient of determination (R^2) and root mean square error (*RMSE*).

2.6. Preparation of carboxymethyl cellulose (CMC)-Lignin film

CMC–lignin films were prepared using a solution casting method adapted from Zhu et al. [47], with minor modification. Briefly, CMC solution was prepared by dissolving CMC at a concentration of 2% (w/v) in water at 80 °C for 30 min. Glycerol was then added at 30% (w/w based on CMC) as a plasticizer and mixed until homogeneous. Separately, recovered lignin was dispersed in 1 mol/L NaOH at 4% (w/w based on CMC) and stirred until a uniform lignin dispersion was obtained. The lignin loading of 4% (w/w based on CMC) was selected by adapting the CMC–DES lignin film formulation reported by Zhu et al. [47], and was used as a fixed comparative loading in this study. This loading was chosen to evaluate how lignin source and pretreatment chemistry influence CMC–lignin film properties, rather than to optimize lignin content. Lignin can improve CMC films by introducing hydrophobic aromatic domains, phenolic antioxidant sites, and possible hydrogen-bonding interactions with the CMC matrix. These interactions may enhance water resistance, moisture-barrier performance, antioxidant activity, and tensile reinforcement. However, excessive lignin loading may also promote aggregation, phase separation, film roughness, brittleness, and reduced elongation at break. Therefore, further formulation studies using different lignin loadings are required to determine the optimum balance between mechanical strength, flexibility, water resistance, antioxidant activity, and film processability. The CMC solution and lignin dispersion were subsequently mixed at a volume ratio of 1:1 and maintained at 80 °C for 1 h to obtain the film-forming solution. The resulting solution was cast onto a mold and dried in a hot-air oven at 60 °C for 12 h to obtain the CMC-lignin film. Since no neutralization or washing step was applied after NaOH-assisted lignin dispersion, the resulting films are discussed as preliminary functional CMC–lignin composite films. Further residual alkali analysis,

migration testing, and safety evaluation are required before direct food-contact packaging application.

2.7. Analytical method

2.7.1. Determination of sugars in liquid hydrolysate and solid compositional analysis

The sugar concentrations in hydrolysates obtained from compositional hydrolysis and enzymatic hydrolysis were quantified using high-performance liquid chromatography (HPLC). The analysis was performed using a Thermo Scientific Vanquish Core HPLC system (Thermo Scientific, USA), equipped with a HyperREZ XP Carbohydrate Pb++ column (8 μm, 300 × 7.7 mm) and a refractive index (RI) detector. Separation was carried out using HPLC-grade water as the mobile phase, with the operating conditions set at a flow rate of 0.6 mL/min, column temperature of 85 °C, and system pressure of 9 bar.

The chemical composition of the biomass was determined according to the NREL analytical protocol reported by Sluiter et al. [64]. In brief, the biomass was subjected to acid hydrolysis using concentrated sulfuric acid to convert structural carbohydrates into monomeric sugars for quantification. This method was also used to determine lignin fractions, including acid-soluble lignin (ASL) and acid-insoluble lignin (AIL).

The influence of DES pretreatment on OPEFB fractionation was assessed based on solid recovery and the removal efficiency of individual biomass components. Solid recovery represents the percentage of residual solid retained after pretreatment relative to the initial OPEFB mass, while component removal indicates the extent to which each major component was solubilized or removed during pretreatment. These values were calculated using Eqs. (23) and (24):

$$\textit{Recovered solids}\ (\%) = \left(\frac{\textit{mass of pretreated OPEFB}\ (g)}{\textit{initial mass of OPEFB}\ (g)}\right) \times 100 \tag{23}$$

$$R_i\ (\%) = \left(1 - \frac{\text{mass of component } i \text{ in pretreated OPEFB (g)}}{\text{mass of component } i \text{ in initial OPEFB (g)}}\right) \times 100 \tag{24}$$

Where R_i refers to the removal percentage of a specific OPEFB component, namely hemicellulose, cellulose, or lignin.

In addition, the lignin recovery yield (Y_L) obtained from each pretreatment condition was calculated by comparing the mass of isolated lignin with the initial lignin content in OPEFB, as shown below:

$$Y_L = \frac{\text{isolated lignin (g)}}{\text{initial lignin content in OPEFB (g)}} \times 100 \tag{25}$$

2.7.2. Crystallinity, morphology, and functional group analyses of pretreated OPEFB

The effects of pretreatment conditions on the structural characteristics of OPEFB were further evaluated by examining changes in crystallinity, surface morphology, and functional groups. The crystallinity of the solid fractions obtained from untreated and hydrothermally pretreated OPEFB was determined by X-ray diffraction (XRD) analysis based on Segal's method [65]. XRD patterns were recorded using an X'Pert PRO diffractometer (PANalytical BV, Netherlands) equipped with Cu Kα radiation, operated at 40 kV and 30 mA. The crystallinity index (CrI) was calculated according to Eq. (26).

$$\textit{CrI}\ (\%) = \frac{I_{002} - I_{am}}{I_{002}} \times 100\% \tag{26}$$

where I_{002} represents the diffraction intensity of the 002 cellulose crystalline plane at $2\theta = 22.6^{\circ}$, while I_{am} denotes the intensity associated with the amorphous cellulose region at $2\theta = 18^{\circ}$.

The surface morphology of OPEFB before and after pretreatment was examined using scanning electron microscopy (SEM; Hitachi FlexSEM 1000, Japan) to observe pretreatment-induced structural disruption [66]. In addition, Fourier transform infrared (FTIR) spectroscopy was performed using an Agilent Cary 630 FTIR Spectrometer (USA) to identify alterations in the functional groups of the OPEFB samples after pretreatment [37].

2.7.3. Lignin characterizations

The recovered lignin samples were characterized by its purity, FTIR, GPC/SEC, and 2D HSQC NMR. Lignin purity was determined by compositional analysis according to the NREL lignin determination procedure, considering acid-insoluble and acid-soluble lignin fractions relative to the dried recovered lignin mass. FTIR analysis was performed using a Cary 630 FTIR Spectrometer (Agilent Technologies, USA) over a wavenumber range of 4000–650 cm^{-1} to identify the characteristic functional groups of lignin. GPC/SEC analysis was conducted using a system equipped with a refractive index detector and a TSKgel SuperAW5000 column. THF was used as the mobile phase at a flow rate of 0.3 mL/min, with an injection volume of 20 μL. The column and pump temperatures were maintained at 40 °C, and molecular weight parameters, including Mn, Mw, and Mw/Mn, were calculated using polystyrene standards in THF. The structural characteristics of the recovered lignin were further analyzed using 2D HSQC NMR on a Bruker Avance Neo-Ascend 500 MHz spectrometer operating at 500 MHz for ^{1}H and 125 MHz for ^{13}C. This characterization was conducted to evaluate the structural differences between lignin recovered from ChCl-LA and ChCl-Gly-$FeCl_3$ DES pretreatment systems. The 2D-HSQC spectra were interpreted based on representative lignin aromatic and side-chain regions. Manual integration was performed for selected cross-peak regions corresponding to S, G, H/p-coumarate-related aromatic units, β-O-4-related, β–5-related, β–β/overlapped oxygenated linkage regions, and methoxy groups. The integrated values were used as semi-quantitative structural indicators. The $S_{2,6}$ and H/p-coumarate-related aromatic integrals were divided by two to account for two equivalent aromatic positions, while linkage-related regions were normalized to the total corrected aromatic integral and expressed per 100 aromatic units. Weak, overlapping, or poorly resolved contours were interpreted cautiously and were not treated as absolute lignin structural contents.

2.7.4. Characterizations of CMC-lignin film

The properties of the CMC-based films were evaluated by FTIR, water contact angle, water vapor transmission rate (WVTR), tensile strength, and antioxidant. FTIR spectra were recorded using a Cary 630 FTIR Spectrometer (Agilent Technologies, USA) over a wavenumber range of 4000–650 cm^{-1} to identify functional groups and possible interactions between CMC and lignin. Water contact angle analysis was performed using a DataPhysics OCA-Series instrument by placing water droplets on the film surface using the sessile drop method. Three measurements were recorded for each sample.

The WVTR was measured using the gravimetric cup method. Film samples were mounted on WVTR cups, and mass changes were measured using an analytical balance (OHAUS). The analysis was performed in duplicate, and the results were reported as mean values with standard deviations. Mechanical properties were determined by tensile strength testing using rectangular film strips with dimensions of 30 mm × 5 mm. The test was conducted with a deformation length of 30 mm, trigger force of 4.5 g, and crosshead speed of 1.0 mm/s. Tensile strength and elongation at break were calculated from the recorded force and deformation data, while antioxidant activity was determined using the DPPH assay and expressed as IC_{50}.

3. Results and discussions

3.1. Modified severity factor determination on xylan degradation and delignification of OPEFB

This study evaluated the applicability of the CDF and CHF to describe lignin removal and xylan hydrolysis during DES pretreatment of OPEFB.

The fitted parameters for the CDF and CHF models are summarized in Table 1, while the correlations between residual lignin (L_{res}), residual xylan (X_{res}), and their corresponding modified severity factors are presented in Fig. 2. CDF was used to represent the severity of delignification, whereas CHF was used to represent the severity of xylan hydrolysis. These parameters integrate the effects of reaction temperature, residence time, and acid/catalyst contribution into single kinetic descriptors. This approach is relevant because ChCl:LA and ChCl:Gly:$FeCl_3$ are both acidic DESs, but they differ in catalytic behavior. ChCl:LA mainly provides Brønsted acidity through lactic acid, whereas ChCl:Gly:$FeCl_3$ introduces Fe^{3+}-based Lewis acidity [26,35].

As shown in Fig. 2a and b, the residual lignin fraction (Lres) decreased with increasing CDF in both DES systems, indicating that the proposed CDF descriptor adequately represented the progress of delignification during OPEFB pretreatment. In the ChCl:LA system, Lres decreased sharply at low CDF and subsequently approached a residual level of approximately 0.16 after CDF exceeded 2. A similar decreasing trend was observed in the ChCl:Gly:$FeCl_3$ system, although the CDF range was broader. In this system, Lres decreased rapidly at low CDF, followed by a slower decline after CDF exceeded 5, suggesting that additional increases in pretreatment severity produced progressively smaller improvements in lignin removal. The nonlinear decline of L_{res} suggests that delignification did not proceed as a single homogeneous reaction, but rather followed a biphasic pattern involving fast-removing and slow-removing lignin fractions. The fast-removing fraction can be associated with more accessible lignin domains, labile ether linkages, and lignin–carbohydrate linkages that are readily cleaved during the early stage of DES pretreatment [58,59,67]. In contrast, the slow-removing fraction likely corresponds to lignin structures that are more condensed, less accessible, or more strongly embedded within the cell wall matrix. Therefore, the plateau-like behavior observed at higher CDF values may indicate that the easily removable lignin fraction had been largely solubilized, while further delignification was limited by the persistence of recalcitrant lignin domains. In the ChCl:LA system, the rapid decrease in Lres at relatively low CDF suggests that the Brønsted-acidic DES effectively promoted lignin solubilization within a narrower severity window [22,26]. Conversely, the broader CDF range observed for ChCl:Gly:$FeCl_3$ indicates that $FeCl_3$-assisted DES pretreatment required higher effective severity to approach a comparable residual lignin level. This behavior may also be associated with partial lignin condensation, pseudo-lignin formation, or lignin redeposition under more severe acidic conditions, which has been reported during acid-catalyzed biomass pretreatment and is further evaluated in this study through solid FTIR and lignin structural characterization [34,54,68]. High coefficients of determination were obtained for both ChCl:LA ($R^2 = 0.996$) and ChCl:Gly:$FeCl_3$ ($R^2 = 0.977$), confirming that CDF captured the severity-dependent delignification behavior with good accuracy. The apparent activation energy for lignin removal was higher in ChCl:Gly:$FeCl_3$ (87.84 kJ/mol) than in ChCl:LA (63.47 kJ/mol), suggesting that delignification in the $FeCl_3$-containing DES was more temperature-sensitive. This higher temperature dependency is consistent with the catalytic role of Fe^{3+}, where elevated temperature may intensify Lewis acid-assisted cleavage of lignin-associated and ether-type linkages during metal salt-assisted pretreatment [69,70]. However, the higher activation energy also implies that lignin removal in ChCl:Gly:$FeCl_3$ is less readily promoted at lower severity than in ChCl:LA. The relatively high

$\alpha_{L,Fe}$ value also reflects the broader severity scale required to describe delignification in the $FeCl_3$-assisted system, whereas ChCl:LA produced effective lignin solubilization over a narrower CDF range.

Similar to delignification, in Fig. 2c and d xylan removal also exhibited biphasic behavior. At low CHF, Xres decreased rapidly, indicating the hydrolysis of the fast-hydrolyzing xylan fraction. This fraction is likely located in more accessible regions of the biomass cell wall and is therefore more susceptible to acid-catalyzed cleavage, as previously observed for biphasic xylan hydrolysis during acidic pretreatment of lignocellulosic biomass [13,58,59]. At higher CHF values, the decrease in Xres became slower, indicating that the remaining xylan belonged to a slow-hydrolyzing fraction. This resistant fraction may be more strongly associated with cellulose and lignin through hydrogen bonding or lignin–carbohydrate complexes, making it less accessible to hydrolytic attack [55,71]. The stronger xylan hydrolysis observed in ChCl:Gly:$FeCl_3$ can be attributed to the Lewis acidity of Fe^{3+}, which may coordinate with oxygen-containing glycosidic linkages and facilitate their cleavage [30,31,72]. Thus, the $FeCl_3$-containing DES appears particularly effective in disrupting hemicellulose, including both readily accessible and more resistant xylan fractions.

The fitted CHF parameters in Table 1 also indicate that the proposed model effectively described xylan hydrolysis in both DES systems. The CHF model gave R^2 values of 0.969 for ChCl:LA and 0.996 for ChCl:Gly:$FeCl_3$, confirming good agreement between experimental and predicted residual xylan fractions. The apparent activation energy for xylan hydrolysis was higher in ChCl:Gly:$FeCl_3$ (69.87 kJ/mol) than in ChCl:LA (49.54 kJ/mol), indicating that xylan removal in the $FeCl_3$-containing DES was more strongly governed by temperature. This finding is consistent with the broader CHF range observed in ChCl:Gly:$FeCl_3$ and supports the interpretation that Fe^{3+} intensifies hemicellulose hydrolysis at elevated temperatures, as reported in metal chloride-assisted pretreatment systems [34,73,74]. In contrast, the lower activation energy in ChCl:LA suggests that xylan removal can proceed more readily under milder Brønsted-acidic conditions, although the overall extent of xylan removal was lower than that obtained using ChCl:Gly:$FeCl_3$.

The fitted fast- and slow-fraction parameters provide additional insight into the heterogeneous nature of OPEFB fractionation. For lignin removal, the slow-removing fraction represents lignin that remains difficult to solubilize after the more labile lignin domains have been extracted. For xylan hydrolysis, the slow-hydrolyzing fraction represents xylan that remains protected within the biomass matrix. Therefore, the biphasic behavior observed for both L_{res} and X_{res} reflects the heterogeneous distribution and accessibility of lignin and hemicellulose in OPEFB, consistent with previous kinetic interpretations of lignocellulosic fractionation using severity-based descriptors [58,59,63]. The comparison between ChCl:LA and ChCl:Gly:$FeCl_3$ further indicates that

Table 1
Fitted parameters for CDF and CHF models on delignification and xylan hydrolysis for each DES system.

Model	Parameter	Unit	Fitted value	Parameter	Unit	Fitted value
	ChCl:LA			ChCl:Gly:$FeCl_3$		
CDF	$E_{a,L,LA}$	kJ/mol	63.47	$E_{a,L,Fe}$	kJ/mol	87.84
	$\theta_{L,LA}$	–	0.20	$\theta_{L,Fe}$	–	0.23
	$f_{L,LA}$	–	0.02	$f_{L,Fe}$	–	0.01
	$\alpha_{L,LA}$	–	2.71	$\alpha_{L,Fe}$	–	28.01
	$\beta_{L,LA}$	L/mol	3.12	$\beta_{L,Fe}$	L/mol	1.41
	R^2	–	0.996	R^2	–	0.977
CHF	$E_{a,X,LA}$	kJ/mol	49.54	$E_{a,X,Fe}$	kJ/mol	69.87
	$\theta_{X,LA}$	–	0.43	$\theta_{X,Fe}$	–	0.24
	$f_{X,LA}$	–	0.10	$f_{X,Fe}$	–	0.05
	$\alpha_{X,LA}$	–	15.42	$\alpha_{X,Fe}$	–	23.29
	$\beta_{X,LA}$	L/mol	−1.37	$\beta_{X,Fe}$	L/mol	0.69
	R^2	–	0.969	R^2	–	0.996

Ea is expressed in kJ/mol. C_i is the concentration of the dominant active component in the DES system, expressed in mol/L: C_{LA} for ChCl:LA and C_{FeCl_3} for ChCl:Gly:$FeCl_3$. The coefficient β_i is expressed in L/mol so that $\beta_i C_i$ is dimensionless. All CDF and CHF values were calculated using temperature in K, pretreatment time in h, and active component concentration in mol/L. Because the active component concentration was fixed within each DES system, β_i represents an empirical acid/catalyst contribution for the selected DES formulation.

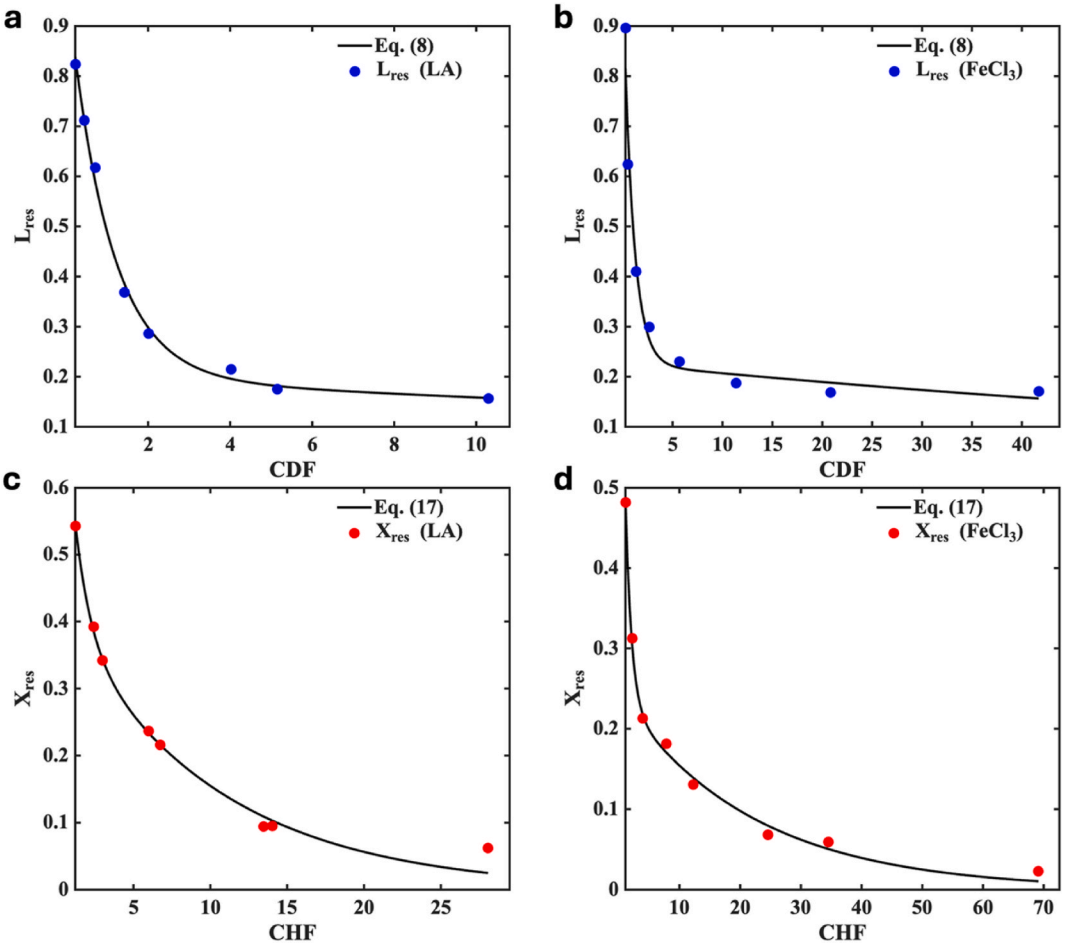

Fig. 2. Correlation of residual lignin and xylan with modified severity factors during DES pretreatment. Residual lignin content, L_{res}, as a function of CDF for (a) ChCl:LA and (b) ChCl:Gly:$FeCl_3$, and residual xylan content, X_{res}, as a function of CHF for (c) ChCl:LA and (d) ChCl:Gly:$FeCl_3$.

the two DES systems deconstruct OPEFB through different dominant pathways. ChCl:LA favors efficient lignin solubilization, which is consistent with previous reports showing that lactic acid-based acidic DESs promote cleavage of lignin–carbohydrate linkages, xylan elimination, and lignin dissolution through Brønsted acidity and hydrogen-bonding interactions [23,25,26]. In contrast, ChCl:Gly:$FeCl_3$ more strongly promotes xylan hydrolysis, in agreement with studies showing that Fe^{3+} or metal chloride-assisted pretreatment enhances hemicellulose depolymerization through Lewis acid-catalyzed cleavage of glycosidic linkages [30,31,74].

Overall, the CDF and CHF models successfully described the severity-dependent fractionation behavior of OPEFB during DES pretreatment. The high fitting accuracy obtained for both descriptors confirms that lignin removal and xylan hydrolysis can be represented separately using response-specific severity factors. ChCl:LA promoted effective delignification within a relatively narrow CDF range, supporting the strong lignin-solubilizing ability commonly reported for ChCl:LA and other organic acid-based DES systems [23,25,26]. Meanwhile, ChCl:Gly:$FeCl_3$ generated stronger xylan hydrolysis over a broader CHF range, reflecting the hydrolytic contribution of Fe^{3+} in the DES matrix [73–75]. These findings demonstrate that the effective severity of DES pretreatment depends not only on temperature and residence time, but also on the acid type and catalytic mechanism of the solvent system. Therefore, CHF and CDF provide useful empirical descriptors for comparing Brønsted-acidic and Lewis acid-assisted DES pretreatments of OPEFB. By unifying temperature, residence time, and acid or catalytic contribution into response-specific severity parameters, these descriptors can support process comparison, operating-window selection, and future scale-up evaluation of DES pretreatment systems. This agrees with previous studies applying combined or modified severity factors to interpret carbohydrate hydrolysis, delignification, and enzymatic digestibility [55,59,63,76].

3.2. *Effect of DES pretreatment variables on OPEFB biomass and lignin recovery*

The effect of DES pretreatment severity on OPEFB fractionation is presented in Fig. 3. The pretreatment conditions were primarily arranged according to the actual operating variables, namely temperature and residence time, while the corresponding CHF and CDF values were included as severity descriptors to support comparison between the two DES systems. In this figure, the upper axis denotes the actual pretreatment condition, whereas CHF and CDF provide unified severity values that reflect the combined influence of temperature, time, and acid or catalytic contribution. The use of severity descriptors is beneficial because it allows different pretreatment conditions to be interpreted through a common scale, facilitates comparison between solvent systems, and supports the identification of an effective operating window for future process development and scale-up evaluation [36,52,53,55]. Fig. 3a and b shows the chemical composition of the recovered solid fractions, while Fig. 3c and d presents hemicellulose removal, cellulose recovery, delignification, and lignin yield. These responses are important because an effective pretreatment should remove non-cellulosic barriers, preserve sufficient cellulose for enzymatic hydrolysis, and recover lignin as a useable product stream.

The untreated OPEFB initially contained approximately 38.6%

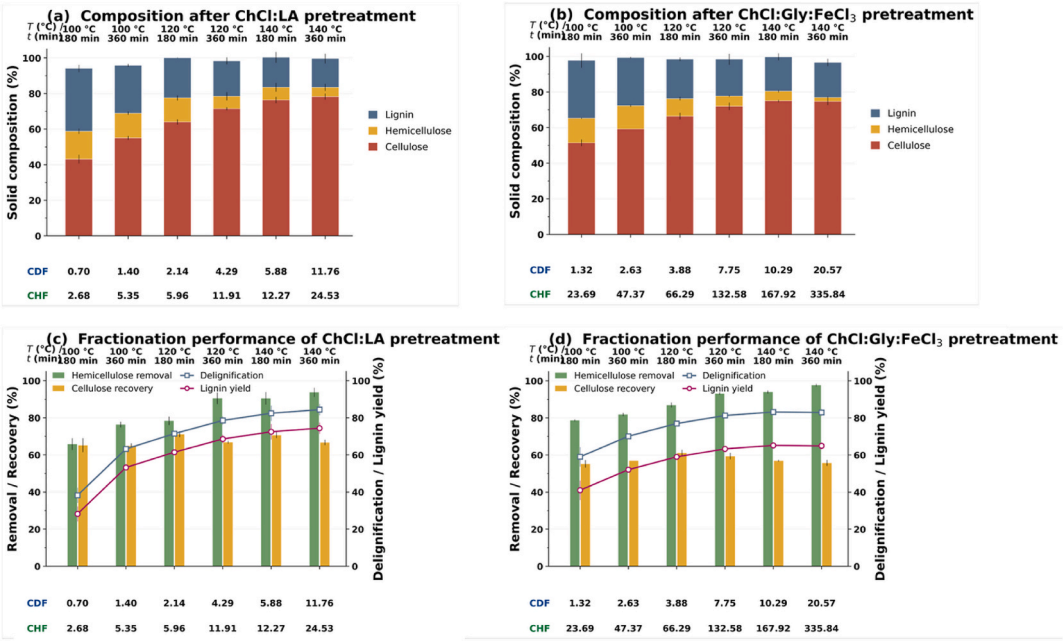

Fig. 3. Severity-dependent compositional and fractionation responses of two DES systems. (a,b) Chemical composition of the recovered solid fraction after pretreatment with ChCl:LA & ChCl:Gly:$FeCl_3$. (c,d) Hemicellulose removal, cellulose recovery, delignification and lignin yield of ChCl:LA & ChCl:Gly:$FeCl_3$ system.

cellulose, 26.8% hemicellulose, and 33.2% lignin. After DES pretreatment, the relative composition of the recovered solid shifted substantially, reflecting the selective removal of non-cellulosic components. For the ChCl:LA system, the cellulose proportion in the recovered solid increased markedly with increasing pretreatment severity, from approximately 43% to 78%. In parallel, the hemicellulose fraction decreased from approximately 16% to below 6%, while the lignin fraction decreased from approximately 35% to 16%. This compositional shift indicates that ChCl:LA effectively removed both hemicellulose and lignin, resulting in a cellulose-enriched solid residue. The most pronounced cellulose enrichment and lignin removal were obtained at the highest tested condition of 140 °C for 6 h, indicating that the ChCl:LA system continued to respond positively to increased temperature and residence time within the investigated range. This trend is consistent with previous reports on ChCl:LA and other organic acid-based DES systems, where increasing pretreatment severity enhanced lignin dissolution, xylan removal, and cellulose enrichment [23,26,77,78]. The increase in cellulose content should be interpreted as an enrichment effect caused by the preferential solubilization of non-cellulosic components rather than the formation of additional cellulose. Such cellulose enrichment is favorable for enzymatic hydrolysis because hemicellulose and lignin removal can open the cell wall structure, reduce physical shielding, and improve enzyme accessibility [53,79–81].

A similar cellulose enrichment trend was observed in the ChCl:Gly:$FeCl_3$ system. The cellulose content increased from approximately 51% to 75%, while the hemicellulose content decreased from approximately 14% to below 3%. This result confirms that ChCl:Gly:$FeCl_3$ was highly effective in removing hemicellulose from OPEFB. However, compared with ChCl:LA, the lignin fraction in the recovered solid remained slightly higher, particularly at high severity. This indicates that the $FeCl_3$-containing DES promoted stronger hemicellulose hydrolysis but was comparatively less selective for lignin solubilization [31,33]. The strong hemicellulose removal can be attributed to the Lewis acidity of Fe^{3+}, which can catalyze glycosidic bond cleavage in xylan, as commonly reported for metal chloride-assisted pretreatment systems [30,33]. In contrast, lignin recovery is governed not only by bond cleavage but also by lignin solvation, precipitation behavior, and the accessibility of lignin within the biomass matrix [26,82]. This distinction is important because ChCl:LA and other organic acid-based DESs are often reported to be particularly effective for lignin solubilization through Brønsted acidity and hydrogen-bonding interactions, whereas $FeCl_3$-containing systems may exert stronger hydrolytic effects toward hemicellulose [33,75,83].

The fractionation performance of ChCl:LA is shown in Fig. 3c. Hemicellulose removal increased from approximately 66% to more than 90% as CHF increased, confirming the hydrolytic effect of the lactic acid-based DES on the hemicellulose fraction. Delignification also increased from approximately 39% to around 85% with increasing CDF, indicating that ChCl:LA effectively promoted lignin solubilization [84,85]. This behavior is consistent with previous studies showing that organic acid-based DESs, particularly ChCl:LA, can promote lignin dissolution and xylan elimination through Brønsted acidity, hydrogen-bonding interactions, and cleavage of lignin–carbohydrate linkages [23,29,39]. Therefore, ChCl:LA appears to provide a balanced fractionation environment in which both hemicellulose and lignin are removed while cellulose is relatively preserved.

Cellulose recovery in the ChCl:LA system remained relatively high, ranging from approximately 64% to 72% across the tested conditions. Although increasing temperature and residence time enhanced delignification and hemicellulose removal, cellulose recovery did not increase proportionally. This indicates that the most suitable operating window should balance three competing outcomes: extensive hemicellulose removal, high delignification, and sufficient cellulose preservation [86–88]. In this context, CHF and CDF are useful because these helps distinguish whether the improvement in fractionation is mainly associated with hydrolytic severity or delignification severity, rather than relying only on temperature and time as independent variables [55,63]. Within the tested range, the highest temperature and longest residence time provided the most favorable fractionation outcome for ChCl:LA, especially when lignin recovery was considered.

For the ChCl:Gly:$FeCl_3$ system, hemicellulose removal was already high at the lowest severity and increased further to approximately 95–97% at higher CHF values, as shown in Fig. 3d. This confirms that the $FeCl_3$-containing DES exerted stronger hydrolytic activity toward hemicellulose than ChCl:LA. The high CHF range of ChCl:Gly:$FeCl_3$ supports the role of Fe^{3+} as a Lewis acid catalyst that facilitates xylan cleavage [33,43,53]. Similar behavior has been reported in metal chloride-assisted pretreatment systems, where Fe^{3+} or other metal ions enhanced hemicellulose depolymerization and improved subsequent

enzymatic digestibility [33,34].

In contrast, delignification in ChCl:Gly:$FeCl_3$ increased from approximately 60% to around 83%, but the improvement became less pronounced at higher CDF. This trend agrees with the CDF-based model in Subsection 3.1, where residual lignin decreased rapidly at low CDF and then approached a plateau at higher severity. Notably, increasing the residence time from 3 h to 6 h at 140 °C did not produce a substantial additional improvement in the ChCl:Gly:$FeCl_3$ system. This indicates that the fractionation response of the $FeCl_3$-containing DES approached an effective plateau at high temperature, where the easily removable lignin fraction had been solubilized, and the remaining lignin was more resistant to be removed.

Lignin yield increased with pretreatment severity in both DES systems, confirming that higher severity promoted lignin solubilization and subsequent precipitation from the DES liquor. In ChCl:LA, lignin yield increased from approximately 29% to around 75%, whereas in ChCl:Gly:$FeCl_3$ it increased from approximately 41% to around 65%. The higher final lignin yield in ChCl:LA indicates that this system was more favorable for lignin recovery, likely because lactic acid-based DESs provide strong lignin solvation and facilitate lignin dissolution through Brønsted acidity and hydrogen-bonding interactions. Recent studies also reported high lignin extraction and recovery from ChCl:LA-based systems, supporting the suitability of this solvent for lignin-focused fractionation [23,25,26,39]. Although ChCl:Gly:$FeCl_3$ achieved strong hemicellulose removal and relatively high delignification, its lower final lignin yield suggests that part of the lignin may have remained in the solid residue or been less efficiently recovered from the DES liquor.

Overall, Fig. 3 demonstrates that the two acidic DES systems produced distinct fractionation profiles. ChCl:LA provided more balanced fractionation, combining high delignification, high lignin yield, and good cellulose enrichment. In contrast, ChCl:Gly:$FeCl_3$ showed stronger hemicellulose removal and higher hydrolytic severity, producing a cellulose-rich solid that is favorable for enzymatic hydrolysis, but with comparatively lower lignin recovery. These differences confirm that the pretreatment outcome depends not only on severity level but also on the acid type and catalytic mechanism of the DES system. The severity-factor approach is therefore valuable because it converts multiple operational variables into comparable response-oriented descriptors, helping to identify whether additional severity still improves fractionation or whether the system has approached a plateau. This is particularly relevant for process scale-up, where increasing temperature or residence time is only beneficial if it produces meaningful gains in component separation and product recovery. Therefore, ChCl:LA is more suitable when lignin recovery is prioritized, particularly because the highest temperature and longest residence time still improved its fractionation outcome. Conversely, ChCl:Gly:$FeCl_3$ is more effective when extensive hemicellulose removal and cellulose accessibility are the main targets, although extending the treatment from 3 h to 6 h at 140 °C provides limited additional benefit.

3.3. Solid characterization of pretreated OPEFB

Structural characterization of untreated and DES-pretreated OPEFB was conducted using SEM, XRD, and FTIR to verify whether the fractionation behavior observed in Section 3.2 was reflected in the physical morphology, cellulose crystallinity, and functional group characteristics of the recovered solids. In Section 3.2, ChCl:LA was shown to increase the cellulose proportion while decreasing both hemicellulose and lignin contents, whereas ChCl:Gly:$FeCl_3$ produced stronger hemicellulose removal but retained a comparatively higher lignin fraction in the recovered solid. These compositional trends indicate that the two DES systems deconstructed OPEFB through different dominant pathways. However, compositional changes alone do not fully describe biomass recalcitrance because enzymatic accessibility also depends on fiber morphology, cellulose ordering, and the persistence of lignin- or hemicellulose-associated functional groups. Therefore, SEM, XRD, and FTIR were used as complementary techniques to evaluate whether the chemical fractionation trends were accompanied by structural disruption and cellulose enrichment. Similar combined characterization approaches have been used to connect biomass composition, crystallinity, functional groups, and enzymatic accessibility after pretreatment [79,89].

To compare temperature-dependent structural changes under a consistent residence-time basis, SEM, XRD, and FTIR analyses were conducted on OPEFB solids pretreated at 100, 120, and 140 °C for 3 h. The SEM images of untreated and DES-pretreated OPEFB are shown in Fig. S1, where panels a–c correspond to ChCl:LA-pretreated samples, panels d–f correspond to ChCl:Gly:$FeCl_3$-pretreated samples, and panel g represents untreated OPEFB. The untreated OPEFB showed a relatively compact and covered surface, suggesting that the native fiber structure was still protected by the lignin–hemicellulose matrix and other amorphous components. After DES pretreatment, both DES systems altered the OPEFB surface morphology, as indicated by surface roughening, partial fiber exposure, localized surace disruption, and erosion. These features suggest that DES pretreatment weakened the compact lignocellulosic architecture and increased the exposure of the pretreated fiber surface. Similar morphological changes have been reported after acidic DES pretreatment, where removal of lignin and hemicellulose opened the biomass structure and improved cellulose accessibility [25,86]. Comparable surface disruption has also been observed after metal salt-assisted pretreatment, where catalytic hydrolysis of hemicellulose weakens the cell-wall matrix [90].

For ChCl:LA-pretreated OPEFB, the surface morphology became rougher and more irregular after pretreatment. At 100 °C for 3 h, surface roughening was already observed, while the sample treated at 140 °C for 3 h showed more visible fiber exposure and fibrillation. This morphology is consistent with the compositional data in Section 3.2, where ChCl:LA produced substantial cellulose enrichment together with high delignification and lignin yield. The enhanced surface opening can be attributed to the combined effects of Brønsted acidity and hydrogen-bonding interactions in the lactic acid-based DES. Liu et al. [26] reported that acidic DES can promote cleavage of lignin–carbohydrate complexes, while H. Li et al. (2021) showed that acidic DES pretreatment enhances bamboo delignification and lignin fractionation. More recently, Rodrigues et al. [43] also demonstrated that ChCl:LA-based pretreatment can enhance lignin extraction and cellulose-to-glucose conversion. In the ChCl:Gly:$FeCl_3$ system, the pretreated OPEFB also showed clear surface modification. The samples treated at 100 and 120 °C for 3 h showed surface disruption and localized pits, whereas the sample treated at 140 °C for 3 h exhibited stronger erosion and a more porous structure. This is consistent with the composition and removal data in Section 3.2, where ChCl:Gly:$FeCl_3$ produced extensive hemicellulose removal. Fe^{3+}-assisted Lewis acidity can intensify xylan hydrolysis and weaken the polysaccharide matrix. Kamireddy et al. [31] described the role of metal chloride salts in improving lignocellulosic deconstruction, while Tang et al. [34] showed that metallic chlorides can alter lignin structure and improve enzymatic hydrolysis. Yang et al. [91] further demonstrated that metal-salt coordinated ChCl:Gly DES systems can promote lignocellulosic pretreatment through coordinated acidity and hydrogen-bond interactions.

The XRD patterns and crystallinity index (CrI) values of untreated and DES-pretreated OPEFB are shown in Fig. S2. Untreated OPEFB showed a CrI of 65.6%. After ChCl:LA pretreatment, the CrI increased markedly to 82.0%, 80.8%, and 81.0% at 100, 120, and 140 °C, respectively. The increase in CrI indicates that ChCl:LA preferentially removed amorphous components, mainly hemicellulose and lignin, thereby enriching the crystalline cellulose fraction in the recovered solid. This interpretation agrees with Section 3.2 composition data, where the cellulose proportion increased while hemicellulose and lignin contents decreased. The relatively stable CrI values at higher temperatures further suggest that the crystalline cellulose structure was largely preserved during ChCl:LA pretreatment, even though non-cellulosic

components were extensively removed. Li et al. [92] similarly reported that acidic DES pretreatment can enhance apparent crystallinity by removing lignin and hemicellulose. Da Costa Lopes et al. [93] also associated selective hemicellulose/lignin degradation with improved enzymolysis efficiency. The broader role of DES pretreatment in removing amorphous barriers and improving cellulose accessibility has also been highlighted in recent reviews [43]. A different crystallinity trend was observed for ChCl:Gly:$FeCl_3$-pretreated OPEFB. The CrI remained almost unchanged at 100 °C (65.5%), increased to 70.2% at 120 °C, and then decreased to 63.3% at 140 °C. The initial increase can be attributed to the preferential removal of amorphous components, particularly hemicellulose and part of the lignin fraction, which enriched the cellulose-rich solid. Similar increases in apparent crystallinity after pretreatment have been associated with the removal of amorphous lignin and hemicellulose fractions [43,79,92]. However, the decrease in CrI at 140 °C suggests that the $FeCl_3$-assisted DES treatment did not simply enrich crystalline cellulose. Instead, the stronger Lewis-acid-assisted deconstruction may have partially altered the ordering of the cellulose-rich solid or increased the relative contribution of less ordered cellulose domains. Since CrI calculated using the Segal method is an apparent crystallinity index, this result should not be interpreted alone as direct evidence of cellulose degradation. Rather, it should be considered together with compositional analysis, SEM morphology, FTIR spectra, and enzymatic hydrolysis results, as biomass digestibility is influenced by multiple structural and chemical features rather than crystallinity alone ([81,89]. In this context, the lower apparent CrI at high ChCl:Gly:$FeCl_3$ severity may contribute to improved cellulase accessibility by exposing less ordered or more accessible cellulose domains. Nevertheless, excessive severity must still be controlled because metallic chloride pretreatment can alter lignin and carbohydrate structures under severe conditions, which may reduce cellulose recovery or increase carbohydrate loss during pretreatment [25,34,94].

The FTIR spectra of untreated and DES-pretreated OPEFB are shown in Fig. S3. The main bands observed in the spectra were located at approximately 3333, 2907, 1729, 1603, 1509, 1371, 1327, 1238, 1110, and 1030 cm^{-1}. The broad band around 3333 cm^{-1}, corresponding to O–H stretching vibrations, decreased after DES pretreatment. This change indicates disruption of the hydrogen-bonding network among cellulose, hemicellulose, and lignin, which is consistent with the removal of matrix-forming amorphous components discussed in Section 3.2. The peak around 2907 cm^{-1}, assigned to C–H stretching vibrations in polysaccharides and lignin, also decreased after pretreatment, suggesting partial removal or structural alteration of carbohydrate and lignin components. These changes confirm that both DES systems modified the chemical environment of the OPEFB solid fraction. Similar changes in O–H and C–H stretching bands have been used to indicate hydrogen-bond disruption and biomass matrix deconstruction after DES pretreatment [23]. In the carbonyl region, the band around 1729 cm^{-1}, commonly attributed to C=O stretching of acetyl and ester groups in hemicellulose, became weaker after DES pretreatment. This decrease supports the removal of hemicellulose, consistent with the high hemicellulose removal shown in Fig. 3. The reduction of bands in the 1238–1371 cm^{-1} region, including peaks around 1371, 1327, and 1238 cm^{-1}, further indicates disruption and solubilization of hemicellulose- and lignin-associated structures. Meanwhile, the bands around 1110 and 1030 cm^{-1} are associated mainly with polysaccharide C–O–C and C–O stretching vibrations, reflecting changes in the carbohydrate-rich solid after pretreatment. H. Li et al. [25] reported similar FTIR changes after acidic DES delignification of bamboo. Huo et al. [23] also linked the reduction of hemicellulose- and lignin-associated bands with improved enzymolysis after DES pretreatment. For ChCl:LA-based pretreatment, Rodríguez-Rebelo et al. [83] further associated lignin extraction and hemicellulose removal with improved cellulose conversion. The lignin-related aromatic skeletal vibration bands around 1603 and 1509 cm^{-1} were also reduced after pretreatment. The decrease was more evident in the ChCl:LA-pretreated solid, supporting the stronger lignin solubilization and higher lignin yield obtained with the lactic acid-based DES. This agrees with the fractionation results in Section 3.2, where ChCl:LA showed more balanced hemicellulose removal and delignification. The efficient lignin removal by acidic DESs has been attributed to the ability of organic acid-based DES systems to disrupt lignin-associated linkages and improve lignin solvation [27,92]. In contrast, the persistence of lignin-related bands in ChCl:Gly:$FeCl_3$-pretreated solids suggests that part of the lignin remained associated with the recovered solid fraction. This observation is consistent with the comparatively lower lignin recovery of ChCl:Gly:$FeCl_3$, despite its strong hemicellulose removal. Tang et al. [34] also showed that metallic chloride pretreatment can strongly affect biomass deconstruction while modifying lignin structure. Therefore, FTIR analysis supports the interpretation that ChCl:LA was more favorable for lignin removal, whereas ChCl:Gly:$FeCl_3$ primarily promoted hemicellulose-directed deconstruction.

Overall, SEM, XRD, and FTIR analyses confirmed that the two DES systems modified OPEFB through different structural pathways. ChCl:LA effectively disrupted the lignin–hemicellulose matrix, reduced lignin-associated FTIR bands, and preserved high apparent cellulose crystallinity, explaining the cellulose enrichment and high lignin recovery observed in the fractionation data. This behavior is consistent with previous reports showing that organic acid-based DESs promote lignin solubilization, lignin–carbohydrate complex cleavage, and cellulose enrichment [23,26,28]. In contrast, ChCl:Gly:$FeCl_3$ produced stronger hemicellulose-directed disruption, surface erosion, and partial reduction in apparent CrI at high temperature. These changes suggest that the $FeCl_3$-containing DES increased cellulose accessibility not only by removing hemicellulose but also by opening the cell-wall structure and exposing less ordered cellulose domains. Similar effects of Fe^{3+} or metallic chloride-assisted pretreatment on hemicellulose disruption, lignocellulose deconstruction, and enzymatic digestibility have been reported previously [33,34,95]. Therefore, ChCl:LA is more favorable for balanced delignification, lignin recovery, and cellulose enrichment, whereas ChCl:Gly:$FeCl_3$ is more effective for generating a highly digestible cellulose-rich solid through hemicellulose removal and structural accessibility improvement. This integrated structural interpretation provides the basis for the enzymatic hydrolysis behavior discussed in the next section.

3.4. Effect of pretreatment on OPEFB saccharification

The effect of DES pretreatment on OPEFB saccharification was evaluated by correlating enzymatic hydrolysis yield (Y_{EH}) with CHF and CDF, as shown in Fig. 4. CHF represents the severity of xylan hydrolysis, while CDF represents the severity of delignification. Therefore, both factors were used to determine whether hemicellulose removal and lignin removal contributed to the improvement of enzymatic digestibility after ChCl:LA and ChCl:Gly:$FeCl_3$ pretreatment.

For the ChCl:LA system, Y_{EH} increased with increasing CHF, as shown in Fig. 4a. The enzymatic hydrolysis yield increased from 46.6% at low CHF to 75.8% at the highest CHF. The increase was rapid at low-to-moderate CHF and then approached a plateau at higher CHF values. This trend indicates that xylan removal strongly improved cellulose accessibility during the early stage of pretreatment. However, after most accessible hemicellulose had been removed, further increase in CHF only slightly improved enzymatic hydrolysis. The fitted model showed a good correlation between CHF and Y_{EH}, with $R^2 = 0.883$ and RMSE = 3.20%, confirming that CHF can describe the contribution of hemicellulose hydrolysis to enzymatic digestibility. A similar trend was observed when Y_{EH} was correlated with CDF for ChCl:LA, as shown in Fig. 4b. The hydrolysis yield increased with increasing CDF and reached a plateau at higher delignification severity. The correlation between CDF and Y_{EH} gave a slightly higher fitting accuracy, with $R^2 = 0.924$ and

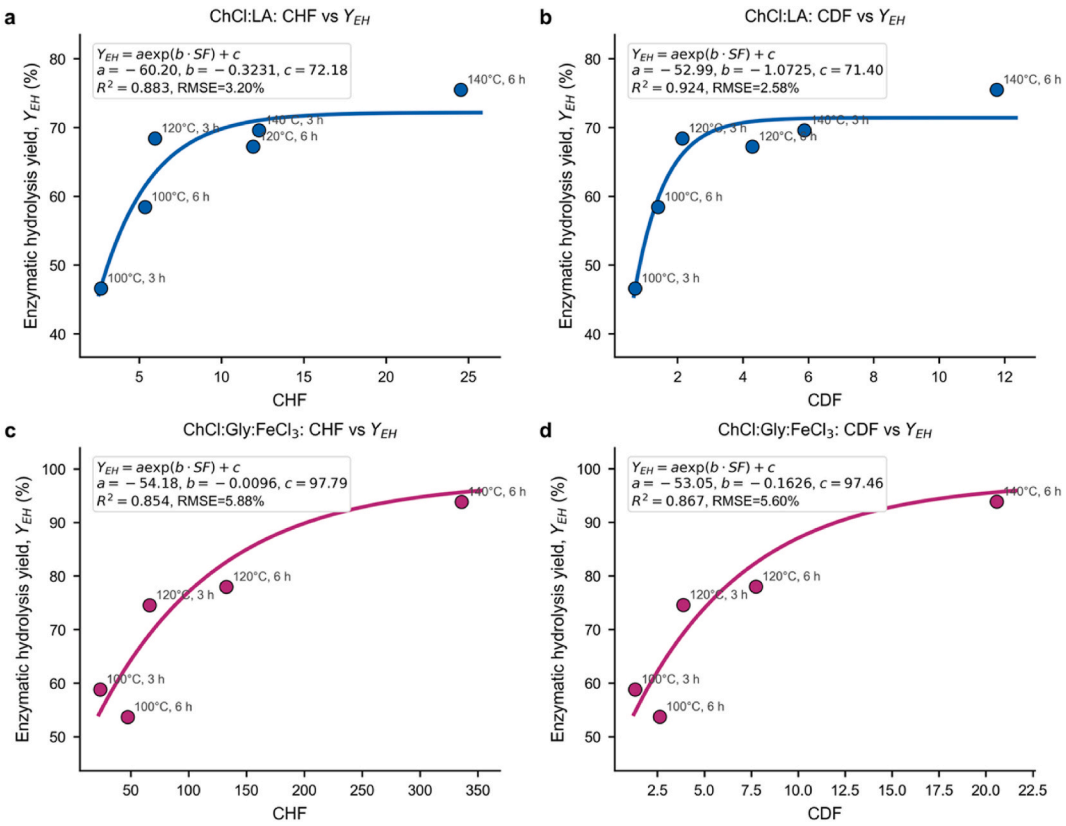

Fig. 4. Effects of modified severity factors on enzymatic hydrolysis yield of DES-pretreated OPEFB. Correlation of Y_{EH} with (a) CHF and (b) CDF for ChCl:LA, and with (c) CHF and (d) CDF for ChCl:Gly:$FeCl_3$.

RMSE = 2.58%. This suggests that, in the ChCl:LA system, lignin removal had a strong contribution to enzymatic hydrolysis improvement. This result is consistent with the fractionation data, where ChCl:LA showed effective delignification and lignin recovery. The removal of lignin likely reduced the physical barrier around cellulose and decreased non-productive enzyme binding, resulting in higher cellulose digestibility [82,96].

For the ChCl:Gly:$FeCl_3$ system, Y_{EH} also increased with increasing CHF, as shown in Fig. 4c. The hydrolysis yield increased from approximately 54–59% at low CHF to 93.8% at the highest CHF. Compared with ChCl:LA, ChCl:Gly:$FeCl_3$ reached a much broader CHF range and achieved a higher final Y_{EH}. This confirms that the $FeCl_3$-containing DES strongly enhanced OPEFB digestibility, mainly through extensive hemicellulose removal and improved cellulose accessibility. The Lewis acidity of Fe^{3+} can promote cleavage of glycosidic linkages in xylan, thereby reducing the hemicellulose barrier surrounding cellulose microfibrils and increasing cellulase access to the cellulose-rich solid [25,33]. The CHF–Y_{EH} model gave $R^2 = 0.854$ and RMSE = 5.88%, indicating a reasonable correlation, although the deviation was higher than that of the ChCl:LA model. This relatively larger deviation suggests that the hydrolysis behavior of ChCl:Gly:$FeCl_3$-pretreated OPEFB was not governed by hemicellulose removal alone, but also by additional structural and compositional factors.

The high enzymatic hydrolysis yield of ChCl:Gly:$FeCl_3$-pretreated OPEFB should also be interpreted together with the structural characterization results. Although the apparent CrI decreased at 140 °C, this decrease does not contradict the high hydrolysis yield. Enzymatic digestibility of lignocellulosic biomass is not governed by crystallinity alone, but by the combined effects of hemicellulose removal, lignin removal, cellulose exposure, accessible surface area, pore formation, and enzyme accessibility [82,97]. In the ChCl:Gly:$FeCl_3$ system, extensive hemicellulose removal reduced the xylan barrier surrounding cellulose microfibrils, while partial delignification and surface erosion decreased physical shielding and improved cellulase penetration into the recovered solid. The lower apparent CrI may also indicate partial deordering of the cellulose-rich fraction, which can increase the proportion of less ordered or more accessible cellulose domains. Therefore, the 93.8% hydrolysis yield was likely caused by the combined effects of hemicellulose removal, partial lignin removal, surface disruption, and increased cellulose accessibility, rather than by a single structural factor.

The relationship between CDF and Y_{EH} for ChCl:Gly:$FeCl_3$ is shown in Fig. 4d. The hydrolysis yield increased with increasing CDF and gradually approached a high plateau. The CDF–Y_{EH} model showed $R^2 = 0.867$ and RMSE = 5.60%, slightly better than the CHF-based correlation for the same DES system. This indicates that delignification also contributed to enzymatic hydrolysis improvement in ChCl:Gly:$FeCl_3$, although the effect was less direct than in ChCl:LA. This may be because ChCl:Gly:$FeCl_3$ primarily promoted hemicellulose removal, while part of the lignin remained in the recovered solid or may have undergone condensation or redeposition at higher severity. Such residual or modified lignin may still affect enzymatic hydrolysis through physical shielding or non-productive enzyme adsorption [7,23]. Therefore, the saccharification behavior of ChCl:Gly:$FeCl_3$ should be interpreted as a combined result of xylan removal, partial delignification, surface disruption, apparent cellulose deordering, and improved cellulose accessibility.

The different behavior between the two DES systems shows that enzymatic digestibility was controlled by multiple structural and compositional factors rather than by CHF or CDF alone. In ChCl:LA, the stronger CDF–hydrolysis relationship suggests that lignin removal played a major role in improving saccharification by reducing physical shielding and non-productive enzyme adsorption. Similar effects of lignin removal on improved enzymatic digestibility have been reported in previous lignocellulosic pretreatment studies [7,96,98]. In ChCl:Gly:

$FeCl_3$, the high final hydrolysis yield was mainly associated with stronger hydrolytic severity, extensive hemicellulose removal, surface disruption, and increased cellulose accessibility, although delignification still contributed to the overall improvement. These results agree with previous reports showing that enzymatic hydrolysis increases after pretreatment because enhances cellulose exposure, lignin removal reduces physical shielding and non-productive adsorption, and structural disruption increases enzyme-accessible surface area [81,82,99].

Overall, DES pretreatment significantly improved the enzymatic hydrolysis of OPEFB. ChCl:LA increased the hydrolysis yield up to 75.8%, while ChCl:Gly:$FeCl_3$ achieved a higher maximum yield of 93.8%. The results confirm that modified severity factors can be used to describe saccharification performance, but they should be interpreted together with compositional and structural changes. CHF mainly reflects the contribution of xylan hydrolysis to cellulose accessibility, whereas CDF reflects the contribution of lignin removal to reducing biomass recalcitrance, consistent with previous severity-based interpretations of enzymatic digestibility [55,58,63]. Therefore, the highest enzymatic hydrolysis yield was obtained when hemicellulose and lignin barriers were sufficiently disrupted, the cell-wall structure was opened, and the cellulose-rich solid became more accessible to cellulase.

The enzyme loading used in this study should also be considered when interpreting the saccharification results. A cellulase dosage of 20 FPU/g dry substrate was selected to evaluate the digestibility potential of raw and DES-pretreated OPEFB under enzyme-sufficient conditions, rather than to optimize enzyme economy. Reported cellulase loadings in lignocellulosic hydrolysis studies vary widely depending on biomass type, pretreatment method, enzyme formulation, substrate loading, and the denominator used for enzyme dosage. Low cellulase loadings of approximately 2–5 FPU/g have been reported in some optimized or assisted hydrolysis systems [100,101], whereas broader optimization studies have evaluated higher loadings extending to 40 FPU/g or above [102–104]. Intermediate loadings around 15–30 FPU/g are also frequently used in laboratory-scale lignocellulosic hydrolysis studies, including dry-matter- or substrate-based enzyme dosage [105–108]. Therefore, the 20 FPU/g dry substrate used in this work is within the commonly reported laboratory-scale range for evaluating biomass digestibility.

Nevertheless, enzyme-loading bases reported in the literature are not always directly interchangeable. Some studies express cellulase loading as FPU/g dry matter or FPU/g substrate, whereas others use FPU/g glucan or FPU/g cellulose [101–103]. These bases can lead to different apparent enzyme dosages because they depend on the cellulose or glucan content of the substrate. Therefore, the enzyme loading in the present study should be interpreted specifically as a dry-substrate-based comparative condition. Under this enzyme-sufficient condition, differences in hydrolysis yield mainly reflect pretreatment-induced changes in substrate accessibility, including hemicellulose removal, delignification, surface disruption, cellulose exposure, and reduced biomass recalcitrance. Thus, the high hydrolysis yield obtained for ChCl:Gly:$FeCl_3$--pretreated OPEFB indicates that this pretreatment produced a highly digestible cellulose-rich solid.

From a practical perspective, however, the enzyme dosage used here should not be regarded as an optimized industrial dosage. Enzyme loading is an important contributor to the operating cost of lignocellulosic sugar production, and enzyme-reduction strategies such as enzyme recycling, high-solids hydrolysis, optimized enzyme cocktails, and process additives have been widely explored to improve process feasibility [100,104,109]. Therefore, future work should evaluate lower cellulase dosages, enzyme recycling, higher-solid hydrolysis, and enzyme–substrate interactions after DES pretreatment to determine the minimum enzyme requirement for economically favorable glucose production.

The stability of cellulase during the 72 h hydrolysis period should also be considered when interpreting the saccharification data. The hydrolysis condition used in this study, 50 °C and pH 4.8 for 72 h, is commonly applied in laboratory-scale lignocellulosic hydrolysis studies, including studies using pretreated lignocellulosic biomass and empty fruit bunch substrates (Yang et al., 2017; Luo et al., 2019; Fabbrizi et al., 2022). Nevertheless, cellulase is a protein catalyst, and partial activity loss may occur during prolonged incubation because of thermal denaturation, product inhibition, non-productive adsorption on residual lignin, and enzyme binding to insoluble biomass solids ([104]; Chen et al., 2016; Santos et al., 2026). Therefore, the 72-h hydrolysis yield should be interpreted as a standardized endpoint digestibility measurement rather than a direct measurement of intrinsic cellulase stability.

In the present work, all raw and DES-pretreated OPEFB samples were hydrolyzed under identical enzyme loading, temperature, pH, agitation, and incubation time. Therefore, any gradual enzyme deactivation would be expected to affect all treatments under the same experimental protocol, allowing the hydrolysis results to remain valid for comparative evaluation among pretreatment conditions. The relatively lower R^2 values observed in some severity–hydrolysis correlations, especially for ChCl:Gly:$FeCl_3$, should not be attributed solely to cellulase instability. They may also reflect the heterogeneous nature of pretreated OPEFB, differences in residual lignin, non-productive enzyme adsorption, cellulose accessibility, surface morphology, crystallinity, and the nonlinear relationship between severity descriptors and enzymatic digestibility [37,55,63]. However, the possible contribution of enzyme deactivation during prolonged hydrolysis is now acknowledged as a limitation. Future work should include time-course hydrolysis analysis, residual cellulase activity measurement, protein adsorption analysis, glucose and cellobiose monitoring, and enzyme-recycling or enzyme-stability evaluation to better separate substrate accessibility effects from enzyme deactivation effects.

3.5. Recovered lignin characterization and fabrication of CMC-lignin film

3.5.1. Recovered lignin characterization

The recovered DES lignins were further characterized to evaluate their suitability as functional additives for CMC-based composite films. As shown in Table 2, both DES systems produced lignin with high purity, reaching 91.7% for ChCl:LA lignin and 93.1% for ChCl:Gly:$FeCl_3$ lignin. These values indicate that the DES pretreatment not only promoted lignin solubilization from OPEFB but also enabled the recovery of lignin with relatively low carbohydrate contamination. High lignin purity is important for film applications because residual polysaccharides and inorganic impurities may reduce compatibility with the polymer matrix and weaken the contribution of lignin to hydrophobicity, mechanical reinforcement, and antioxidant functionality. Similar observations have been reported for DES-extracted lignins, where high purity, lower molecular weight, and more homogeneous structure improved compatibility with CMC and enhanced the physicochemical performance of CMC–lignin films [47].

The molecular weight distribution of the recovered lignin also differed between the two DES systems. ChCl:LA lignin showed higher Mn and Mw values of 1998 and 2541 g/mol, respectively, with a dispersity of 1.591. In contrast, ChCl:Gly:$FeCl_3$ lignin exhibited lower Mn and Mw values of 1344 and 2139 g/mol, respectively, with a narrower dispersity of 1.272. The lower molecular weight and narrower distribution of ChCl:Gly:$FeCl_3$ lignin suggest that the Lewis-acid-assisted DES system promoted more extensive lignin depolymerization or selective solubilization of lower-molecular-weight lignin fragments. This behavior may be associated with the catalytic role of Fe^{3+} in cleaving ether linkages and disrupting lignin–carbohydrate interactions during

Table 2
Molecular weight and purity of recovered DES lignin.

DES Lignin	Purity	Mn	Mw	Mw/Mn
ChCl:LA	91.7%	1998	2541	1.591
ChCl:Gly:$FeCl_3$	93.1%	1344	2139	1.272

pretreatment [33]. Lower-molecular-weight lignin can be beneficial for film formation because it may disperse more easily in the CMC matrix and form more uniform intermolecular interactions. However, excessive depolymerization may also increase the amount of phenolic hydroxyl groups and polar functionalities, which can influence surface wettability and water vapor transport [40,45].

The FTIR spectra of the recovered lignins are presented in Fig. S4. Both ChCl:LA and ChCl:Gly:$FeCl_3$ lignins exhibited typical lignin absorption bands, confirming that the recovered fractions retained the main aromatic lignin structure. The broad band at around 3200–3400 cm^{-1} corresponds to O–H stretching vibrations from phenolic and aliphatic hydroxyl groups, while the bands near 2920 cm^{-1} are associated with C–H stretching of methyl and methylene groups [110]. The characteristic aromatic skeletal vibrations of lignin were observed around 1600, 1510, and 1420 cm^{-1}, indicating the preservation of the aromatic backbone after DES pretreatment [111]. In addition, bands in the region of 1260–1210 cm^{-1} and 1120–1030 cm^{-1} can be assigned to guaiacyl/syringyl-related C–O vibrations and ether linkages, suggesting the presence of typical lignin units in both recovered samples [50]. These results support the successful isolation of lignin from the DES filtrate and are consistent with the high lignin purity values obtained from compositional analysis. The presence of hydroxyl- and aromatic-related bands is also important for the subsequent CMC–lignin film application, because phenolic hydroxyl groups contribute to antioxidant activity, while the aromatic structure of lignin contributes to hydrophobicity, UV-absorbing capability, and barrier performance [40,47]. Similar FTIR features have been reported for DES lignin incorporated into CMC films, where preserved aromatic and hydroxyl functionalities contributed to improved physicochemical and antioxidant properties of the resulting films [46,47].

The structural features of the recovered DES lignins were further evaluated by 2D-HSQC NMR, as shown in Fig. S5, and the semi-quantitative structural indicators are summarized in Table S1. In the aromatic region, signals at approximately δ_C/δ_H 103–106/6.4–6.8 ppm were assigned to syringyl $S_{2,6}$ correlations, signals around 110–120/6.7–7.3 ppm were assigned to guaiacyl aromatic correlations, and signals near 127–132/7.2–7.8 ppm were assigned cautiously to H-type or p-coumarate-related aromatic structures because this region may overlap with other phenolic aromatic signals in grass-type lignins [47,112–114]. Semi-quantitative integration showed that both recovered lignins were S-rich. ChCl:LA lignin showed 45.9% S, 23.2% G, and 30.9% H/p-coumarate-related units, with an S/G ratio of 1.98, whereas ChCl:Gly:$FeCl_3$ lignin showed 53.4% S, 24.4% G, and 22.2% H/p-coumarate-related units, with an S/G ratio of 2.19. These aromatic correlations indicate that both DES systems recovered lignin fractions that still retained the main aromatic lignin framework.

The side-chain region provides clearer evidence for the difference between preserved structure and depolymerization. ChCl:LA lignin showed a higher β-O-4-related signal, estimated at 22.9 per 100 aromatic units, compared with 16.7 per 100 aromatic units for ChCl:Gly:$FeCl_3$ lignin. Because β-O-4 aryl ether linkages are major native lignin interunit linkages, their higher relative abundance in ChCl:LA lignin suggests that the Brønsted-acidic ChCl:LA system solubilized lignin while preserving more of the native-like side-chain framework. In contrast, the lower β-O-4-related signal in ChCl:Gly:$FeCl_3$ lignin indicates stronger cleavage of aryl ether-type linkages, supporting lignin depolymerization under Fe^{3+}-assisted Lewis acidic conditions. This interpretation is consistent with previous studies showing that $FeCl_3$ and other metal chloride-assisted systems can promote lignocellulose deconstruction, oxygen-containing bond cleavage, and lignin structural modification [29,32,34,70]. The β–5-related and β–β/overlapped oxygenated linkage regions were also estimated, but these values were interpreted cautiously because technical lignins often show weak or overlapping contours in the side-chain region ([47,112].

This structural difference is consistent with the GPC/SEC results, where ChCl:Gly:$FeCl_3$ lignin exhibited lower molecular weight and narrower dispersity than ChCl:LA lignin. The lower molecular weight of ChCl:Gly:$FeCl_3$ lignin suggests that $FeCl_3$-assisted DES pretreatment promoted more extensive lignin fragmentation. Such depolymerization can increase the accessibility of phenolic hydroxyl groups, explaining the stronger antioxidant activity of the CMC–ChCl:Gly:$FeCl_3$ lignin film, as reflected by its lower IC_{50} value[46,47]. Meanwhile, the relatively more preserved aromatic framework and higher molecular weight of ChCl:LA lignin may contribute to better hydrophobicity and moisture-barrier behavior, as shown by its higher water contact angle and lower WVTR. Therefore, Fig. S5 supports the conclusion that the pretreatment chemistry controlled not only lignin extraction but also the downstream functional performance of the recovered lignin in CMC-based packaging films.

3.5.2. Characterization of CMC-Lignin film

FTIR spectra of the CMC–DES lignin films is shown in Fig. 5. The spectra confirmed the successful incorporation of recovered lignin into the CMC matrix. The broad absorption band around 3200–3400 cm^{-1} can be assigned to O–H stretching vibrations from hydroxyl groups in CMC, glycerol, and lignin. The bands near 2920 cm^{-1} are associated with C–H stretching of aliphatic groups, while the absorption bands around 1590–1600 cm^{-1} and 1410–1420 cm^{-1} are related to carboxylate groups of CMC and aromatic skeletal vibrations of lignin. The presence of lignin-related bands in the composite films indicates that the recovered DES lignin was successfully incorporated into the CMC network. In addition, possible shifts or intensity changes in the O–H and carboxylate regions suggest intermolecular hydrogen bonding between hydroxyl groups of CMC and phenolic/aliphatic hydroxyl groups of lignin. Such interactions are important because they can improve matrix cohesion, reduce free volume, and contribute to the enhanced mechanical and barrier properties of the films. Previous studies on CMC–DES lignin films similarly attributed improved film performance to the compatibility and intermolecular interactions between DES lignin and CMC [46,47].

The antioxidant, physical, and mechanical properties of CMC-DES lignin films were summarized In Table 3. The incorporation of DES lignin improved the antioxidant activity of the CMC films, as indicated by the decrease in IC_{50} values from 50.3 g/mL for neat CMC to 20.8 g/mL for CMC–ChCl:LA lignin and 12.6 g/mL for CMC–ChCl:Gly:$FeCl_3$ lignin. Since a lower IC_{50} value indicates stronger radical scavenging ability, the ChCl:Gly:$FeCl_3$ lignin film showed the highest antioxidant performance among the tested films. This enhancement can be attributed to the aromatic and phenolic structures of lignin, which can donate hydrogen atoms or electrons to neutralize free radicals [40,45]. The

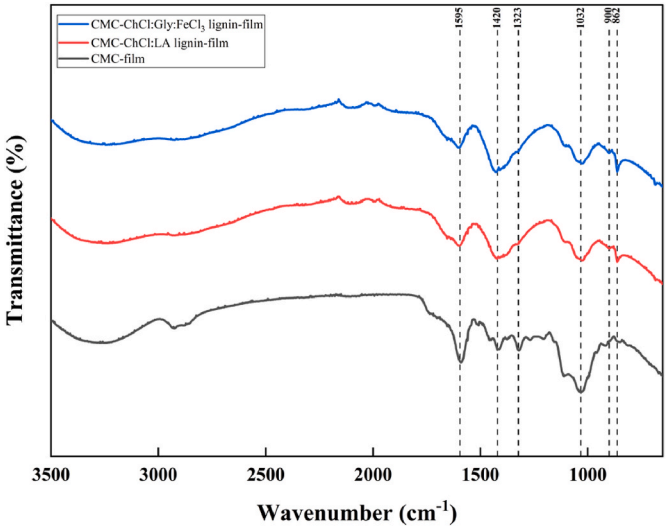

Fig. 5. FTIR Spectra of CMC-lignin film.

Table 3
Antioxidant, physical, and mechanical properties of CMC-DES lignin films.

CMC-lignin film	Antioxidant (IC_{50}) (μg/mL)	Water contact angle (°)	WVTR (g/m^{2}h)	Thickness (mm)	Tensile strength (MPa)	Elongation at break (%)
CMC	50.3	68.5 ± 0.3	19.95 ± 0.74	0.1	8.05	39
CMC-ChCl-LA lignin	20.8	70.7 ± 0.2	13.94 ± 0.16	0.12	12.13	21.83
CMC-ChCl-Gly-$FeCl_3$	12.6	65.8 ± 0.7	15.84 ± 0.72	0.13	13.08	20.67

stronger antioxidant activity of the ChCl:Gly:$FeCl_3$ lignin film may be related to its lower molecular weight and higher purity, which could increase the accessibility of phenolic hydroxyl groups within the film matrix. This interpretation agrees with previous reports showing that lignin-containing films exhibit improved antioxidant activity due to phenolic hydroxyl groups from syringyl, guaiacyl, and p-hydroxyphenyl units ([115]; [41]). In food packaging applications, this antioxidant function is valuable because it may help reduce oxidative deterioration, lipid oxidation, and quality loss during storage.

The surface wettability of the films was also affected by lignin incorporation. The neat CMC film showed a water contact angle of 68.5°, confirming its hydrophilic nature. After lignin addition, the contact angle increased slightly to 70.7° for CMC–ChCl:LA lignin, indicating improved surface hydrophobicity. This increase can be attributed to the aromatic and hydrophobic domains of lignin, which reduce the exposure of hydrophilic CMC groups at the film surface. In contrast, the CMC–ChCl:Gly:$FeCl_3$ lignin film showed a lower contact angle of 65.8°, despite having higher purity and stronger antioxidant activity. This result suggests that the ChCl:Gly:$FeCl_3$ lignin may contain a greater proportion of accessible polar groups, particularly phenolic hydroxyl groups generated through lignin depolymerization [47]. Therefore, while lignin generally contributes hydrophobic aromatic domains, the final wettability of the composite film depends on the balance between hydrophobic aromatic structures and exposed polar functionalities. A similar trend has been reported in lignin-based films, where the incorporation of lignin can increase hydrophobicity, but the extent depends strongly on lignin structure, purity, molecular weight, and phenolic hydroxyl content (Syahidah et al., 2025).

The WVTR results further demonstrate the role of DES lignin in improving the moisture barrier properties of CMC films. The neat CMC film showed the highest WVTR of 19.95 g/m^{2}h, reflecting the water-sensitive nature of the CMC matrix. Incorporation of ChCl:LA lignin reduced the WVTR to 13.94 g/m^{2}h, while ChCl:Gly:$FeCl_3$ lignin reduced it to 15.84 g/m^{2}h. These reductions indicate that recovered DES lignin can hinder water vapor diffusion through the CMC film. The improved barrier performance can be explained by two complementary mechanisms. First, the hydrophobic aromatic structure of lignin can decrease water affinity within the film matrix. Second, lignin particles or domains can create a more tortuous diffusion pathway, thereby slowing water vapor transport across the film [46,116]. The slightly better WVTR reduction observed for CMC–ChCl:LA lignin may be consistent with its higher contact angle, suggesting a more hydrophobic surface and stronger resistance to water vapor transmission. Previous studies have also shown that lignin incorporation can reduce water vapor permeability in biopolymer films by improving matrix compactness and introducing hydrophobic domains [47,117].

Mechanical testing showed that DES lignin incorporation improved the tensile strength of the CMC films. The tensile strength increased from 8.05 MPa for neat CMC to 12.13 MPa for CMC–ChCl:LA lignin and 13.08 MPa for CMC–ChCl:Gly:$FeCl_3$ lignin. This enhancement indicates that lignin acted as a reinforcing component within the CMC matrix. The improvement may result from hydrogen bonding and physical interactions between CMC chains and lignin functional groups, which strengthen the composite network and improve stress transfer during tensile loading. The slightly higher tensile strength of the ChCl:Gly:$FeCl_3$ lignin film may be associated with its lower molecular weight and narrower dispersity, which could promote more uniform dispersion and stronger interfacial interaction with CMC. However, the elongation at break decreased from 39% for neat CMC to 21.83% and 20.67% for the ChCl:LA and ChCl:Gly:$FeCl_3$ lignin films, respectively. This reduction suggests that lignin increased film rigidity and restricted CMC chain mobility (Syahidah et al., 2025)[118,119]. Therefore, DES lignin improved strength but reduced flexibility, reflecting a typical reinforcement effect in biopolymer composite films.

Overall, the recovered DES lignins from OPEFB demonstrated strong potential as functional additives for CMC-based films. Both lignins improved antioxidant activity, reduced WVTR, and increased tensile strength compared with neat CMC. ChCl:LA lignin gave better surface hydrophobicity and moisture barrier performance, while ChCl:Gly:$FeCl_3$ lignin provided stronger antioxidant activity and higher tensile strength. These differences indicate that the pretreatment chemistry not only affects lignin recovery and enzymatic glucose production but also determines the downstream functionality of recovered lignin in packaging materials. Thus, the DES fractionation strategy developed in this work supports an integrated OPEFB biorefinery concept, in which the cellulose-rich solid fraction is converted into glucose and the recovered lignin is valorized as an active reinforcing component for biodegradable CMC-based packaging films.

3.6. Process mass balance analysis of DES-enzymatic hydrolysis process

Process mass balance analysis was conducted to evaluate the integrated performance of DES pretreatment and enzymatic hydrolysis on the basis of 100 g raw OPEFB. While the previous sections separately discussed fractionation behavior, structural modification, enzymatic digestibility, and lignin-based film performance, the mass balance provides a more practical assessment of how effectively the initial biomass was converted into two major product streams: glucose from the cellulose-rich solid and recovered lignin from the DES liquor. This evaluation is important because a pretreatment condition with high enzymatic hydrolysis yield does not necessarily provide the highest overall glucose recovery on a raw biomass basis, particularly if excessive solid loss or cellulose degradation occurs during pretreatment. Similarly, high delignification is only beneficial for lignin valorization when the solubilized lignin can be effectively recovered.

The glucose and lignin yields obtained from the ChCl:LA and ChCl:Gly:$FeCl_3$ systems are shown in Fig. 6. In the ChCl:LA system, increasing pretreatment severity generally improved both enzymatic glucose production and lignin recovery. The best-performing ChCl:LA condition within the investigated range was 140 °C for 6 h, producing approximately 21.6 g glucose and 24.7 g recovered lignin per 100 g raw OPEFB. This result is consistent with the fractionation behavior discussed in Section 3.2, where ChCl:LA promoted strong delignification, high lignin yield, and cellulose enrichment at higher severity. Although the enzymatic hydrolysis yield of ChCl:LA-pretreated solid was lower than that of the ChCl:Gly:$FeCl_3$ system, its higher lignin recovery demonstrates the advantage of ChCl:LA when lignin valorization is considered as an important output of the process. In contrast, the ChCl:Gly:$FeCl_3$ system produced slightly higher glucose recovery, reaching approximately 21.7 g glucose per 100 g raw OPEFB, while the recovered lignin yield was approximately 23.1 g per 100 g raw OPEFB. The higher glucose production agrees with the stronger enzymatic hydrolysis performance observed in Section 3.4, where ChCl:Gly:$FeCl_3$-pretreated OPEFB achieved the highest enzymatic hydrolysis yield. This behavior can be

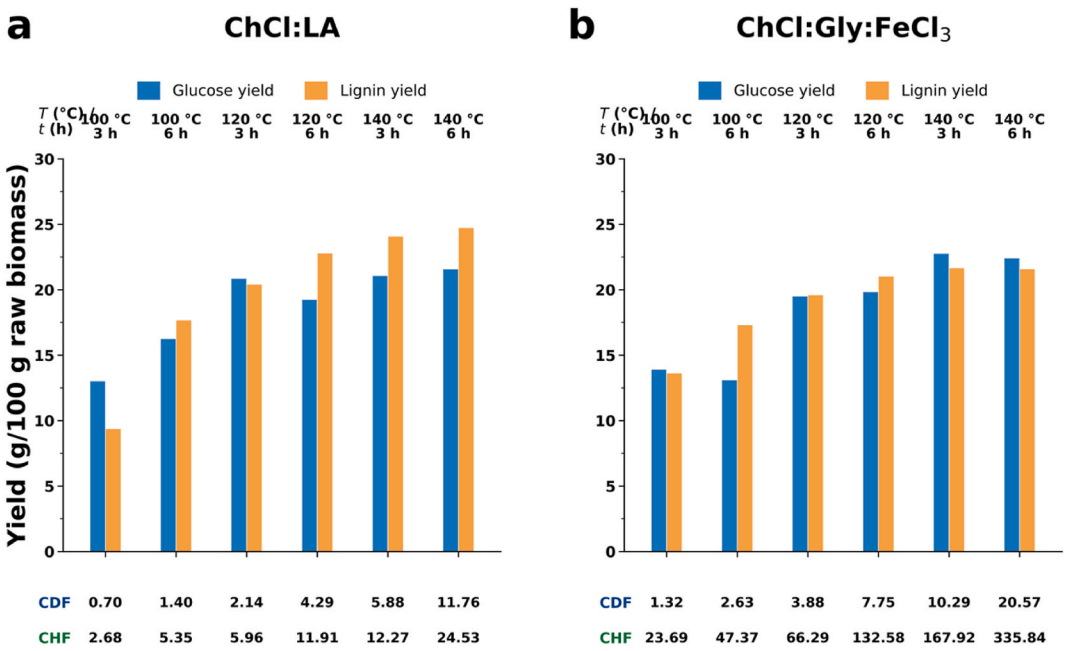

Fig. 6. Glucose and lignin yield on a 100 g raw OPEFB basis (a) ChCl:LA system + Enzymatic hydrolysis & (b) ChCl:Gly:$FeCl_3$+enzymatic hydrolysis.

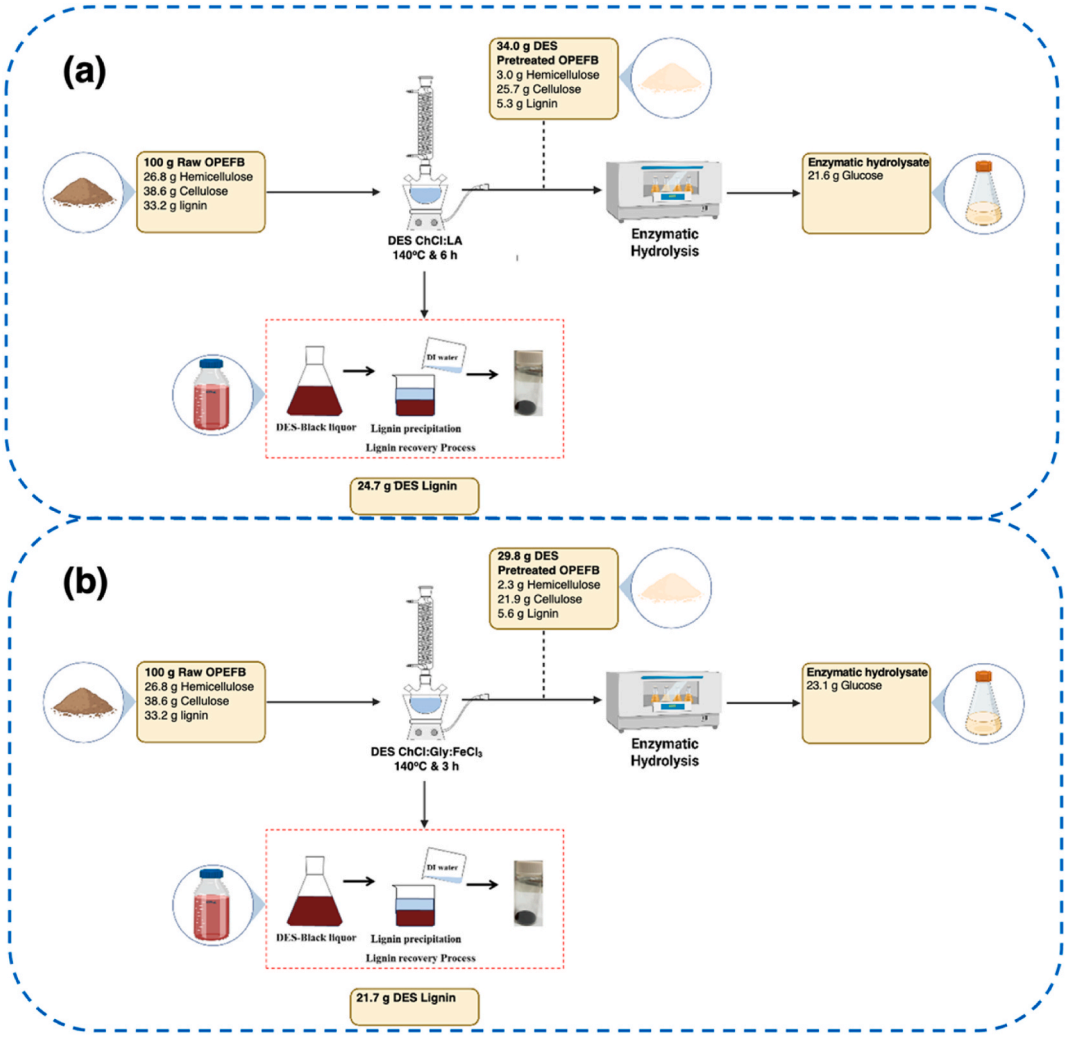

Fig. 7. Process mass balances of highest total glucose and lignin in (a) ChCl:LA DES and (b) ChCl:Gly:$FeCl_3$ DES with basis 100 g raw OPEFB.

attributed to the strong hydrolytic effect of Fe^{3+}, which promoted extensive hemicellulose removal and improved cellulose accessibility [33,95]. However, the lignin yield was slightly lower than that obtained using ChCl:LA, confirming that the $FeCl_3$-containing DES was more favorable for carbohydrate accessibility than for maximizing lignin recovery.

It should also be noted that the glucose recoveries reported in this mass balance were calculated from the standardized 72 h enzymatic hydrolysis endpoint used for all samples. Therefore, these values are suitable for comparing the relative digestibility of the two DES-pretreated solids under identical hydrolysis conditions, although future time-course and residual-enzyme-activity analyses would be needed to evaluate the contribution of enzyme stability to absolute glucose yield.

The detailed process mass balances for the best-performing conditions of both DES systems are presented in Fig. 7. This analysis further confirms that evaluating pretreatment performance only from enzymatic hydrolysis yield may be misleading, because the final glucose recovery also depends on solid recovery, cellulose preservation, and the amount of cellulose remaining in the pretreated solid. For ChCl:LA pretreatment, the highest integrated product recovery was obtained at 140 °C for 6 h. Under this condition, the process generated 21.6 g glucose and 24.7 g recovered lignin from 100 g raw OPEFB. This result indicates that ChCl:LA provided a balanced fractionation route, where a substantial portion of lignin was solubilized and recovered while the cellulose-rich residue remained sufficiently digestible for glucose production. The higher recovered lignin mass agrees with the stronger delignification and lignin yield discussed in Section 3.2, confirming the suitability of ChCl:LA for lignin-oriented OPEFB fractionation. For ChCl:Gly:$FeCl_3$, the best-performing mass balance within the investigated range was obtained at 140 °C for 3 h, producing 21.7 g glucose and 23.1 g recovered lignin per 100 g raw OPEFB. Although this DES system achieved the highest enzymatic hydrolysis yield, the raw-biomass-based glucose recovery was only slightly higher than that of ChCl:LA. This indicates that the strong hydrolytic action of Fe^{3+} improved cellulose accessibility, but the overall glucose recovery was also constrained by the amount of cellulose retained in the solid fraction after pretreatment [33,70]. Therefore, the mass balance highlights an important distinction between enzymatic digestibility and overall glucose recovery. A highly digestible solid does not necessarily give proportionally higher glucose production if pretreatment also causes greater solid loss or partial carbohydrate degradation.

Comparison of the two mass balances shows that both DES systems converted OPEFB into similar amounts of glucose, but through different mechanistic routes. ChCl:LA produced slightly lower glucose but higher recovered lignin, whereas ChCl:Gly:$FeCl_3$ produced slightly higher glucose but lower recovered lignin. This difference should not be attributed to a single factor such as delignification, hemicellulose removal, or crystallinity alone. Instead, glucose recovery on a raw-biomass basis depends on the combined effects of solid recovery, cellulose preservation, cellulose enrichment, hemicellulose removal, lignin removal, cellulose accessibility, and enzymatic hydrolysis efficiency. In the ChCl:Gly:$FeCl_3$ system, strong Lewis-acid-assisted hemicellulose removal, surface disruption, and partial reduction in apparent CrI produced a highly digestible cellulose-rich solid, consistent with the highest enzymatic hydrolysis yield. Similar effects of $FeCl_3$ or metal chloride-assisted pretreatment on xylan disruption and enzymatic digestibility have been reported previously [30,33,95]. However, its glucose recovery on a 100 g raw OPEFB basis was only slightly higher than that of ChCl:LA because total glucose production was also constrained by the amount of cellulose retained after pretreatment. In contrast, ChCl:LA provided a more balanced fractionation route, combining strong delignification, high lignin recovery, cellulose enrichment, and sufficient cellulose preservation. Therefore, the mass balance highlights the distinction between digestibility of the recovered solid and total glucose recovery from the initial biomass.

As shown in Table 4, previous OPEFB pretreatment studies achieved different balances between enzymatic sugar production and lignin recovery. The peracetic acid–sulfuric acid pretreatment produced a higher recalculated enzymatic glucose yield than the present DES systems, indicating its strong effectiveness in improving cellulose digestibility. However, lignin was not recovered as an isolated product stream in that process; therefore, its contribution was mainly sugar-oriented [42]. Similarly, the ionosolv pretreatment using [DMBA][HSO_4] generated relatively high glucose release and recovered lignin, but the estimated recovered lignin yield was substantially lower than that obtained in the present DES systems [44]. In the sequential hydrothermal–organosolv process, both lignin and reducing sugar were recovered, but the lignin yield and enzymatic sugar recovery on a raw OPEFB basis were lower than those obtained in the present DES-based process [65].

In comparison, the present ChCl:LA and ChCl:Gly:$FeCl_3$ pretreatments produced similar glucose recovery, 21.6 and 21.7 g/100 g raw OPEFB, respectively, while also recovering 24.7 and 23.1 g lignin/100 g raw OPEFB. Although the glucose recovery was lower than that reported for peracetic acid–sulfuric acid pretreatment, the present process provided a more balanced product distribution because both the carbohydrate and lignin fractions were recovered as useable streams. This distinction is important for biorefinery development, where the economic and environmental value of pretreatment depends not only on sugar production but also on the valorization of lignin as a co-product [109].

Although the present DES pretreatment demonstrated effective OPEFB fractionation and dual recovery of glucose and lignin, DES loading and solvent recyclability remain important considerations for scale-up. In this study, the OPEFB-to-DES ratio was fixed at 1:15 (w/w), which was selected as a laboratory-scale comparative condition to ensure sufficient wetting, mixing, heat transfer, and contact between biomass and the DES phase. Relatively high solvent loading is frequently applied in laboratory-scale DES pretreatment to reduce mass-transfer limitations and provide sufficient solvent capacity for lignin solubilization and lignocellulose deconstruction [32,49,51,114]. However, direct translation of this solvent loading to industrial scale may increase solvent inventory, reactor volume, heating requirement, downstream separation load, and overall operating cost. Previous techno-economic and process-design studies have emphasized that solvent recovery efficiency, solvent-to-biomass ratio, energy demand, and recycling stability are key

Table 4
Previous fractionation study of OPEFB.

Process	Conditions	Recovered Lignin (per 100 g raw OPEFB)	EH Glucose (per 100 g raw OPEFB)	References
Ionosolv pretreatment coupled EH	[DMBA][HSO_4]: H_2O = 80:20 wt%, biomass/solvent ratio 1:10, 170 °C, 1 h & EH	8	25	[44]
PA– H_2SO_4 pretreatment coupled EH	PA 200 mM, H_2SO_4 100 mM, 140 °C, 5 min	-	28.4	[42]
Sequential HT &H_2SO_4 -organosolv pretreatment	HT: 180 °C, 30 min, 10 mM H_2SO_4, Organosolv: EtOh 80%, 185 °C,	9.1	12.6	[65]
DES pretreatment & EH	ChCl:LA (1:2) 140 °C & 6 h	24.7	21.6	This study
DES pretreatment & EH	ChCl:Gly:$FeCl_3$ 140 °C & 3 h	23.1	21.7	This study

HT: hydrothermal; DES: deep eutectic solvent; DMBA: N,N,N-dimethylbutylamine; EH: enzymatic hydrolysis; PA: paracetic acid.

determinants of the feasibility of DES-based lignocellulose pretreatment [19,120,121]. Therefore, the 1:15 ratio used in this work should be interpreted as a laboratory-scale solvent loading rather than an optimized industrial solvent-to-biomass ratio.

DES recovery is also a critical factor because lignin regeneration was performed by adding water to the DES filtrate. Water addition reduces DES solvent strength and promotes lignin precipitation, but it also dilutes the DES phase and creates an additional requirement for water removal before solvent reuse [29,49,51]. In our previous study on coconut husk fractionation using hydrothermal and ChCl:LA DES pretreatment, DES recycling was performed after lignin recovery by removing ethanol and water through rotary evaporation at approximately 50 °C, and the recovered DES was directly reused in subsequent pretreatment cycles without additional purification. The recycled DES remained effective over multiple cycles, but its performance gradually decreased. Hemicellulose removal declined from 79.96% in the first cycle to 68.0% in the fourth cycle, lignin removal decreased from 64.18% to 49.7%, and lignin yield decreased from 50.2% to 37.4% [49]. Similar decreases in recycled DES performance have been associated with solvent dilution, reduced acidity, impurity accumulation, and saturation by solubilized lignocellulosic fragments [29,32]. This decline may reduce the ability of recycled DES to disrupt lignin–carbohydrate complexes and maintain consistent lignin solubilization across repeated cycles.

These findings indicate that DES recycling is feasible but requires further optimization to maintain pretreatment efficiency across repeated cycles. For the present OPEFB system, the current study should therefore be regarded as a laboratory-scale proof of concept rather than an industrially optimized process. Future work should evaluate lower DES-to-biomass ratios, high-solids pretreatment, DES recycling over multiple cycles, solvent make-up requirements, impurity accumulation, ethanol and water recovery, and the energy demand for DES reconcentration [19,121,122]. These evaluations are necessary to improve the economic and practical feasibility of DES-based lignocellulose fractionation.

Beyond solvent loading and recyclability, the practical comparison between ChCl:LA and ChCl:Gly:$FeCl_3$ should also consider residence time, solvent formulation, catalyst requirement, apparent activation energy, solvent recovery, and process-energy implications, because these parameters strongly influence the economic feasibility of DES-based lignocellulose pretreatment [19,120–122]. Based on the fitted CDF and CHF models, ChCl:Gly:$FeCl_3$ showed higher apparent activation energies than ChCl:LA for both lignin removal and xylan hydrolysis. The apparent activation energy for lignin removal was 87.84 kJ/mol in ChCl:Gly:$FeCl_3$ and 63.47 kJ/mol in ChCl:LA, while that for xylan hydrolysis was 69.87 kJ/mol in ChCl:Gly:$FeCl_3$ and 49.54 kJ/mol in ChCl:LA. These values indicate that fractionation in the $FeCl_3$-containing DES was more temperature-sensitive, which is consistent with the broader CDF and CHF ranges observed for ChCl:Gly:$FeCl_3$. In contrast, the lower apparent activation energies of ChCl:LA suggest that lignin solubilization and xylan removal can proceed more readily within a narrower Brønsted-acidic severity window.

The best-performing conditions for both DES systems used the same pretreatment temperature of 140 °C, but different residence times. ChCl:LA required 6 h and produced 21.6 g glucose and 24.7 g recovered lignin per 100 g raw OPEFB, whereas ChCl:Gly:$FeCl_3$ required only 3 h and produced 21.7 g glucose and 23.1 g recovered lignin per 100 g raw OPEFB. Therefore, although ChCl:Gly:$FeCl_3$ had higher apparent activation energies, its Lewis-acid-assisted catalytic effect allowed comparable glucose recovery at a shorter holding time. This may offer an advantage in terms of reducing the energy associated with maintaining the reactor at the target temperature. However, apparent activation energy should not be directly equated with total process-energy consumption. Total process energy also depends on DES heat capacity, viscosity, mixing requirement, solvent-to-biomass ratio, heat recovery, ethanol and water removal, DES reconcentration, solvent loss, and solvent reuse efficiency [19,49,122].

In addition, the incorporation of $FeCl_3$ introduces additional process considerations, including catalyst cost, salt recovery, possible corrosion control, impurity accumulation during recycling, and potential effects of residual metal species on downstream lignin and hydrolysate applications. Although Lewis-acid-mediated DES systems can intensify lignocellulose fractionation by promoting hemicellulose disruption, lignin cleavage, and cellulose accessibility, metal chloride addition may also increase process complexity through catalyst handling and recovery requirements [29,30,34,50,70]. Therefore, ChCl:LA may be more attractive when simpler solvent formulation and lignin recovery are prioritized, whereas ChCl:Gly:$FeCl_3$ may be more suitable when shorter pretreatment time and enzymatic glucose production are emphasized [19,120]. Nevertheless, this comparison should be regarded as a preliminary feasibility interpretation rather than a complete techno-economic or energy analysis. A rigorous comparison would require quantitative data on solvent cost, DES heat capacity, viscosity, heating duty, evaporation duty, solvent loss, catalyst make-up, DES recycling stability, equipment compatibility, corrosion risk, wastewater generation, and product purification requirements [19,70,120].

Considering these process-level trade-offs, ChCl:LA showed a stronger advantage for lignin-oriented fractionation because it produced the highest recovered lignin yield, used a simpler Brønsted-acidic DES formulation, and later gave better moisture-barrier performance in the CMC–lignin film. Conversely, ChCl:Gly:$FeCl_3$ gave slightly higher glucose recovery and produced lignin that contributed stronger antioxidant activity and tensile reinforcement. Therefore, the present DES pretreatment route is not merely a saccharification-enhancement strategy, but a dual-product OPEFB valorization approach in which the cellulose-rich fraction is converted into glucose and the recovered lignin is further upgraded into functional CMC-based packaging material.

4. Conclusions

This study demonstrated an integrated OPEFB valorization strategy through DES pretreatment, enzymatic glucose production, lignin recovery, and CMC–lignin composite film development. The two DES systems exhibited distinct fractionation behaviors: ChCl:LA promoted stronger lignin solubilization and higher lignin recovery, whereas ChCl:Gly:$FeCl_3$ enhanced hemicellulose removal and enzymatic hydrolysis through Lewis acid-assisted deconstruction. The CDF and CHF models successfully described the severity-dependent delignification and xylan hydrolysis behavior, confirming that pretreatment performance was governed by the combined effects of temperature, residence time, and the acidic or catalytic nature of the DES. On a 100 g raw OPEFB basis, ChCl:LA pretreatment at 140 °C for 6 h produced 21.6 g glucose and 24.7 g recovered lignin, while ChCl:Gly:$FeCl_3$ pretreatment at 140 °C for 3 h produced 21.7 g glucose and 23.1 g recovered lignin. The recovered DES lignins were successfully incorporated into CMC-based films, where ChCl:LA lignin provided better water resistance and moisture-barrier performance, while ChCl:Gly:$FeCl_3$ lignin contributed stronger antioxidant activity and tensile reinforcement. Overall, this work confirms that OPEFB can be converted through a multiproduct biorefinery pathway, in which the cellulose-rich fraction is utilized for glucose production and the recovered lignin is upgraded into functional biodegradable packaging films. Future studies should focus on DES recyclability, solvent recovery, techno-economic assessment, life-cycle evaluation, and scale-up validation to further assess the industrial feasibility and sustainability of this integrated process.

CRediT authorship contribution statement

Candra Wijaya: Conceptualization, Data curation, Formal analysis, Investigation, Methodology, Visualization, Writing – original draft. **Andika Prastika:** Data curation, Formal analysis, Investigation. **Olivia Izzati Atiqa:** Data curation, Formal analysis, Investigation. **Tabina**

Raissa Apol: Data curation, Formal analysis, Investigation. **Urania Noor Lintang Pertiwi:** Data curation, Formal analysis, Investigation. **Lieke Riadi:** Supervision, Writing – review & editing. **Maktum Muharja:** Methodology, Supervision, Writing – review & editing. **Arief Widjaja:** Conceptualization, Funding acquisition, Methodology, Project administration, Supervision, Writing – review & editing.

Declaration of competing interest

The authors declare that they have no known competing financial interests or personal relationships that could have appeared to influence the work reported in this paper.

Acknowledgments

This research is funded by the Indonesian Endowment Fund for Education (LPDP) under the EQUITY Program (Contract No. 4299/B3/DT.03.08/2025)

Appendix A. Supplementary data

Supplementary data to this article can be found online at https://doi.org/10.1016/j.biombioe.2026.109859.

Data availability

Data will be made available on request.

References

[1] C.P. Bosah, S. Li, G.K.M. Ampofo, I. Sangare, A continental and global assessment of the role of energy consumption, total natural resource rent, and economic growth as determinants of carbon emissions, Sci. Total Environ. 892 (2023) 164592, https://doi.org/10.1016/J.SCITOTENV.2023.164592.

[2] H. Chen, C. Sun, Y. Hu, C. Xia, F. Sun, Z. Zhang, Reaction characteristics of metal-salt coordinated deep eutectic solvents during lignocellulosic pretreatment, J. Environ. Chem. Eng. 11 (2023) 109531, https://doi.org/10.1016/J.JECE.2023.109531.

[3] R. Li, Y. Zheng, X. Zhao, Q. Yong, X. Meng, A. Ragauskas, C. Huang, Recent advances in biomass pretreatment using biphasic solvent systems, Green Chem. 25 (2023) 2505–2523, https://doi.org/10.1039/D3GC00271C.

[4] K. Mishra, S. Singh Siwal, A. Kumar Saini, V.K. Thakur, Recent update on gasification and pyrolysis processes of lignocellulosic and algal biomass for hydrogen production, Fuel 332 (2023), https://doi.org/10.1016/j.fuel.2022.126169.

[5] M. Wang, X. Fu, Y. Chang, J. Wei, H. Cui, Recent advancements in deep eutectic solvent (DES) pretreatment: applications, mechanisms, and integration with emerging technologies for biorefinery, Ind. Crops Prod. 229 (2025) 121028, https://doi.org/10.1016/j.indcrop.2025.121028.

[6] Z. Chen, Y. Wang, H. Cheng, H. Zhou, Hemicellulose degradation: an overlooked issue in acidic deep eutectic solvents pretreatment of lignocellulosic biomass, Ind. Crops Prod. 187 (2022) 115335, https://doi.org/10.1016/J.INDCROP.2022.115335.

[7] M. Li, B. Jiang, W. Wu, S. Wu, Y. Yang, J. Song, M. Ahmad, Y. Jin, Current understanding and optimization strategies for efficient lignin-enzyme interaction: a review, Int. J. Biol. Macromol. 195 (2022) 274–286, https://doi.org/10.1016/J.IJBIOMAC.2021.11.188.

[8] E.J. Panakkal, K. Cheenkachorn, S. Chuetor, P. Tantayotai, N. Raina, Y.S. Cheng, M. Sriariyanun, Optimization of deep eutectic solvent pretreatment for bioethanol production from napier grass, Sustain. Energy Technol. Assessments 54 (2022) 102856, https://doi.org/10.1016/J.SETA.2022.102856.

[9] H.A. Ruiz, M. Galbe, G. Garrote, D.M. Ramirez-Gutierrez, E. Ximenes, S.-N. Sun, D. Lachos-Perez, R.M. Rodríguez-Jasso, R.-C. Sun, B. Yang, M.R. Ladisch, Severity factor kinetic model as a strategic parameter of hydrothermal processing (steam explosion and liquid hot water) for biomass fractionation under biorefinery concept, Bioresour. Technol. 342 (2021) 125961, https://doi.org/10.1016/j.biortech.2021.125961.

[10] S. Suhartini, N.A. Rohma, E. Mardawati, Kasbawati, N. Hidayat, L. Melville, Biorefining of oil palm empty fruit bunches for bioethanol and xylitol production in Indonesia: a review, Renew. Sustain. Energy Rev. 154 (2022) 111817, https://doi.org/10.1016/j.rser.2021.111817.

[11] W. Fatriasari, W. Ulwan, T. Aminingsih, F.P. Sari, Fitria, L. Suryanegara, A. H. Iswanto, M. Ghozali, L.N. Kholida, M.H. Hussin, A. Fudholi, E. Hermiati, Optimization of maleic acid pretreatment of oil palm empty fruit bunches (OPEFB) using response surface methodology to produce reducing sugars, Ind. Crops Prod. 171 (2021), https://doi.org/10.1016/j.indcrop.2021.113971.

[12] D. Ouyang, T. Liu, A.A. Astimar, H.L.N. Lau, S.S. Teh, J. Nursyairah, D. Liu, X. Zhao, Model-based process intensification of dilute acid pre-hydrolysis of oil palm empty fruit bunch biomass for pretreatment and furfural production, Bioresour. Technol. 372 (2023), https://doi.org/10.1016/j.biortech.2023.128626.

[13] C. Wijaya, U.N.L. Pertiwi, T.R. Apol, I.P.N. Rohmah, M. Muharja, T. Widjaja, L. Riadi, A. Widjaja, Enhancing enzymatic digestibility and lignin production of oil palm empty fruit bunch (OPEFB) by green deep eutectic solvent, Bull. Chem. React. Eng. Catal. 21 (2026) 412–427, https://doi.org/10.9767/bcrec.20526.

[14] E.F. Ahmad, P. Lestari, K. Oginawati, Y. Yulizar, J. Sianturi, M.M. Munir, A. Adawiah, Soda-anthraquinone-catalyzed delignification of coconut husk waste, Bull. Chem. React. Eng. Catal. 21 (2026) 128–136, https://doi.org/10.9767/bcrec.20537.

[15] C. Huang, X. Zhao, Y. Zheng, W. Lin, C. Lai, Q. Yong, A.J. Ragauskas, X. Meng, Revealing the mechanism of surfactant-promoted enzymatic hydrolysis of dilute acid pretreated bamboo, Bioresour. Technol. 360 (2022), https://doi.org/10.1016/j.biortech.2022.127524.

[16] M.M. Kininge, P.R. Gogate, Intensification of alkaline delignification of sugarcane bagasse using ultrasound assisted approach, Ultrason. Sonochem. 82 (2022) 105870, https://doi.org/10.1016/j.ultsonch.2021.105870.

[17] A. Ovejero-Pérez, V. Rigual, J.C. Domínguez, M.V. Alonso, M. Oliet, F. Rodriguez, Organosolv and ionosolv processes for autohydrolyzed poplar fractionation: lignin recovery and characterization, Int. J. Biol. Macromol. 197 (2022) 131–140, https://doi.org/10.1016/j.ijbiomac.2021.12.079.

[18] B.B. Hansen, S. Spittle, B. Chen, D. Poe, Y. Zhang, J.M. Klein, A. Horton, L. Adhikari, T. Zelovich, B.W. Doherty, B. Gurkan, E.J. Maginn, A. Ragauskas, M. Dadmun, T.A. Zawodzinski, G.A. Baker, M.E. Tuckerman, R.F. Savinell, J. R. Sangoro, Deep eutectic solvents: a review of fundamentals and applications, Chem. Rev. 121 (2021) 1232–1285, https://doi.org/10.1021/acs.chemrev.0c00385.

[19] J. Peng, H. Xu, W. Wang, Y. Kong, Z. Su, B. Li, Techno-economic analysis of bioethanol preparation process via deep eutectic solvent pretreatment, Ind. Crops Prod. 172 (2021) 114036, https://doi.org/10.1016/J.INDCROP.2021.114036.

[20] B. Soares, A.M. da Costa Lopes, A.J.D. Silvestre, P.C. Rodrigues Pinto, C.S. R. Freire, J.A.P. Coutinho, Wood delignification with aqueous solutions of deep eutectic solvents, Ind. Crops Prod. 160 (2021), https://doi.org/10.1016/j.indcrop.2020.113128.

[21] H. Yu, Z. Xue, R. Shi, F. Zhou, T. Mu, Lignin dissolution and lignocellulose pretreatment by carboxylic acid based deep eutectic solvents, Ind. Crops Prod. 184 (2022), https://doi.org/10.1016/j.indcrop.2022.115049.

[22] X. Liang, Y. Zhu, B. Qi, S. Li, J. Luo, Y. Wan, Structure-property-performance relationships of lactic acid-based deep eutectic solvents with different hydrogen bond acceptors for corn stover pretreatment, Bioresour. Technol. 336 (2021) 125312, https://doi.org/10.1016/j.biortech.2021.125312.

[23] D. Huo, Y. Sun, Q. Yang, F. Zhang, G. Fang, H. Zhu, Y. Liu, Selective degradation of hemicellulose and lignin for improving enzymolysis efficiency via pretreatment using deep eutectic solvents, Bioresour. Technol. 376 (2023), https://doi.org/10.1016/j.biortech.2023.128937.

[24] S. Kumar, S. Sharma, S.M. Arumugam, C. Miglani, S. Elumalai, Biphasic separation approach in the DES biomass fractionation facilitates lignin recovery for subsequent valorization to phenolics, ACS Sustain. Chem. Eng. 8 (2020) 19140–19154, https://doi.org/10.1021/acssuschemeng.0c07747.

[25] H. Li, X. Li, T. You, D. Li, H. Nawaz, X. Zhang, F. Xu, Insights into alkaline choline chloride-based deep eutectic solvents pretreatment for populus deltoides: lignin structural features and modification mechanism, Int. J. Biol. Macromol. 193 (2021) 319–327, https://doi.org/10.1016/J.IJBIOMAC.2021.10.134.

[26] Q. Liu, T. Yuan, Q. Fu, jin Bai, Y. yuan, F. Peng, C. li Yao, Choline chloride-lactic acid deep eutectic solvent for delignification and nanocellulose production of moso bamboo, Cellulose 26 (2019) 9447–9462, https://doi.org/10.1007/s10570-019-02726-0.

[27] S. Hong, X.J. Shen, B. Pang, Z. Xue, X.F. Cao, J.L. Wen, Z.H. Sun, S.S. Lam, T. Q. Yuan, R.C. Sun, In-depth interpretation of the structural changes of lignin and formation of diketones during acidic deep eutectic solvent pretreatment, Green Chem. 22 (2020) 1851–1858, https://doi.org/10.1039/d0gc00006j.

[28] W.X. Li, W.Z. Xiao, Y.Q. Yang, Q. Wang, X. Chen, L.P. Xiao, R.C. Sun, Insights into bamboo delignification with acidic deep eutectic solvents pretreatment for enhanced lignin fractionation and valorization, Ind. Crops Prod. 170 (2021), https://doi.org/10.1016/j.indcrop.2021.113692.

[29] Y. Bai, X.F. Zhang, Z. Wang, T. Zheng, J. Yao, Deep eutectic solvent with bifunctional brønsted-lewis acids for highly efficient lignocellulose fractionation, Bioresour. Technol. 347 (2022), https://doi.org/10.1016/j.biortech.2022.126723.

[30] L. Chen, R. Chen, S. Fu, FeCl3 pretreatment of three lignocellulosic biomass for ethanol production, ACS Sustain. Chem. Eng. 3 (2015) 1794–1800, https://doi.org/10.1021/acssuschemeng.5b00377.

[31] S.R. Kamireddy, J. Li, M. Tucker, J. Degenstein, Y. Ji, Effects and mechanism of metal chloride salts on pretreatment and enzymatic digestibility of corn stover, Ind. Eng. Chem. Res. 52 (2013) 1775–1782, https://doi.org/10.1021/ie3019609.

[32] Z.K. Wang, S. Hong, J. long Wen, C.Y. Ma, L. Tang, H. Jiang, J.J. Chen, S. Li, X. J. Shen, T.Q. Yuan, Lewis acid-facilitated deep eutectic solvent (DES) pretreatment for producing high-purity and antioxidative lignin, ACS Sustain. Chem. Eng. 8 (2020) 1050–1057, https://doi.org/10.1021/acssuschemeng.9b05846.

[33] X. Chen, H. Yang, L. Zhang, Z. Li, Y. Xue, R. Wang, X. Fan, S. Sun, Green construction and release mechanism of lignin-based double-layer coated urea,

Biotechnol. Biofuels Bioprod. 16 (2023) 97, https://doi.org/10.1186/s13068-023-02355-7.
[34] W. Tang, X. Wu, C. Huang, Z. Ling, C. Lai, Q. Yong, Revealing the influence of metallic chlorides pretreatment on chemical structures of lignin and enzymatic hydrolysis of waste wheat straw, Bioresour. Technol. 342 (2021) 125983, https://doi.org/10.1016/J.BIORTECH.2021.125983.
[35] Q. Wei, C. Shi, D. Wang, J. Yang, Z. Shi, J.-L. Wen, H.-Y. Yang, Metal chloride mediated choline chloride-lactic acid deep eutectic solvent pretreatment of bamboo for improved cellulose saccharification and lignin recovery, Int. J. Biol. Macromol. 305 (2025) 141107, https://doi.org/10.1016/j.ijbiomac.2025.141107.
[36] A.R. Abouelela, P.Y.S. Nakasu, J.P. Hallett, Influence of pretreatment severity factor and hammett acidity on softwood fractionation by an acidic protic ionic liquid, ACS Sustain. Chem. Eng. 11 (2023) 2404–2415, https://doi.org/10.1021/acssuschemeng.2c06076.
[37] C. Wijaya, N.L. Sangadji, M. Muharja, T. Widjaja, L. Riadi, E. Elaine, R. Lau, A. Widjaja, Prediction by a modified severity factor in $FeCl_3$-catalyzed hydrothermal fractionation of coconut husk: enhancing hemicellulose hydrolysis and enzymatic digestibility of cellulose, Bioresour. Technol. Rep. (2025) 102282, https://doi.org/10.1016/j.biteb.2025.102282.
[38] A. Varilla-Mazaba, J.A. Raggazo-Sánchez, M. Calderón-Santoyo, J. Gómez-Rodríguez, M.G. Aguilar-Uscanga, Optimization of lignin extraction by response surface methodology from sugarcane bagasse using deep eutectic solvents (DES), Ind. Crops Prod. 184 (2022) 115040, https://doi.org/10.1016/J.INDCROP.2022.115040.
[39] Y. Zhang, Y. Guo, X. Xie, V.M. Chernyshev, Y. Liu, W. Qi, Effects of phosphoric acid/hydrogen peroxide, ammonia/hydrogen peroxide and deep eutectic solvent pretreatments on component separation and enzymatic saccharification of Glycyrrhiza residue, Ind. Crops Prod. 196 (2023) 116525, https://doi.org/10.1016/J.INDCROP.2023.116525.
[40] M. Michelin, A.M. Marques, L.M. Pastrana, J.A. Teixeira, M.A. Cerqueira, Carboxymethyl cellulose-based films: effect of organosolv lignin incorporation on physicochemical and antioxidant properties, J. Food Eng. 285 (2020) 110107, https://doi.org/10.1016/J.JFOODENG.2020.110107.
[41] M. Zubair, Z. Rauf, S. Fatima, A. Ullah, Lignin-derived bionanocomposites as functional food packaging materials, Sustain. Food Technol. 2 (2024) 945–966, https://doi.org/10.1039/D4FB00105B.
[42] L. Darus, S. Susana, H. Sihombing, A.R.I. Utami, M. Mel, Enzymatic hydrolysis enhancement of oil palm empty fruit bunch by Peracetic-sulfuric acid pretreatment, Chem. Eng. J. 429 (2022), https://doi.org/10.1016/j.cej.2021.132452.
[43] B.G. Rodrigues, Á.H.M. José, C.A. Prado, D. Rodrigues, R.C.L.B. Rodrigues, Optimizing corncob pretreatment with eco-friendly deep eutectic solvents to enhance lignin extraction and cellulose-to-glucose conversion, Int. J. Biol. Macromol. 283 (2024) 137432, https://doi.org/10.1016/J.IJBIOMAC.2024.137432.
[44] S.M.S.N. Shikh Zahari, Y. Liu, P. Yao, M.S. Ideris, H.H. Azman, J.P. Hallett, OPEFB pretreatment using the low-cost N,N,N-dimethylbutylammonium hydrogen sulfate ionic liquid under varying conditions, Sci. Rep. 13 (2023), https://doi.org/10.1038/s41598-023-48722-0.
[45] M.T. Haqiqi, W. Bankeeree, P. Lotrakul, P. Pattananuwat, H. Punnapayak, R. Ramadhan, T. Kobayashi, R. Amirta, S. Prasongsuk, Antioxidant and UV-Blocking properties of a carboxymethyl cellulose–lignin composite film produced from oil palm empty fruit bunch, ACS Omega 6 (2021) 9653–9666, https://doi.org/10.1021/ACSOMEGA.1C00249.
[46] Y. He, H.C. Ye, T.T. You, F. Xu, Sustainable and multifunctional cellulose-lignin films with excellent antibacterial and UV-shielding for active food packaging, Food Hydrocoll. 137 (2023) 108355, https://doi.org/10.1016/J.FOODHYD.2022.108355.
[47] Y. Zhu, H. Li, Q.S. Zhao, B. Zhao, Effect of DES lignin incorporation on physicochemical, antioxidant and antimicrobial properties of carboxymethyl cellulose-based films, Int. J. Biol. Macromol. 263 (2024) 130294, https://doi.org/10.1016/J.IJBIOMAC.2024.130294.
[48] B. Hames, R. Ruiz, C. Scarlata, A. Sluiter, J. Sluiter, D. Templeton, Preparation of Samples for Compositional Analysis: Laboratory Analytical Procedure (LAP); Issue Date 08/08/2008, 2008.
[49] C. Wijaya, N.L. Sangadji, M. Muharja, T. Widjaja, L. Riadi, A. Widjaja, An integrated green fractionation of coconut husk: hydrothermal and deep eutectic solvent pretreatment for enhanced sugar and lignin production, Bioresour. Technol. Rep. 29 (2025) 102078, https://doi.org/10.1016/j.biteb.2025.102078.
[50] C. He, Feiyue Shen, D. Tian, M. Huang, L. Zhao, Q. Yu, Fei Shen, Lewis acid/base mediated deep eutectic solvents intensify lignocellulose fractionation to facilitate enzymatic hydrolysis and lignin nanosphere preparation, Int. J. Biol. Macromol. 254 (2024) 127853, https://doi.org/10.1016/j.ijbiomac.2023.127853.
[51] C. Alvarez-Vasco, R. Ma, M. Quintero, M. Guo, S. Geleynse, K.K. Ramasamy, M. Wolcott, X. Zhang, Unique low-molecular-weight lignin with high purity extracted from wood by deep eutectic solvents (DES): a source of lignin for valorization, Green Chem. 18 (2016) 5133–5141, https://doi.org/10.1039/c6gc01007e.
[52] R. Wang, K. Wang, M. Zhou, J. Xu, J. Jiang, Efficient fractionation of moso bamboo by synergistic hydrothermal-deep eutectic solvents pretreatment, Bioresour. Technol. 328 (2021) 124873, https://doi.org/10.1016/J.BIORTECH.2021.124873.
[53] Y. Guo, J. Zhang, C. Wang, M. Liu, J. You, L. Yin, M. Shi, Green pretreatment of lignocellulosic biomasses via deep eutectic solvents, Sustain. Chem. Pharm. 39 (2024) 101569, https://doi.org/10.1016/J.SCP.2024.101569.
[54] G. Wan, Q. Zhang, M. Li, Z. Jia, C. Guo, B. Luo, S. Wang, D. Min, How pseudo-lignin is generated during dilute sulfuric acid pretreatment, J. Agric. Food Chem. 67 (2019) 10116–10125, https://doi.org/10.1021/acs.jafc.9b02851.
[55] X. Jiang, R. Zhai, H. Li, C. Li, Q. Deng, M. Jin, Understanding acid hydrolysis of corn stover during densification pretreatment for quantitative predictions of enzymatic hydrolysis efficiency using modified pretreatment severity factor, Bioresour. Technol. 386 (2023) 129487, https://doi.org/10.1016/j.biortech.2023.129487.
[56] H. Zhou, J.Y. Zhu, X. Luo, S.Y. Leu, X. Wu, R. Gleisner, B.S. Dien, R.E. Hector, D. Yang, X. Qiu, E. Horn, J. Negron, Bioconversion of beetle-killed lodgepole pine using SPORL: process scale-up design, lignin coproduct, and high solids fermentation without detoxification, Ind. Eng. Chem. Res. 52 (2013) 16057–16065, https://doi.org/10.1021/ie402873y.
[57] L. Zhu, W. Tang, C. Ma, Y.-C. He, Efficient co-production of reducing sugars and xylooligosaccharides via clean hydrothermal pretreatment of rape straw, Bioresour. Technol. 388 (2023) 129727, https://doi.org/10.1016/j.biortech.2023.129727.
[58] Q. Ma, J. Zhu, R. Gleisner, R. Yang, J.Y. Zhu, Valorization of wheat straw using a recyclable hydrotrope at low temperatures (≤90 °c), ACS Sustain. Chem. Eng. 6 (2018) 14480–14489, https://doi.org/10.1021/acssuschemeng.8b03135.
[59] Q. Gao, Z. Tang, Y.C. He, Valorization of wheat straw through enhancement of cellulose accessibility, xylan elimination and lignin removal by choline chloride: p-toluenesulfonic acid pretreatment, Int. J. Biol. Macromol. 301 (2025), https://doi.org/10.1016/j.ijbiomac.2025.140335.
[60] Q. Yuan, S. Liu, M.G. Ma, X.X. Ji, S.E. Choi, C. Si, The kinetics studies on hydrolysis of hemicellulose, Front. Chem. 9 (2021) 781291, https://doi.org/10.3389/FCHEM.2021.781291/FULL.
[61] L. Schoofs, H. Hilker, N. Conen, A. Jupke, H. Klose, P.M. Grande, Time-resolved analysis of lignocellulose extraction in a biphasic, acid-catalyzed flow-through system, ACS Sustain. Chem. Eng. 14 (2026) 7099–7108, https://doi.org/10.1021/acssuschemeng.5c05534.
[62] Z. Tang, C. Wu, W. Tang, M. Huang, C. Ma, Y.C. He, Enhancing enzymatic saccharification of sunflower straw through optimal tartaric acid hydrothermal pretreatment, Bioresour. Technol. 385 (2023), https://doi.org/10.1016/j.biortech.2023.129279.
[63] H. Ji, Y. Song, X. Zhang, T. Tan, Using a combined hydrolysis factor to balance enzymatic saccharification and the structural characteristics of lignin during pretreatment of hybrid poplar with a fully recyclable solid acid, Bioresour. Technol. 238 (2017) 575–581, https://doi.org/10.1016/j.biortech.2017.04.092.
[64] A. Sluiter, B. Hames, R. Ruiz, C. Scarlata, J. Sluiter, D. Templeton, Determination of Ash in Biomass: Laboratory Analytical Procedure (LAP); Issue Date: 7/17/2005, 2008.
[65] N.L. Sangadji, C. Wijaya, M. Muharja, E. Elaine, H.F. Sangian, R. Lau, A. Widjaja, Two step fractionation of oil palm empty fruit bunches integrating hydrothermal-organosolv pretreatment for enhanced lignin extraction and enzymatic hydrolysis efficiency, Case Stud. Chem. Environ. Eng. (2025) 101275, https://doi.org/10.1016/j.cscee.2025.101275.
[66] P.D. Sutrisna, R.P. Hadi, C. Wijaya, J. Liliani, C. Robby, Cellulose acetate-based mixed matrix membrane for methylene blue wastewater treatment, in: AIP Conference Proceedings, American Institute of Physics Inc, 2023, https://doi.org/10.1063/5.0112184.
[67] A. Mittal, T.B. Vinzant, R. Brunecky, S.K. Black, H.M. Pilath, M.E. Himmel, D. K. Johnson, Investigation of the role of lignin in biphasic xylan hydrolysis during dilute acid and organosolv pretreatment of corn stover, Green Chem. 17 (2015) 1546–1558, https://doi.org/10.1039/c4gc02258k.
[68] Y. Zhu, B. Qi, X. Liang, J. Luo, Y. Wan, Comparison of corn stover pretreatments with lewis acid catalyzed choline chloride, glycerol and choline chloride-glycerol deep eutectic solvent, Polymers 13 (2021), https://doi.org/10.3390/POLYM13071170. Page 1170 13, 1170.
[69] C. He, Feiyue Shen, D. Tian, M. Huang, L. Zhao, Q. Yu, Fei Shen, Lewis acid/base mediated deep eutectic solvents intensify lignocellulose fractionation to facilitate enzymatic hydrolysis and lignin nanosphere preparation, Int. J. Biol. Macromol. 254 (2024) 127853, https://doi.org/10.1016/J.IJBIOMAC.2023.127853.
[70] Feiyue Shen, S. Wu, M. Huang, L. Zhao, J. He, Y. Zhang, S. Deng, J. Hu, D. Tian, Fei Shen, Integration of lignin microcapsulated pesticide production into lignocellulose biorefineries through FeCl3-mediated deep eutectic solvent pretreatment, Green Chem. 24 (2022) 5242–5254, https://doi.org/10.1039/D2GC01255C.
[71] T.M. Curry, M.J. Peña, B.R. Urbanowicz, An update on xylan structure, biosynthesis, and potential commercial applications, Cell Surf. (2023), https://doi.org/10.1016/j.tcsw.2023.100101.
[72] H. Wei, X. Chen, J. Shekiro, E. Kuhn, W. Wang, Y. Ji, E. Kozliak, M.E. Himmel, M. P. Tucker, Kinetic modelling and experimental studies for the effects of fe2+ ions on xylan hydrolysis with dilute-acid pretreatment and subsequent enzymatic hydrolysis, Catalysts 8 (2018), https://doi.org/10.3390/catal8010039.
[73] I. Romero, J.C. López-Linares, M. Moya, E. Castro, Optimization of sugar recovery from rapeseed straw pretreated with FeCl3, Bioresour. Technol. 268 (2018) 204–211, https://doi.org/10.1016/j.biortech.2018.07.112.
[74] X. Wu, Chen Huang, W. Tang, Caoxing Huang, C. Lai, Q. Yong, Use of metal chlorides during waste wheat straw autohydrolysis to overcome the self-buffering effect, Bioresour. Technol. 268 (2018) 259–265, https://doi.org/10.1016/J.BIORTECH.2018.07.132.
[75] W. Tang, X. Wu, C. Huang, Z. Ling, C. Lai, Q. Yong, Comprehensive understanding of the effects of metallic cations on enzymatic hydrolysis of humic acid-pretreated waste wheat straw, Biotechnol. Biofuels 14 (2021) 25, https://doi.org/10.1186/s13068-021-01874-5.

[76] W. Zhu, C.J. Houtman, J.Y. Zhu, R. Gleisner, K.F. Chen, Quantitative predictions of bioconversion of aspen by dilute acid and SPORL pretreatments using a unified combined hydrolysis factor (CHF), Process Biochem. 47 (2012) 785–791, https://doi.org/10.1016/j.procbio.2012.02.012.
[77] Y. Li, Z. Lin, X. Wang, Z. Duan, P. Lu, S. Li, D. Ji, Z. Wang, G. Li, D. Yu, W. Liu, High-hydrophobic ZIF-8@PLA composite aerogel and application for oil-water separation, Sep. Purif. Technol. 270 (2021) 118794, https://doi.org/10.1016/J.SEPPUR.2021.118794.
[78] B. Zhang, C. Peng, S. Zhang, M. Zhang, D. Li, X. Wang, B. Mao, Comprehensive analysis of the combined flocculation and filtration process for microalgae harvesting at various operating parameters, Sci. Total Environ. 857 (2023), https://doi.org/10.1016/j.scitotenv.2022.159658.
[79] R. Kumar, G. Mago, V. Balan, C.E. Wyman, Physical and chemical characterizations of corn stover and poplar solids resulting from leading pretreatment technologies, Bioresour. Technol. 100 (2009) 3948–3962, https://doi.org/10.1016/j.biortech.2009.01.075.
[80] H. Li, X. Li, D. Li, J. Zhang, H. Nawaz, T. You, F. Xu, Highly-efficient pretreatment using alkaline enhanced aqueous deep eutectic solvent to unlock poplar for high yield of fermentable sugars: synergistic removal of lignin and mannan, Bioresour. Technol. 351 (2022) 126993, https://doi.org/10.1016/J.BIORTECH.2022.126993.
[81] Y. Su, P. Wang, C. Lai, C. Huang, Z. Ling, Q. Yong, Revealing key factors influencing enzymatic digestibility of hydrothermally pretreated poplar in comparison with corn stover, Ind. Crops Prod. 194 (2023), https://doi.org/10.1016/j.indcrop.2023.116297.
[82] S.L. Sunar, R.K. Oruganti, D. Bhattacharyya, D. Shee, T.K. Panda, Deep eutectic solvent pretreatment of sugarcane bagasse for efficient lignin recovery and enhanced enzymatic hydrolysis, J. Ind. Eng. Chem. 139 (2024) 539–553, https://doi.org/10.1016/j.jiec.2024.05.030.
[83] F. Rodríguez-Rebelo, B. Rodríguez-Martínez, P.G. Del-Río, M.N. Collins, G. Garrote, B. Gullón, Assessment of deep eutectic solvents (DES) to fractionate paulownia wood within a biorefinery scheme: cellulosic bioethanol production and lignin isolation, Ind. Crops Prod. 216 (2024) 118761, https://doi.org/10.1016/j.indcrop.2024.118761.
[84] S.O. Anuchi, K.L.S. Campbell, J.P. Hallett, Effective pretreatment of lignin-rich coconut wastes using a low-cost ionic liquid, Sci. Rep. 12 (1 12) (2022) 1–11, https://doi.org/10.1038/s41598-022-09629-4, 2022.
[85] A.R. Mankar, A. Pandey, K.K. Pant, Microwave-assisted extraction of lignin from coconut coir using deep eutectic solvents and its valorization to aromatics, Bioresour. Technol. 345 (2022) 126528, https://doi.org/10.1016/J.BIORTECH.2021.126528.
[86] C. Ji, R. Weng, C. Yu, Y. Fan, J. Ouyang, Insights into acidic deep eutectic solvent-mediated softwood pretreatment for high fermentable sugar yield and efficient lignin recovery, Ind. Crops Prod. 227 (2025), https://doi.org/10.1016/j.indcrop.2025.120779.
[87] G. Miao, F. Ge, Y. Hu, H. Li, S. Yu, Y. He, S. Chen, F. Xu, Z. Chen, J. Xu, Mechanisms and mass-transfer kinetics of hemicellulose and lignin dissolution during deep eutectic solvent pretreatment, AIChE J. (2025), https://doi.org/10.1002/aic.70116.
[88] M.F. Syakir Bahazin, N.I. Amalin Mohd Isa, N.A. Natasha Mohd Azlan, M. R. Anuar, K.F. Pa'ee, T.L. Kelly Yong, Valorization of oil palm biomass: investigating chcl:lactic acid deep eutectic solvents for efficient furfural production, Biomass Bioenergy 200 (2025) 107971, https://doi.org/10.1016/J.BIOMBIOE.2025.107971.
[89] J. Yan, O. Oyedeji, J.H. Leal, B.S. Donohoe, T.A. Semelsberger, C. Li, A.N. Hoover, E. Webb, E.A. Bose, Y. Zeng, C.L. Williams, K.D. Schaller, N. Sun, A.E. Ray, D. Tanjore, Characterizing variability in lignocellulosic biomass: a review, ACS Sustain. Chem. Eng. (2020), https://doi.org/10.1021/acssuschemeng.9b06263.
[90] S.C. Sun, Y. Xu, C.Y. Ma, C. Zhang, C. Zuo, D. Sun, J.L. Wen, T.Q. Yuan, Green and efficient fractionation of bamboo biomass via synergistic hydrothermal-alkaline deep eutectic solvents pretreatment: valorization of carbohydrates, Renew. Energy 217 (2023) 119175, https://doi.org/10.1016/J.RENENE.2023.119175.
[91] B. Yang, B. Fan, Y.C. He, Metal salt-assisted hydrogen peroxide-malonic acid pretreatment for effectively enhancing delignification and saccharification of rapeseed straw, Ind. Crops Prod. 230 (2025), https://doi.org/10.1016/j.indcrop.2025.121076.
[92] P. Li, W. Qian, S. Wu, Y. Liu, Acidic deep eutectic solvents for lignocellulose pretreatment: insights into lignin extraction efficiency and structural transformation, ACS Sustain. Chem. Eng. 13 (2025) 9987–10018, https://doi.org/10.1021/acssuschemeng.5c02184.
[93] A.M. Da Costa Lopes, J.R.B. Gomes, J.A.P. Coutinho, A.J.D. Silvestre, Novel insights into biomass delignification with acidic deep eutectic solvents: a mechanistic study of β-O-4 ether bond cleavage and the role of the halide counterion in the catalytic performance, Green Chem. 22 (2020) 2474–2487, https://doi.org/10.1039/C9GC02569C.
[94] P. Moodley, Y. Sewsynker-Sukai, E.B. Gueguim Kana, Progress in the development of alkali and metal salt catalysed lignocellulosic pretreatment regimes: potential for bioethanol production, Bioresour. Technol. 310 (2020) 123372, https://doi.org/10.1016/j.biortech.2020.123372.
[95] H. Zhang, W. Chen, X. Han, Y. Zeng, J. Zhang, Z. Gao, J. Xie, Intensification of sugar production by using tween 80 to enhance metal-salt catalyzed pretreatment and enzymatic hydrolysis of sugarcane bagasse, Bioresour. Technol. 339 (2021), https://doi.org/10.1016/j.biortech.2021.125522.
[96] Z. Zhao, X. Chen, M.F. Ali, A.A. Abdeltawab, S.M. Yakout, G. Yu, Pretreatment of wheat straw using basic ethanolamine-based deep eutectic solvents for improving enzymatic hydrolysis, Bioresour. Technol. 263 (2018) 325–333, https://doi.org/10.1016/J.BIORTECH.2018.05.016.
[97] Y. Yuan, B. Jiang, H. Chen, W. Wu, S. Wu, Y. Jin, H. Xiao, Recent advances in understanding the effects of lignin structural characteristics on enzymatic hydrolysis, Biotechnol. Biofuels 14 (1 14) (2021) 1–20, https://doi.org/10.1186/S13068-021-02054-1, 2021.
[98] S. Hou, B. Shen, D. Zhang, R. Li, X. Xu, K. Wang, C. Lai, Q. Yong, Understanding of promoting enzymatic hydrolysis of combined hydrothermal and deep eutectic solvent pretreated poplars by tween 80, Bioresour. Technol. 362 (2022), https://doi.org/10.1016/j.biortech.2022.127825.
[99] H. Zhang, M. Fan, X. Li, A. Zhang, J. Xie, Enhancing enzymatic hydrolysis of sugarcane bagasse by ferric chloride catalyzed organosolv pretreatment and tween 80, Bioresour. Technol. 258 (2018) 295–301, https://doi.org/10.1016/j.biortech.2018.03.004.
[100] X. Shi, L. Wang, L. Sun, H. Chen, Sufficient premixing enhances enzymatic hydrolysis efficiency of lignocellulose at high-solids loading, Chem. Eng. J. 444 (2022) 136612, https://doi.org/10.1016/j.cej.2022.136612.
[101] J. Yang, X. Zhang, Q. Yong, S. Yu, Three-stage enzymatic hydrolysis of steam-exploded corn stover at high substrate concentration, Bioresour. Technol. 102 (2011) 4905–4908, https://doi.org/10.1016/j.biortech.2010.12.047.
[102] D.H. Fockink, M.B. Urio, J.H. Sánchez, L.P. Ramos, Enzymatic hydrolysis of steam-treated sugarcane bagasse: effect of enzyme loading and substrate total solids on its fractal kinetic modeling and rheological properties, Energy Fuel. 31 (2017) 6211–6220, https://doi.org/10.1021/acs.energyfuels.7b00818.
[103] M.G. Ganter de Moura, T.A. da Silva, A.Z. Filho, M.L. Corazza, L.P. Ramos, Fed-batch enzymatic hydrolysis of steam-exploded sugarcane bagasse, Bioresources 18 (2023) 3160–3177, https://doi.org/10.15376/biores.18.2.3160-3177.
[104] J.K. Kim, J. Yang, S.Y. Park, J.-H. Yu, K.H. Kim, Cellulase recycling in high-solids enzymatic hydrolysis of pretreated empty fruit bunches, Biotechnol. Biofuels 12 (2019) 138, https://doi.org/10.1186/s13068-019-1476-x.
[105] D. Ludwig, B. Michael, T. Hirth, S. Rupp, S. Zibek, High solids enzymatic hydrolysis of pretreated lignocellulosic materials with a powerful stirrer concept, Appl. Biochem. Biotechnol. 172 (2014) 1699–1713, https://doi.org/10.1007/s12010-013-0607-2.
[106] M.H. Sipponen, M. Österberg, Aqueous ammonia pre-treatment of wheat straw: process optimization and broad spectrum dye adsorption on nitrogen-containing lignin, Front. Chem. 7 (2019), https://doi.org/10.3389/fchem.2019.00545.
[107] F. Xin, H. Zhang, W. Wong, Bioethanol production from horticultural waste using crude fungal enzyme mixtures produced by solid state fermentation, Bioenergy Res. 6 (2013) 1030–1037, https://doi.org/10.1007/s12155-013-9330-7.
[108] V.P. Zambare, A.V. Zambare, D. Barh, L.P. Christopher, Optimization of enzymatic hydrolysis of prairie cordgrass for improved ethanol production, J. Renew. Sustain. Energy 4 (2012), https://doi.org/10.1063/1.4729587.
[109] A.K. Chandel, V.K. Garlapati, A.K. Singh, F.A.F. Antunes, S.S. da Silva, The path forward for lignocellulose biorefineries: bottlenecks, solutions, and perspective on commercialization, Bioresour. Technol. 264 (2018) 370–381, https://doi.org/10.1016/j.biortech.2018.06.004.
[110] Y. Xiao, J. Qi, Z. Yu, W. Zhao, W. Shao, N. Li, Y. Kong, L. Li, W. Wei, Pretreatment of corncob powder by choline chloride-urea-ethanolamine to co-produce glucose, xylose and lignin nanospheres, Ind. Crops Prod. 206 (2023) 117695, https://doi.org/10.1016/J.INDCROP.2023.117695.
[111] Y. Guo, L. Xu, F. Shen, J. Hu, M. Huang, J. He, Y. Zhang, S. Deng, Q. Li, D. Tian, Insights into lignocellulosic waste fractionation for lignin nanospheres fabrication using acidic/alkaline deep eutectic solvents, Chemosphere 286 (2022) 131798, https://doi.org/10.1016/j.chemosphere.2021.131798.
[112] Z. Guo, Z. Ling, C. Wang, X. Zhang, F. Xu, Integration of facile deep eutectic solvents pretreatment for enhanced enzymatic hydrolysis and lignin valorization from industrial xylose residue, Bioresour. Technol. 265 (2018) 334–339, https://doi.org/10.1016/j.biortech.2018.06.027.
[113] M. Karlsson, J. Romson, T. Elder, Å. Emmer, M. Lawoko, Lignin structure and reactivity in the organosolv process studied by NMR spectroscopy, mass spectrometry, and density functional theory, Biomacromolecules 24 (2023) 2314–2326, https://doi.org/10.1021/acs.biomac.3c00186.
[114] X.J. Shen, J.L. Wen, Q.Q. Mei, X. Chen, D. Sun, T.Q. Yuan, R.C. Sun, Facile fractionation of lignocelluloses by biomass-derived deep eutectic solvent (DES) pretreatment for cellulose enzymatic hydrolysis and lignin valorization, Green Chem. 21 (2019) 275–283, https://doi.org/10.1039/c8gc03064b.
[115] Syahidah, A.S.R.D. Lestari, A. Arif, I. Taskirawati, Fardhatillah Makkarennu, R. Zhafira, M.R.A. Pratama, S. Sulaeha, S.H. Anita, M. Ghozali, F.P. Sari, A. D. Martino, W. Fatriasari, Lignin from the sugar palm's fiber (Arenga pinnata merr.) as a potential active compound in packaging, Case Stud. Chem. Environ. Eng. 11 (2025), https://doi.org/10.1016/j.cscee.2025.101133.
[116] C.E. de A. Padilha, C. da C. Nogueira, B.R.A. Alencar, Í.B.S. de Abreu, E.D. Dutra, J.A.C. Ruiz, D.F. de S. Souza, E.S. dos Santos, Production and application of lignin-based chemicals and materials in the cellulosic ethanol production: an overview on lignin closed-loop biorefinery approaches, Waste Biomass Valor. (2021), https://doi.org/10.1007/s12649-021-01455-5.
[117] H. Mostafa, M. Hamdi, J.O. Airouyuwaa, F. Hamed, Y. Wang, S. Maqsood, Lignin and green solvent extracted phenolic compounds from date palm leaves as functional ingredients for the formulation of soy protein isolate biocomposite packaging materials: a circular packaging concept, Int. J. Biol. Macromol. 279 (2024) 134843, https://doi.org/10.1016/J.IJBIOMAC.2024.134843.
[118] I. Korbag, S. Mohamed Saleh, Studies on the formation of intermolecular interactions and structural characterization of polyvinyl alcohol/lignin film, Int. J. Environ. Stud. 73 (2016) 226–235, https://doi.org/10.1080/00207233.2016.1143700.

[119] A. Wichaphian, P. Yasan, W. Pathom-aree, S. Lumyong, N. Suwannarach, J. Kumla, S. Chaipoot, S. Hoijang, T. Krasian, P. Worajittiphon, W. Punyodom, B. Cheirsilp, G. Wang, S. Srinuanpan, From agricultural waste to active films: enhanced crystallinity of spent mushroom substrate-derived cellulose via deep eutectic solvent-based microwave-assisted pretreatment and its application in reinforcing CMC-Based composite films, J. Agric. Food Res. 20 (2025), https://doi.org/10.1016/j.jafr.2025.101759.

[120] J.F. Leal Silva, P.Y.S. Nakasu, A.C. da Costa, R. Maciel Filho, S.C. Rabelo, Techno-economic analysis of the production of 2G ethanol and technical lignin via a protic ionic liquid pretreatment of sugarcane bagasse, Ind. Crops Prod. 189 (2022), https://doi.org/10.1016/j.indcrop.2022.115788.

[121] P. Li, C. Yang, Z. Jiang, Y. Jin, W. Wu, Lignocellulose pretreatment by deep eutectic solvents and related technologies: a review, J. Bioresour. Bioprod. (2022), https://doi.org/10.1016/j.jobab.2022.11.004.

[122] H.A. Ruiz, W.G. Sganzerla, V. Larnaudie, R.J. Veersma, G. van Erven, Shiva, L. J. Ríos-González, R.M. Rodríguez-Jasso, G. Rosero-Chasoy, M.D. Ferrari, M. A. Kabel, T. Forster-Carneiro, C. Lareo, Advances in process design, techno-economic assessment and environmental aspects for hydrothermal pretreatment in the fractionation of biomass under biorefinery concept, Bioresour. Technol. 369 (2023) 128469, https://doi.org/10.1016/j.biortech.2022.128469.

1-s2.0-S0961953426009359-main.pdf

Institut Teknologi Sepuluh Nopember, Jurusan Teknik Informatika

Document Details

Submission ID
trn:oid:::3117:613881120

Submission Date
Aug 12, 2026, 5:28 PM GMT+7

Download Date
Aug 12, 2026, 5:35 PM GMT+7

File Name
1-s2.0-S0961953426009359-main.pdf

File Size
5.8 MB

22 Pages

22,905 Words

132,803 Characters

11% Overall Similarity

The combined total of all matches, including overlapping sources, for each database.

Filtered from the Report

- Bibliography
- Quoted Text
- Cited Text

Exclusions

- 1 Excluded Source

Match Groups

182 Not Cited or Quoted 11%
Matches with neither in-text citation nor quotation marks

0 Missing Quotations 0%
Matches that are still very similar to source material

0 Missing Citation 0%
Matches that have quotation marks, but no in-text citation

0 Cited and Quoted 0%
Matches with in-text citation present, but no quotation marks

Top Sources

7% Internet sources
9% Publications
0% Submitted works (Student Papers)

Match Groups

- **182** Not Cited or Quoted 11%
  Matches with neither in-text citation nor quotation marks
- **0** Missing Quotations 0%
  Matches that are still very similar to source material
- **0** Missing Citation 0%
  Matches that have quotation marks, but no in-text citation
- **0** Cited and Quoted 0%
  Matches with in-text citation present, but no quotation marks

Top Sources

7% Internet sources
9% Publications
0% Submitted works (Student Papers)

Top Sources

The sources with the highest number of matches within the submission. Overlapping sources will not be displayed.

1	Internet	repository.ubaya.ac.id 2%
2	Internet	journal.bcrec.id <1%
3	Internet	link.springer.com <1%
4	Publication	Yuan Zhu, Hang Li, Qing-Sheng Zhao, Bing Zhao. "Effect of DES lignin incorporatio... <1%
5	Publication	Bingxue Sun, Huaitao Jiang, Guan-Ping Jin, Shi-Kui Han, Bolin Liu, Xiaoli Ge, Xiaoy... <1%
6	Publication	Francisco W. Maciel-Silva, Luiz E.N. Castro, William Gustavo Sganzerla, Josiel Marti... <1%
7	Publication	Candra Wijaya, Ningsi Lick Sangadji, Maktum Muharja, Tri Widjaja, Lieke Riadi, El... <1%
8	Publication	Yuan Zhu, Tian-Xiao Yang, Ben-Kun Qi, Hang Li, Qing-Sheng Zhao, Bing Zhao. "Aci... <1%
9	Publication	Candra Wijaya, Ningsi Lick Sangadji, Maktum Muharja, Tri Widjaja, Lieke Riadi, Ar... <1%
10	Internet	cris.vtt.fi <1%

11 Internet

assets-eu.researchsquare.com <1%

12 Publication

Shiva Lall Sunar, Debraj Bhattacharyya, Debaprasad Shee, Tarun K. Panda. "Effici... <1%

13 Publication

Xiaoyu Du, Yanan Wang, Zhiwei Gong, Wenwen Chen, Wei Zhou, Qishuai Ma, Wen... <1%

14 Publication

Euis Hermiati, Hana Nur Fitriana, Dwi Ajias Pramasari, Nanik Rahmani et al. "Inte... <1%

15 Publication

Yu Sheng, Yao-yao Jin, Hai-yan Yang, Zheng-jun Shi, Chun Shi, Da-wei Wang, Tao-h... <1%

16 Publication

Antira Wichaphian, Phonthida Yasan, Wasu Pathom-aree, Saisamorn Lumyong et ... <1%

17 Publication

Adrián Arcís, Estela Lladosa, Helena Poy, Sonia Loras, Carlos Silvestre, Javier Álvar... <1%

18 Publication

Enqing Zhu, Jinyuan Cheng, Leixin Huang, Hangyu Shen et al. "Ultrahigh solid loa... <1%

19 Internet

www.researchsquare.com <1%

20 Publication

Jinwen Guo, Guoce Yu, Jianlong Wang. "Comparative insight into biomass pretrea... <1%

21 Publication

Mohammad Farhan Supriadiputra, Hakun Wirawasista Aparamarta, Arief Widjaja,... <1%

22 Publication

Merdieta Amelia, Holilah, Didik Prasetyoko, RH Fitri Faradilla et al. "Efficient nan... <1%

23 Publication

Xinyuan Zhang, Yiqin Wang, Jie Lu, Miaomiao Liu, Wanting Tan, Yi Cheng, Yehan T... <1%

24 Internet

ir.niist.res.in:8080 <1%

25 Publication
Dawid Mikulski, Grzegorz Kłosowski, Katarzyna Osmolak. "Efficiency of cellulosic ... <1%

26 Publication
Shuang Wang, Wenyang Xu, Yehan Tao, Jinwen Hu, Jian Du, Jie Lu, Yanna Lv, Chen... <1%

27 Publication
Yuan Zhu, Shunan Zhao, Congli Chen, Fangzhou Wang, Shuo Yuan, Kai Zhao, Ruipi... <1%

28 Internet
public-pages-files-2025.frontiersin.org <1%

29 Publication
Penghui Li, Tiantian Li, Shubin Wu. "Process parameters and product characteriza... <1%

30 Publication
Weiqi Wei, Hongdan Zhang, Yongcan Jin. "Comparison of microwave-assisted zinc... <1%

31 Publication
Xuelian Zhou, Xuze Liu, Yunni Zhan, Huiyang Bian et al. "A tailored deep eutectic ... <1%

32 Publication
Yiyi Chen, Chaojie Yang, Jinguang Hu, Mei Huang, Li Zhao, Jinsong He, Shaobo Zh... <1%

33 Publication
Zhu Chen, Yuguang Wang, Haina Cheng, Hongbo Zhou. "Hemicellulose degradati... <1%

34 Internet
betasg.inflibnet.ac.in <1%

35 Internet
repositorio.uam.es <1%

36 Internet
riubu.ubu.es <1%

37 Publication
Lei Zhong, Chao Wang, Guihua Yang, Jiachuan Chen, Feng Xu, Chang Geun Yoo, G... <1%

38 Publication
Sarvesh Kumar, Paula Nousiainen, Donya Kamravamanesh, Rahul Mangayil. "Inte... <1%

39 Publication
D. S. Yamashita. "Benzodioxocin-3-ones and N-acyl-3-amino-3-buten-2-ones: novel... <1%

40 Publication
Huan Chen, Chihe Sun, Yun Hu, Changlei Xia, Fubao Sun, Zhanying Zhang. "Reacti... <1%

41 Publication
Nur Zatul'Iffah Zakaria, Ku Syahidah Ku Ismail, Ahmad Anas Nagoor Gunny, Ham... <1%

42 Publication
Jung Lin Wong, Sabeeha Nushrat Bibi Aisha Khadaroo, Jonathan Lin Yang Cheng, J... <1%

43 Internet
mdpi-res.com <1%

44 Publication
Guohua Miao, Jung Lin Wong, Jiuan Jing Chew, Deni Shidqi Khaerudini, Jaka Sunar... <1%

45 Internet
dfrws.org <1%

46 Publication
Obiakor, Okwudili I.. "Mechanical Fractionation of Wheat Middlings for Applicatio... <1%

47 Publication
Xiaohu Zhao, Wei Tang, Bo Fan, Yu-Cai He, Cuiluan Ma. "Implementing efficient a... <1%

48 Internet
biointerfaceresearch.com <1%

49 Internet
c.coek.info <1%

50 Publication
Bhisma Mahendra, Hilman Imadul Umam, Saniatun Wilda, Natasya Shafira Putri ... <1%

51 Publication
Guojie Song, Meysam Madadi, Chihe Sun, Lishu Shao, Maobing Tu, Ali Abdulkhani... <1%

52 Publication
Nida Arshad, Elizabeth Jayex Panakkal, Aiya Chantarasiri, Peerapong Pornwongth... <1%

53 Publication
Qianli Wang, Jiaqi Chen, Xiaoyan Jiang, Chen Huang, Jun-ichiro Hayashi, Xianzhi M... <1%

54 Internet
burjcdigital.urjc.es <1%

55 Publication
"Nonwoody Plant Lignin for Advanced Applications", Springer Science and Busine... <1%

56 Publication
Azizatul Karimah, Nyoman Jaya Wistara, Widya Fatriasari, Takashi Watanabe, Mo... <1%

57 Publication
Dilay Özuyar, Emir Zafer Hoşgün. "Acidic Deep Eutectic Solvent Pretreatment of S... <1%

58 Publication
Fernando Rodríguez-Rebelo, Beatriz Rodríguez-Martínez, Pablo G. Del-Río, Mauric... <1%

59 Publication
Guojie Song, Meysam Madadi, Xianzhi Meng, Chihe Sun et al. "Double in-situ ligni... <1%

60 Publication
Haichao Li, Xin Li, Tingting You, Deqiang Li, Haq Nawaz, Xueming Zhang, Feng Xu.... <1%

61 Publication
Prado, Desiree Mae S.. "Tailoring Deep Eutectic Solvents for Electrochemical Appli... <1%

62 Publication
Vidhyadevi Udayakumar, Brinda Lakshmi Anguraj. "Optimized deep eutectic solv... <1%

63 Publication
Yadong Yang, Hossein Shahbeik, Alireza Shafizadeh, Shahin Rafiee et al. "Predicti... <1%

64 Internet
constellation.uqac.ca <1%

65 Internet
d21zja6o12zyp0.cloudfront.net <1%

66 Internet
ouci.dntb.gov.ua <1%

67 Publication

Agwu, Kelechi Andrew. "Sustainable Organosolv Pretreatment and Fractionation ... <1%

68 Publication

Bingying Yang, Bo Fan, Yu-Cai He. "Metal salt-assisted hydrogen peroxide-maloni... <1%

69 Publication

Binyuan Gao, Chongran Sun, Tao Yang, Qikun Wen et al. "Biphasic solvent system... <1%

70 Publication

Ericsem Pereira, Débora Tamires Vitor Pereira, Sarita Cândida Rabelo, Roberta Ce... <1%

71 Publication

Helena Poy, Estela Lladosa, Adrián Arcís, Carmen Gabaldón, Sonia Loras. "Microw... <1%

72 Publication

Ho Thi Thuy Huynh, Ninh Thi Tinh, Nguyen Thanh Hoai Nam, Mai Thanh Phong, N... <1%

73 Publication

Hong-li Ma, Ying-chuan Zhang, Fei-xiang Xu, Nian-fang Ma, Ming-fu Li, Gui-hua W... <1%

74 Publication

Jiabin Wang, Xiang Zhou, Rui Zhang, Xinyan You et al. "N-heterocycle-based deep ... <1%

75 Publication

N. V. R. Naidu, N. L. Ramesh, A. Jagannatha Reddy, Nagaraju Kottam et al. "Applie... <1%

76 Publication

Novia Novia, Asyeni Miftahul Jannah, Elda Melwita, Ahmad Fudholi, Vishnu K. Par... <1%

77 Publication

Qi Zheng, Yongwen Ma, Jinquan Wan, Yan Wang, Yingping Long, Xinyu Xia, Xu Su... <1%

78 Publication

Ruoyan Li, Ziyi Jin, Wenna Guan, Chenhuan Lai, Caoxing Huang, Qiang Yong. "Mec... <1%

79 Publication

Shuheng Zhao, Shang Wang, Zhuojie Li, Qiaolong Zhai, Junhao Hu, Kui Wang, Fei ... <1%

80 Publication

Vishal Sharma, Parushi Nargotra, Surbhi Sharma, Bijender Kumar Bajaj. "Efficacy ... <1%

81 Internet
backend.orbit.dtu.dk <1%

82 Internet
biotechnologyforbiofuels.biomedcentral.com <1%

83 Internet
epubl.ktu.edu <1%

84 Internet
www.cellulosechemtechnol.ro <1%

85 Publication
Changliu He, Lihe Zhang, Xi Zhao, Jiayu Xin, Cui Li, ChenXi Li, Xu Zhang. "Pretreat... <1%

86 Publication
Pedro Verdía Barbará, Hemant Choudhary, Pedro S. Nakasu, Amir Al-Ghatta et al. ... <1%

87 Publication
Prakaidao Pomdaeng, Prawat Sukphun, Alissara Reungsang, Chen-Yeon Chu. "Sy... <1%

88 Publication
Rakopoulos, D.C., C.D. Rakopoulos, E.G. Giakoumis, and A.M. Dimaratos. "Studyin... <1%

89 Publication
Xinquan Liang, Yuan Zhu, Benkun Qi, Shiqian Li, Jianquan Luo, Yinhua Wan. "Stru... <1%

90 Publication
Yoon-Jung Shin, Jae-Won Lee. "Tailoring lignin surface properties for enhanced en... <1%

91 Publication
Chenjun He, Feiyue Shen, Dong Tian, Mei Huang, Li Zhao, Qiang Yu, Fei Shen. "Le... <1%

92 Publication
Jiyou Yang, Wanjing Zhang, Yiquan Tang, Mingfei Li, Feng Peng, Jing Bian. "Mild p... <1%

93 Publication
Karthik Ananth Mani, Lokesh Kumar, Nelson Barrios, Sachin Agate et al. "Emerge... <1%

94 Publication
Min Wu, Lin Wang, Ren Zhang, Zhiyu Zhang, Mang Wu, Youhong Wang, Liang Zho... <1%

95 Publication

Rui Lou, Xiao Zhang. "Evaluation of pretreatment effect on lignin extraction from ... <1%

96 Publication

Xue-Dan Hou, Guo-Jian Feng, Mei Ye, Chao-Mei Huang, Yi Zhang. "Significantly en... <1%

Biomass and Bioenergy 217 (2027) 109859

Contents lists available at ScienceDirect

Biomass and Bioenergy

journal homepage: www.elsevier.com/locate/biombioe

Integrated valorization of oil palm empty fruit bunch (OPEFB) by deep eutectic solvent pretreatment: Glucose production enhancement and lignin-CMC composite for sustainable packaging

Candra Wijaya [a,b], Andika Prastika [a], Olivia Izzati Atiqa [a], Tabina Raissa Apol [a], Urania Noor Lintang Pertiwi [a], Lieke Riadi [b], Maktum Muharja [a], Arief Widjaja [a,*]

[a] Department of Chemical Engineering, Institut Teknologi Sepuluh Nopember, Kampus ITS Sukolilo, Surabaya, 60111, Indonesia
[b] Department of Chemical Engineering, Universitas Surabaya (UBAYA), Jalan Raya Kalirungkut (Tenggilis), Surabaya, 60293, Indonesia

ARTICLE INFO

Keywords:
Oil palm empty fruit bunch
Deep eutectic solvent
Fractionation
Enzymatic hydrolysis
CMC-lignin film
Modified severity factor

ABSTRACT

Oil palm empty fruit bunch (OPEFB) is an abundant lignocellulosic residue with potential for integrated biorefinery applications, but its recalcitrant structure limits direct enzymatic conversion and lignin utilization. This study investigated the integrated valorization of OPEFB through deep eutectic solvent (DES) pretreatment using choline chloride–lactic acid (ChCl:LA) and choline chloride–glycerol–$FeCl_3$ (ChCl:Gly:$FeCl_3$) systems for glucose production, lignin recovery, and CMC–lignin composite film development. Modified severity descriptors, namely combined delignification factor (CDF) and combined hydrolysis factor (CHF), were applied to describe severity-dependent lignin removal and xylan hydrolysis. The CDF and CHF models successfully described the severity-dependent fractionation behavior of OPEFB during DES pretreatment. ChCl:LA promoted stronger lignin solubilization and higher lignin recovery, while ChCl:Gly:$FeCl_3$ enhanced hemicellulose removal and enzymatic digestibility through Lewis acid-assisted deconstruction. The highest enzymatic hydrolysis yields reached 75.8% for ChCl:LA and 93.8% for ChCl:Gly:$FeCl_3$. On a 100 g raw OPEFB basis, ChCl:LA pretreatment at 140 °C for 6 h produced 21.6 g glucose and 24.7 g recovered lignin, whereas ChCl:Gly:$FeCl_3$ pretreatment at 140 °C for 3 h produced 21.7 g glucose and 23.1 g recovered lignin. The recovered DES lignins showed high purity and were successfully incorporated into CMC-based films. ChCl:LA lignin improved water resistance and reduced WVTR, while ChCl:Gly:$FeCl_3$ lignin provided stronger antioxidant activity and tensile reinforcement. These findings demonstrate that DES pretreatment enables the dual valorization of OPEFB into fermentable glucose and functional lignin-derived packaging materials, supporting a multiproduct biorefinery pathway for sustainable biomass utilization.

1. Introduction

The transition from fossil-based resources to renewable carbon feedstocks has become increasingly important for the development of sustainable fuels, chemicals, and materials [1,2]. Lignocellulosic biomass is one of the most promising renewable resources because it is abundant, renewable, and composed of carbohydrate and aromatic fractions that can be converted into multiple value-added products [3–5]. However, the efficient utilization of lignocellulosic biomass remains restricted by its naturally recalcitrant structure. Cellulose microfibrils are embedded within hemicellulose and lignin, while lignin–carbohydrate complexes provide additional resistance against chemical and enzymatic deconstruction [6,7]. As a result, pretreatment is required to disrupt the biomass matrix, improve cellulose accessibility, and enable the selective recovery of lignin for further valorization [8,9].

Oil palm empty fruit bunch (OPEFB) is an abundant lignocellulosic residue generated from the palm oil industry, particularly in tropical countries such as Indonesia and Malaysia [10]. OPEFB contains cellulose, hemicellulose, and lignin as its major structural components, making it a promising feedstock for biorefinery applications [11]. The cellulose-rich fraction can be hydrolyzed into glucose and further converted into biofuels or biochemicals, while the lignin fraction can serve as a renewable aromatic polymer for material applications [12,13].

* Corresponding author.
E-mail address: arief.widjaja@its.ac.id (A. Widjaja).

https://doi.org/10.1016/j.biombioe.2026.109859
Received 25 May 2026; Received in revised form 16 July 2026; Accepted 16 July 2026
Available online 20 July 2026

Nevertheless, the compact fiber structure and relatively high lignin content of OPEFB limit its direct enzymatic digestibility. Without suitable pretreatment, lignin can act as a physical barrier and induce non-productive enzyme adsorption, thereby reducing hydrolysis efficiency [7]. Therefore, an effective OPEFB fractionation strategy should not only enhance glucose production but also recover lignin in a form suitable for downstream utilization.

Several pretreatment methods have been reported for lignocellulosic biomass, including dilute acid, alkaline, hydrothermal, organosolv, and ionic liquid-based processes [14–17]. Although these methods can improve enzymatic hydrolysis, they may involve limitations such as high chemical loading, corrosion, severe operating conditions, inhibitor formation, or limited selectivity toward lignin recovery [18,19]. In this context, DESs have emerged as promising green solvents for lignocellulosic biomass fractionation. DESs are commonly formed through hydrogen-bond interactions between a hydrogen-bond acceptor and a hydrogen-bond donor, producing solvent systems with low volatility, tunable acidity, and strong lignin solubilization capacity [20,21]. Choline chloride-based DESs are particularly attractive because they can be combined with various hydrogen-bond donors, including organic acids and polyols, to tailor pretreatment performance [22].

Among acidic DES systems, choline chloride–lactic acid (ChCl:LA) was selected as a representative Brønsted-acidic DES because lactic acid-based DESs have been widely reported to promote lignin dissolution, xylan elimination, and enzymatic digestibility enhancement in lignocellulosic biomass [23–26]. The acidic nature of lactic acid can facilitate the cleavage of ether and ester linkages in lignin and lignin–carbohydrate complexes, while choline chloride contributes hydrogen-bonding and ionic interactions that assist lignin solubilization and cell wall deconstruction [22,27,28]. Therefore, ChCl:LA was chosen to represent a delignification-oriented DES route in which lignin recovery is expected to be a major output. In contrast, choline chloride–glycerol (ChCl:Gly) represents a milder polyol-based DES matrix, but its deconstruction ability can be strengthened by incorporating $FeCl_3$ as a Lewis acid catalyst. Fe^{3+} species can coordinate with oxygen-containing bonds and facilitate the cleavage of glycosidic and ether linkages, thereby enhancing hemicellulose disruption, biomass deconstruction, cellulose accessibility, and subsequent enzymatic hydrolysis [29–32]. Previous studies on metal chloride-assisted pretreatment have also shown that Fe^{3+}-based systems can intensify xylan depolymerization and improve enzymatic digestibility, supporting the use of $FeCl_3$-containing DESs for hydrolysis-oriented fractionation [33–35]. Thus, ChCl:Gly:$FeCl_3$ was selected as a Lewis-acid-assisted DES system to represent a hemicellulose-disruption-oriented route. The comparison between ChCl:LA and ChCl:Gly:$FeCl_3$ was therefore designed not as a random solvent screening, but as a mechanistic comparison between two choline chloride-based DES systems with different dominant catalytic environments, Brønsted-acid-driven delignification and Lewis-acid-assisted hemicellulose deconstruction. This comparison is relevant for determining whether OPEFB valorization should be directed toward higher lignin recovery, higher glucose production, or a balanced dual-product biorefinery strategy.

In addition to experimental evaluation, severity-based parameters can provide a useful framework for interpreting lignocellulosic fractionation. Conventional severity factors generally combine temperature and reaction time, but they do not fully account for solvent acidity, catalyst contribution, or DES composition [9,36]. Therefore, modified severity descriptors such as the combined delignification factor (CDF) and combined hydrolysis factor (CHF) have been proposed to better describe selective lignin removal and carbohydrate hydrolysis under chemically assisted pretreatment systems [13,37]. CDF is particularly relevant for evaluating the collective influence of pretreatment temperature, time, and solvent or catalyst contribution on lignin removal. Meanwhile, CHF can be used to describe the severity-dependent behavior of carbohydrate hydrolysis or enzymatic glucose production. In DES pretreatment, these descriptors may help connect operating conditions with two key outcomes: delignification efficiency and glucose release from the cellulose-rich solid fraction. This is important because excessive pretreatment severity may enhance lignin removal but may also reduce carbohydrate recovery, alter lignin structure, or affect the suitability of recovered lignin for material applications.

Most DES pretreatment studies have primarily focused on improving enzymatic hydrolysis or maximizing lignin removal [38,39]. However, a more complete biorefinery approach requires the valorization of both the carbohydrate-rich solid and the recovered lignin fraction. Lignin is often regarded as a low-value by-product, even though its aromatic structure, phenolic hydroxyl groups, hydrophobicity, antioxidant activity, and ultraviolet-blocking ability make it suitable for functional material applications [40,41]. Previous OPEFB–DES work has demonstrated that DES pretreatment can enhance lignin removal, preserve cellulose, improve enzymatic hydrolysis, and recover lignin as a potential product stream, supporting its relevance for multiproduct biomass utilization [42–44]. However, the direct conversion of recovered DES lignin into functional packaging materials remains less explored, particularly when combined with severity-based interpretation of glucose production and lignin recovery.

Carboxymethyl cellulose (CMC) is a biodegradable cellulose derivative with good film-forming ability, transparency, and compatibility with water-based processing [45]. However, neat CMC films commonly suffer from high water sensitivity, limited moisture barrier properties, and insufficient mechanical stability for broader packaging applications [40]. The incorporation of lignin into CMC films can address some of these limitations by increasing hydrophobic interactions, introducing aromatic UV-absorbing domains, and enhancing antioxidant functionality [46,47]. In this regard, lignin recovered from DES pretreatment may provide additional value beyond its role as a fractionation by-product. Instead, it can be directly utilized as a functional component in lignin-CMC composite films, supporting the development of biodegradable and biomass-derived packaging materials.

Nevertheless, the integration of DES pretreatment, glucose production, lignin recovery, severity-based analysis, and lignin-based composite film fabrication remains insufficiently explored. A pretreatment condition that enhances enzymatic hydrolysis does not always generate lignin with suitable properties for material applications. Conversely, conditions that favor lignin recovery may influence cellulose preservation and glucose release. Therefore, an integrated assessment is needed to determine whether DES pretreatment can simultaneously improve enzymatic glucose production and provide recovered lignin suitable for CMC-based packaging films. Such an approach is important for advancing OPEFB utilization from a single-product sugar platform toward a multiproduct biorefinery system.

This study investigates the integrated valorization of OPEFB through DES pretreatment for glucose production enhancement and lignin-CMC composite film development. Two DES systems, ChCl:LA and ChCl:Gly:$FeCl_3$, were evaluated to determine their effects on biomass fractionation, component removal, CDF- and CHF-related pretreatment behavior, enzymatic glucose release, lignin recovery, and the functional performance of lignin-CMC films. The pretreated solid fractions were subjected to enzymatic hydrolysis to assess glucose production, while the recovered lignin was incorporated into CMC films and evaluated for its physical, mechanical, surface, and barrier-related properties. Unlike previous studies that mainly focused on DES-assisted delignification or enzymatic saccharification, this work integrates severity-based fractionation analysis, carbohydrate conversion, and lignin-derived material development within a single OPEFB valorization pathway. This strategy demonstrates the dual role of OPEFB as a glucose platform and renewable source of functional lignin for sustainable packaging applications.

2. Materials and methods

2.1. Materials

The OPEFB was supplied by PT. Sawit Arum Madani (Blitar, Indonesia). The biomass was washed, dried, and prepared according to the National Renewable Energy Laboratory (NREL) protocol [48], and then ground to a particle size of 40–60 mesh. Lactic acid, glycerol, and ferric chloride hexahydrate ($FeCl_3{\cdot}6H_2O$), all of analytical grade, were purchased from Merck (Germany). Choline chloride and cellulase derived from *Trichoderma reesei* were obtained from Sigma-Aldrich (USA). Unless otherwise specified, all other analytical-grade reagents used in this work were also supplied by Sigma-Aldrich.

2.2. Experimental diagram

A schematic representation of the experimental workflow is presented in Fig. 1. The diagram summarizes the main stages of the study, namely OPEFB preparation, deep eutectic solvent (DES) preparation, DES pretreatment, separation of the pretreated solid and filtrate fractions, lignin regeneration, enzymatic hydrolysis of the solid residue, and the preparation and characterization of CMC–lignin films. For lignin characterization and film fabrication, the lignin sample obtained under the pretreatment condition giving the highest lignin yield was used.

2.3. DES pretreatment and lignin recovery

The experimental procedure was adapted from prior research [49]. The ChCl:LA deep eutectic solvent (DES) was prepared by mixing choline chloride (ChCl) and lactic acid (LA) at a molar ratio of 1:2. Meanwhile, the ChCl:Gly:$FeCl_3$ DES was prepared by mixing ChCl and glycerol (Gly) at a molar ratio of 1:2, followed by the addition of $FeCl_3$ at a concentration of 0.01 mol/L. The $FeCl_3$ concentration was fixed at 0.01 mol/L based on previous Lewis acid-mediated ChCl:Gly DES studies, in which the same catalyst loading was used to intensify lignocellulose fractionation while maintaining a controlled DES formulation [29,50]. In the present work, only one $FeCl_3$ concentration was used because the main objective was not to optimize catalyst loading, but to compare two different DES fractionation mechanisms under controlled formulation conditions: Brønsted-acidic ChCl:LA and Lewis-acid-assisted ChCl:Gly:$FeCl_3$. Maintaining a constant $FeCl_3$ concentration allowed the effects of DES chemistry, temperature, and residence time to be evaluated without additional variation in Lewis acid loading, acidity, ionic strength, viscosity, and mass-transfer behavior. This approach is also consistent with previous studies on Lewis-acid-containing DES systems, where metal chlorides such as $FeCl_3$, $AlCl_3$, $CuCl_2$, and $ZnCl_2$ were evaluated as acid-site contributors to DES-mediated lignocellulose fractionation before further optimization of specific solvent composition or catalyst loading [29].

The mixtures were heated in a closed round-bottom flask at 70 °C under continuous stirring until clear and homogeneous liquids were formed. The mixture was then cooled to room temperature prior to use [51]. For the pretreatment, 4 g of OPEFB was mixed with 60 g of DES in a 250 mL three-neck round-bottom flask and heated at certain temperature and time [52]. The pretreatment variables were temperature, ranging from 100 to 140 °C, and residence time, ranging from 3 to 6 h, for each DES system. The pretreatment temperature and residence-time ranges were selected to evaluate a moderate DES pretreatment window that is commonly used to promote lignocellulosic fractionation while limiting excessive carbohydrate degradation and unnecessary energy input [23,26,52,53]. Temperatures above 140 °C were not included in this study because increasing acidic pretreatment severity may enhance component removal but can also accelerate sugar degradation, lignin condensation, pseudo-lignin formation, and solvent recovery burden, which may reduce the overall benefit of the process [6,27,54]. Therefore, the conditions identified in this study should be interpreted as the best-performing conditions within the investigated range, rather than as globally optimized pretreatment conditions. In addition, the $FeCl_3$ concentration in the ChCl:Gly:$FeCl_3$ system was fixed at 0.01 mol/L to focus the comparison on the effects of DES chemistry, temperature, and

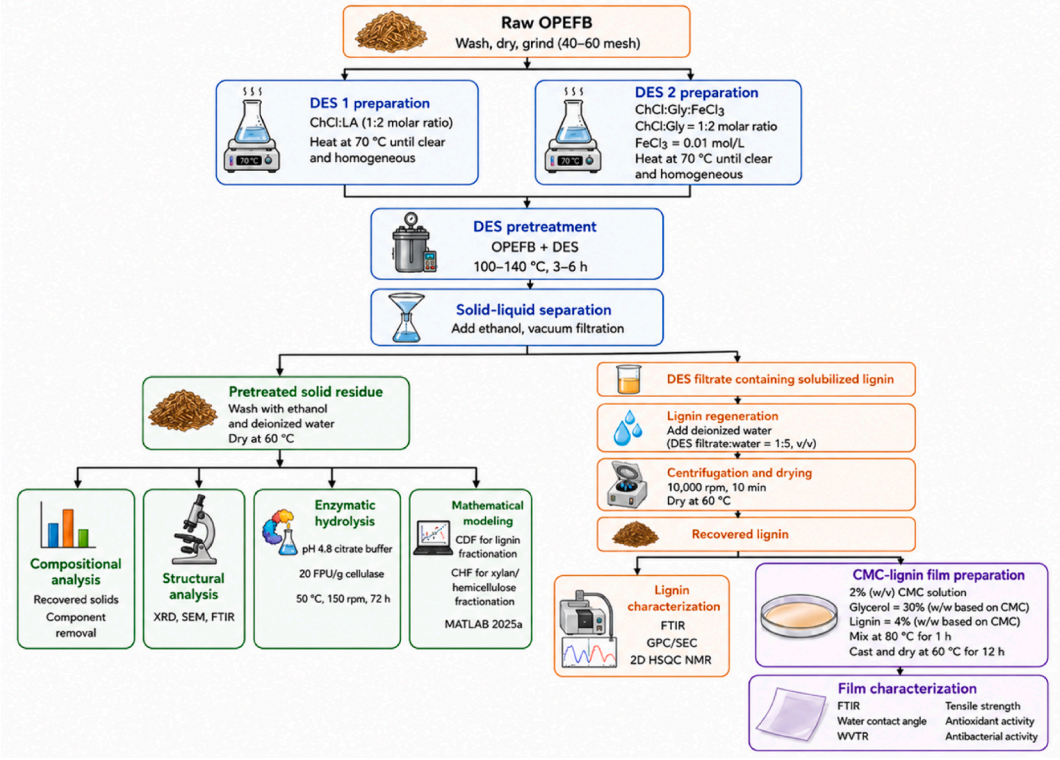

Fig. 1. Experimental workflow for OPEFB fractionation, lignin recovery, and CMC–lignin film fabrication.

residence time under a constant Lewis-acid catalyst loading. The influence of $FeCl_3$ concentration gradient was not evaluated in the present work and should be addressed in future optimization studies.

After pretreatment, 50 mL of ethanol was added to the slurry, and the mixture was vacuum-filtered. The solid residue was sequentially washed with 150 mL of ethanol and 150 mL of deionized water, then dried at 60 °C in an oven prior to further analysis. The DES phase containing solubilized lignin was subjected to lignin regeneration following the method of [51]. Briefly, deionized water was added to the DES filtrate at a ratio of 1:5 (v/v), allowing lignin to precipitate. The precipitate was recovered by centrifugation (HERMLE Z306 universal centrifuge, 10, 000 rpm, 10 min) and subsequently dried at 60 °C before characterization and preparation of lignin composite film. All pretreatment experiments were performed in triplicate to ensure reproducibility.

2.4. Mathematical reaction model

The fractionation behavior of lignocellulosic biomass during deep eutectic solvent pretreatment was modeled using response-specific combined severity factors. Since DES pretreatment simultaneously promotes lignin solubilization and hemicellulose disruption, two separate kinetic descriptors were used: the combined delignification factor (CDF) for lignin fractionation and the combined hydrolysis factor (CHF) for xylan/hemicellulose fractionation. The model was developed to integrate the effects of reaction temperature, pretreatment time, and the concentration of the dominant acidic or catalytic component in each DES system [55–57].

In this study, two DES systems were considered, namely ChCl:LA and ChCl:Gly:$FeCl_3$. For ChCl:LA, lactic acid was assigned as the active acidic component, while for ChCl:Gly:$FeCl_3$, $FeCl_3$ was assigned as the dominant Lewis-acidic catalytic component. Glycerol was considered part of the DES solvent matrix and was not included as an independent kinetic concentration term because the ChCl:Gly ratio was kept constant.

2.4.1. Lignin fractionation model

The removal of lignin from the solid fraction was assumed to follow an apparent pseudo-first-order kinetic model with respect to the residual lignin content. The active acidic or catalytic component of the DES was incorporated as a concentration-dependent term. The rate of lignin removal was expressed as Eq (1).

$$\frac{dL_{res}}{dt} = -k_L(T, C, \ldots)CL_{res} \tag{1}$$

where L_{res} represents the residual lignin fraction remaining in the pretreated solid, T is the reaction temperature (K), C is the concentration of the dominant active component in the DES system, and $k_L(T, C, \ldots)$ is the apparent delignification rate coefficient.

For the ChCl:LA system:

$$C = C_{LA} \tag{2}$$

where C_{LA} represents the lactic acid concentration.

For the ChCl:Gly:$FeCl_3$ system:

$$C = C_{Fe} \tag{3}$$

where C_{Fe} represents the $FeCl_3$ concentration.

The apparent delignification rate coefficient was described using an Arrhenius-type empirical relationship.

$$k_L = exp\left(\alpha_L - \frac{E_{a,L}}{RT} + \beta_L C\right) \tag{4}$$

Where $E_{a,L}$ is the apparent activation energy for lignin removal, R is the universal gas constant, and α_L and β_L are empirical fitted parameters. The term $\beta_L C$ represents the contribution of the active acidic or catalytic component to lignin fractionation [55,56,58].

Accordingly, the combined delignification factor was defined as Eq. (5)

$$CDF = \exp\left(\alpha_L - \frac{E_{a,L}}{RT} + \beta_L C\right)Ct \tag{5}$$

where t is the pretreatment time.

To account for the heterogeneous structure of lignin in the biomass matrix, lignin was divided into two fractions: a fast-removing lignin fraction and a slow-removing lignin fraction [58,59]. The corresponding rate equations were written as:

$$\frac{dL_f}{dt} = -k_L CL_f \tag{6}$$

$$\frac{dL_s}{dt} = -f_L k_L CL_s \tag{7}$$

where L_f and L_s represent the fast- and slow-removing lignin fractions, respectively. The parameter f_L is the relative rate constant of the slow-removing lignin fraction compared with the fast-removing fraction. The initial proportion of slow-removing lignin is denoted as θ_L, while $1 - \theta_L$ represents the fast-removing lignin fraction.

By solving the differential equations, the residual lignin fraction can be expressed as a function of CDF:

$$L_{res} = (1 - \theta_L)\exp(-CDF) + \theta_L \exp(-f_L CDF) \tag{8}$$

For the two DES systems, the CDF can be written separately as:

$$CDF_{LA} = \exp\left(\alpha_{L,LA} - \frac{E_{a,L,LA}}{RT} + \beta_{L,LA}C_{LA}\right)C_{LA}t \tag{9}$$

$$CDF_{Fe} = \exp\left(\alpha_{L,Fe} - \frac{E_{a,L,Fe}}{RT} + \beta_{L,Fe}C_{Fe}\right)C_{Fe}t \tag{10}$$

where CDF_{LA} and CDF_{Fe} represent the combined delignification factors for ChCl:LA and ChCl:Gly:$FeCl_3$ pretreatment, respectively.

The objective function for lignin fractionation was defined as the sum of squared errors between the modeled and experimental residual lignin values.

$$F_L = \sum_{i=1}^{N}\left(L_{res,i}^{model} - L_{res,i}^{exp}\right)^2 \tag{11}$$

where N is the number of experimental data points, while $L_{res,i}^{model}$ and $L_{res,i}^{exp}$ are the predicted and experimentally measured residual lignin fractions, respectively.

2.4.2. Hemicellulose/xylan fractionation model

The fractionation of hemicellulose was modeled based on the removal of xylan from the solid fraction. Similar to lignin removal, xylan solubilization was described using an apparent pseudo-first-order kinetic expression with respect to the residual xylan content [37,60]:

$$\frac{dX_{res}}{dt} = -k_X(T, C, \ldots)CX_{res} \tag{12}$$

where X_{res} represents the residual xylan fraction remaining in the pretreated solid, and $k_X(T, C, \ldots)$ is the apparent xylan hydrolysis or solubilization rate coefficient.

The apparent rate coefficient for xylan fractionation was expressed as:

$$k_X = \exp\left(\alpha_X - \frac{E_{a,X}}{RT} + \beta_X C\right) \tag{13}$$

where $E_{a,X}$ is the apparent activation energy for xylan removal, and α_X and β_X are empirical fitted parameters.

The combined hydrolysis factor was therefore defined as:

$$CHF = \exp\left(\alpha_X - \frac{E_{a,X}}{RT} + \beta_X C\right) Ct \quad (14)$$

In the context of this study, CHF was used to describe the extent of hemicellulose/xylan fractionation during DES pretreatment, rather than enzymatic hydrolysis.

Xylan was also assumed to consist of fast- and slow-removing fractions. The kinetic expressions for these fractions were written as:

$$\frac{dX_f}{dt} = -k_X C X_f \quad (15)$$

$$\frac{dX_s}{dt} = -f_X k_X C X_s \quad (16)$$

where X_f and X_s represent the fast- and slow-removing xylan fractions, respectively. The parameter f_X represents the relative rate constant of the slow-removing xylan fraction compared with the fast-removing fraction. The initial proportion of slow-removing xylan is denoted as θ_X [60,61].

By solving the corresponding differential equations, the residual xylan fraction can be expressed as:

$$X_{res} = (1-\theta_X)\exp(-CHF) + \theta_X \exp(-f_X CHF) \quad (17)$$

For the two DES systems, the CHF can be written separately as:

$$CHF_{LA} = \exp\left(\alpha_{X,LA} - \frac{E_{a,X,LA}}{RT} + \beta_{X,LA} C_{LA}\right) C_{LA} t \quad (18)$$

$$CHF_{Fe} = \exp\left(\alpha_{X,Fe} - \frac{E_{a,X,Fe}}{RT} + \beta_{X,Fe} C_{Fe}\right) C_{Fe} t \quad (19)$$

where CHF_{LA} and CHF_{Fe} represent the combined hydrolysis factors for ChCl:LA and ChCl:Gly:$FeCl_3$ pretreatment, respectively.

The objective function for xylan fractionation was defined as:

$$F_X = \sum_{i=1}^{N} \left(X_{res,i}^{model} - X_{res,i}^{exp}\right)^2 \quad (20)$$

where $X_{res,i}^{model}$ and $X_{res,i}^{exp}$ are the predicted and experimentally measured residual xylan fractions, respectively.

For clarity, the concentration term C_i used in the CDF and CHF equations refers to the molar concentration of the dominant active acidic or catalytic component in the prepared DES formulation, expressed in mol/L. For the ChCl:LA system, C_i corresponds to the effective lactic acid concentration, C_{LA}, calculated from the ChCl:LA molar ratio of 1:2 in the DES mixture. For the ChCl:Gly:$FeCl_3$ system, C_i corresponds to the $FeCl_3$ concentration, C_{FeCl_3}, which was fixed at 0.01 mol/L. Since the active component concentration was fixed within each DES system, C_i was used as a formulation-specific acid/catalyst contribution term, while temperature and residence time represented the varied operating conditions. The coefficient β_i has units of L/mol so that the product $\beta_i C_i$ is dimensionless in the exponential term. Therefore, the CDF and CHF values should be interpreted as empirical response-specific severity descriptors rather than independent optimization parameters for acid or catalyst concentration. All the objective functions were solved by using MATLAB 2025a.

2.5. Enzymatic hydrolysis

The enzymatic hydrolysis of OPEFB was performed using cellulase enzyme according to the procedure adapted from Huo et al. [23]. Briefly, 0.5 g of raw or pretreated solid residue was suspended in a citric acid–sodium citrate buffer solution at pH 4.8. Cellulase was then added at an enzyme loading of 20 FPU/g dry substrate, calculated based on the dry mass of raw or DES-pretreated OPEFB solid. The hydrolysis reaction was conducted in a shaker incubator at 50 °C and 150 rpm for 72 h. The enzymatic hydrolysis yield was calculated using Eq. (21), as described by Ref. [62].

$$\%Y_{EH} = \frac{released\ glucose \times 0.9(g)}{cellulose\ in\ substrate(g)} \times 100\% \quad (21)$$

where $\%Y_{EH}\%$ represents the enzymatic hydrolysis yield obtained from the hydrolysate.

To evaluate the relationship between pretreatment severity and enzymatic digestibility, Y_{EH} was correlated with both the CHF and CDF. CHF represents the severity of xylan or hemicellulose hydrolysis, while CDF represents the severity of lignin removal during DES pretreatment. These two descriptors were selected because enzymatic hydrolysis is affected by both hemicellulose removal and delignification[58,63]. Hemicellulose removal could improve cellulose accessibility by opening the polysaccharide matrix, whereas lignin removal can reduce physical shielding and non-productive enzyme adsorption.

The relationship between enzymatic hydrolysis yield and the modified severity factor was described using an empirical exponential model, as shown in Eq. (22):

$$\%Y_{EH} = a \cdot exp\ (b \cdot CHF) + c \quad (22)$$

where Y_{EH} is the enzymatic hydrolysis yield, SF represents either CHF or CDF, and a, b, and c are fitted parameters. In this model, c represents the asymptotic hydrolysis yield approached at higher pretreatment severity, a describes the difference between the initial and limiting hydrolysis yield, and b represents the sensitivity of enzymatic hydrolysis yield to increasing pretreatment severity. For each DES system, separate correlations were developed between Y_{EH} and CHF, and between Y_{EH} and CDF. The $CHF - Y_{EH}$ correlation was used to evaluate the contribution of hemicellulose/xylan removal to enzymatic digestibility, whereas the $CDF - Y_{EH}$ correlation was used to evaluate the contribution of delignification. The fitting quality was evaluated using the coefficient of determination (R^2) and root mean square error ($RMSE$).

2.6. Preparation of carboxymethyl cellulose (CMC)-Lignin film

CMC–lignin films were prepared using a solution casting method adapted from Zhu et al. [47], with minor modification. Briefly, CMC solution was prepared by dissolving CMC at a concentration of 2% (w/v) in water at 80 °C for 30 min. Glycerol was then added at 30% (w/w based on CMC) as a plasticizer and mixed until homogeneous. Separately, recovered lignin was dispersed in 1 mol/L NaOH at 4% (w/w based on CMC) and stirred until a uniform lignin dispersion was obtained. The lignin loading of 4% (w/w based on CMC) was selected by adapting the CMC–DES lignin film formulation reported by Zhu et al. [47], and was used as a fixed comparative loading in this study. This loading was chosen to evaluate how lignin source and pretreatment chemistry influence CMC–lignin film properties, rather than to optimize lignin content. Lignin can improve CMC films by introducing hydrophobic aromatic domains, phenolic antioxidant sites, and possible hydrogen-bonding interactions with the CMC matrix. These interactions may enhance water resistance, moisture-barrier performance, antioxidant activity, and tensile reinforcement. However, excessive lignin loading may also promote aggregation, phase separation, film roughness, brittleness, and reduced elongation at break. Therefore, further formulation studies using different lignin loadings are required to determine the optimum balance between mechanical strength, flexibility, water resistance, antioxidant activity, and film processability. The CMC solution and lignin dispersion were subsequently mixed at a volume ratio of 1:1 and maintained at 80 °C for 1 h to obtain the film-forming solution. The resulting solution was cast onto a mold and dried in a hot-air oven at 60 °C for 12 h to obtain the CMC-lignin film. Since no neutralization or washing step was applied after NaOH-assisted lignin dispersion, the resulting films are discussed as preliminary functional CMC–lignin composite films. Further residual alkali analysis,

migration testing, and safety evaluation are required before direct food-contact packaging application.

2.7. Analytical method

2.7.1. Determination of sugars in liquid hydrolysate and solid compositional analysis

The sugar concentrations in hydrolysates obtained from compositional hydrolysis and enzymatic hydrolysis were quantified using high-performance liquid chromatography (HPLC). The analysis was performed using a Thermo Scientific Vanquish Core HPLC system (Thermo Scientific, USA), equipped with a HyperREZ XP Carbohydrate Pb++ column (8 μm, 300 × 7.7 mm) and a refractive index (RI) detector. Separation was carried out using HPLC-grade water as the mobile phase, with the operating conditions set at a flow rate of 0.6 mL/min, column temperature of 85 °C, and system pressure of 9 bar.

The chemical composition of the biomass was determined according to the NREL analytical protocol reported by Sluiter et al. [64]. In brief, the biomass was subjected to acid hydrolysis using concentrated sulfuric acid to convert structural carbohydrates into monomeric sugars for quantification. This method was also used to determine lignin fractions, including acid-soluble lignin (ASL) and acid-insoluble lignin (AIL).

The influence of DES pretreatment on OPEFB fractionation was assessed based on solid recovery and the removal efficiency of individual biomass components. Solid recovery represents the percentage of residual solid retained after pretreatment relative to the initial OPEFB mass, while component removal indicates the extent to which each major component was solubilized or removed during pretreatment. These values were calculated using Eqs. (23) and (24):

$$\textit{Recovered solids}\ (\%) = \left(\frac{\textit{mass of pretreated OPEFB}\ (g)}{\textit{initial mass of OPEFB}\ (g)}\right) \times 100 \tag{23}$$

$$R_i\ (\%) = \left(1 - \frac{\text{mass of component } i \text{ in pretreated OPEFB (g)}}{\text{mass of component } i \text{ in initial OPEFB (g)}}\right) \times 100 \tag{24}$$

Where R_i refers to the removal percentage of a specific OPEFB component, namely hemicellulose, cellulose, or lignin.

In addition, the lignin recovery yield (Y_L) obtained from each pretreatment condition was calculated by comparing the mass of isolated lignin with the initial lignin content in OPEFB, as shown below:

$$Y_L = \frac{\text{isolated lignin (g)}}{\text{initial lignin content in OPEFB (g)}} \times 100 \tag{25}$$

2.7.2. Crystallinity, morphology, and functional group analyses of pretreated OPEFB

The effects of pretreatment conditions on the structural characteristics of OPEFB were further evaluated by examining changes in crystallinity, surface morphology, and functional groups. The crystallinity of the solid fractions obtained from untreated and hydrothermally pretreated OPEFB was determined by X-ray diffraction (XRD) analysis based on Segal's method [65]. XRD patterns were recorded using an X'Pert PRO diffractometer (PANalytical BV, Netherlands) equipped with Cu Kα radiation, operated at 40 kV and 30 mA. The crystallinity index (CrI) was calculated according to Eq. (26).

$$\textit{CrI}\ (\%) = \frac{I_{002} - I_{am}}{I_{002}} \times 100\% \tag{26}$$

where I_{002} represents the diffraction intensity of the 002 cellulose crystalline plane at $2\theta = 22.6^{\circ}$, while I_{am} denotes the intensity associated with the amorphous cellulose region at $2\theta = 18^{\circ}$.

The surface morphology of OPEFB before and after pretreatment was examined using scanning electron microscopy (SEM; Hitachi FlexSEM 1000, Japan) to observe pretreatment-induced structural disruption [66]. In addition, Fourier transform infrared (FTIR) spectroscopy was performed using an Agilent Cary 630 FTIR Spectrometer (USA) to identify alterations in the functional groups of the OPEFB samples after pretreatment [37].

2.7.3. Lignin characterizations

The recovered lignin samples were characterized by its purity, FTIR, GPC/SEC, and 2D HSQC NMR. Lignin purity was determined by compositional analysis according to the NREL lignin determination procedure, considering acid-insoluble and acid-soluble lignin fractions relative to the dried recovered lignin mass. FTIR analysis was performed using a Cary 630 FTIR Spectrometer (Agilent Technologies, USA) over a wavenumber range of 4000–650 cm^{-1} to identify the characteristic functional groups of lignin. GPC/SEC analysis was conducted using a system equipped with a refractive index detector and a TSKgel SuperAW5000 column. THF was used as the mobile phase at a flow rate of 0.3 mL/min, with an injection volume of 20 μL. The column and pump temperatures were maintained at 40 °C, and molecular weight parameters, including Mn, Mw, and Mw/Mn, were calculated using polystyrene standards in THF. The structural characteristics of the recovered lignin were further analyzed using 2D HSQC NMR on a Bruker Avance Neo-Ascend 500 MHz spectrometer operating at 500 MHz for ^{1}H and 125 MHz for ^{13}C. This characterization was conducted to evaluate the structural differences between lignin recovered from ChCl-LA and ChCl-Gly-$FeCl_3$ DES pretreatment systems. The 2D-HSQC spectra were interpreted based on representative lignin aromatic and side-chain regions. Manual integration was performed for selected cross-peak regions corresponding to S, G, H/p-coumarate-related aromatic units, β-O-4-related, β–5-related, β–β/overlapped oxygenated linkage regions, and methoxy groups. The integrated values were used as semi-quantitative structural indicators. The $S_{2,6}$ and H/p-coumarate-related aromatic integrals were divided by two to account for two equivalent aromatic positions, while linkage-related regions were normalized to the total corrected aromatic integral and expressed per 100 aromatic units. Weak, overlapping, or poorly resolved contours were interpreted cautiously and were not treated as absolute lignin structural contents.

2.7.4. Characterizations of CMC-lignin film

The properties of the CMC-based films were evaluated by FTIR, water contact angle, water vapor transmission rate (WVTR), tensile strength, and antioxidant. FTIR spectra were recorded using a Cary 630 FTIR Spectrometer (Agilent Technologies, USA) over a wavenumber range of 4000–650 cm^{-1} to identify functional groups and possible interactions between CMC and lignin. Water contact angle analysis was performed using a DataPhysics OCA-Series instrument by placing water droplets on the film surface using the sessile drop method. Three measurements were recorded for each sample.

The WVTR was measured using the gravimetric cup method. Film samples were mounted on WVTR cups, and mass changes were measured using an analytical balance (OHAUS). The analysis was performed in duplicate, and the results were reported as mean values with standard deviations. Mechanical properties were determined by tensile strength testing using rectangular film strips with dimensions of 30 mm × 5 mm. The test was conducted with a deformation length of 30 mm, trigger force of 4.5 g, and crosshead speed of 1.0 mm/s. Tensile strength and elongation at break were calculated from the recorded force and deformation data, while antioxidant activity was determined using the DPPH assay and expressed as IC_{50}.

3. Results and discussions

3.1. Modified severity factor determination on xylan degradation and delignification of OPEFB

This study evaluated the applicability of the CDF and CHF to describe lignin removal and xylan hydrolysis during DES pretreatment of OPEFB.

The fitted parameters for the CDF and CHF models are summarized in Table 1, while the correlations between residual lignin (L_{res}), residual xylan (X_{res}), and their corresponding modified severity factors are presented in Fig. 2. CDF was used to represent the severity of delignification, whereas CHF was used to represent the severity of xylan hydrolysis. These parameters integrate the effects of reaction temperature, residence time, and acid/catalyst contribution into single kinetic descriptors. This approach is relevant because ChCl:LA and ChCl:Gly:$FeCl_3$ are both acidic DESs, but they differ in catalytic behavior. ChCl:LA mainly provides Brønsted acidity through lactic acid, whereas ChCl:Gly:$FeCl_3$ introduces Fe^{3+}-based Lewis acidity [26,35].

As shown in Fig. 2a and b, the residual lignin fraction (Lres) decreased with increasing CDF in both DES systems, indicating that the proposed CDF descriptor adequately represented the progress of delignification during OPEFB pretreatment. In the ChCl:LA system, Lres decreased sharply at low CDF and subsequently approached a residual level of approximately 0.16 after CDF exceeded 2. A similar decreasing trend was observed in the ChCl:Gly:$FeCl_3$ system, although the CDF range was broader. In this system, Lres decreased rapidly at low CDF, followed by a slower decline after CDF exceeded 5, suggesting that additional increases in pretreatment severity produced progressively smaller improvements in lignin removal. The nonlinear decline of L_{res} suggests that delignification did not proceed as a single homogeneous reaction, but rather followed a biphasic pattern involving fast-removing and slow-removing lignin fractions. The fast-removing fraction can be associated with more accessible lignin domains, labile ether linkages, and lignin–carbohydrate linkages that are readily cleaved during the early stage of DES pretreatment [58,59,67]. In contrast, the slow-removing fraction likely corresponds to lignin structures that are more condensed, less accessible, or more strongly embedded within the cell wall matrix. Therefore, the plateau-like behavior observed at higher CDF values may indicate that the easily removable lignin fraction had been largely solubilized, while further delignification was limited by the persistence of recalcitrant lignin domains. In the ChCl:LA system, the rapid decrease in Lres at relatively low CDF suggests that the Brønsted-acidic DES effectively promoted lignin solubilization within a narrower severity window [22,26]. Conversely, the broader CDF range observed for ChCl:Gly:$FeCl_3$ indicates that $FeCl_3$-assisted DES pretreatment required higher effective severity to approach a comparable residual lignin level. This behavior may also be associated with partial lignin condensation, pseudo-lignin formation, or lignin redeposition under more severe acidic conditions, which has been reported during acid-catalyzed biomass pretreatment and is further evaluated in this study through solid FTIR and lignin structural characterization [34,54,68]. High coefficients of determination were obtained for both ChCl:LA ($R^2 = 0.996$) and ChCl:Gly:$FeCl_3$ ($R^2 = 0.977$), confirming that CDF captured the severity-dependent delignification behavior with good accuracy. The apparent activation energy for lignin removal was higher in ChCl:Gly:$FeCl_3$ (87.84 kJ/mol) than in ChCl:LA (63.47 kJ/mol), suggesting that delignification in the $FeCl_3$-containing DES was more temperature-sensitive. This higher temperature dependency is consistent with the catalytic role of Fe^{3+}, where elevated temperature may intensify Lewis acid-assisted cleavage of lignin-associated and ether-type linkages during metal salt-assisted pretreatment [69,70]. However, the higher activation energy also implies that lignin removal in ChCl:Gly:$FeCl_3$ is less readily promoted at lower severity than in ChCl:LA. The relatively high

$\alpha_{L,Fe}$ value also reflects the broader severity scale required to describe delignification in the $FeCl_3$-assisted system, whereas ChCl:LA produced effective lignin solubilization over a narrower CDF range.

Similar to delignification, in Fig. 2c and d xylan removal also exhibited biphasic behavior. At low CHF, Xres decreased rapidly, indicating the hydrolysis of the fast-hydrolyzing xylan fraction. This fraction is likely located in more accessible regions of the biomass cell wall and is therefore more susceptible to acid-catalyzed cleavage, as previously observed for biphasic xylan hydrolysis during acidic pretreatment of lignocellulosic biomass [13,58,59]. At higher CHF values, the decrease in Xres became slower, indicating that the remaining xylan belonged to a slow-hydrolyzing fraction. This resistant fraction may be more strongly associated with cellulose and lignin through hydrogen bonding or lignin–carbohydrate complexes, making it less accessible to hydrolytic attack [55,71]. The stronger xylan hydrolysis observed in ChCl:Gly:$FeCl_3$ can be attributed to the Lewis acidity of Fe^{3+}, which may coordinate with oxygen-containing glycosidic linkages and facilitate their cleavage [30,31,72]. Thus, the $FeCl_3$-containing DES appears particularly effective in disrupting hemicellulose, including both readily accessible and more resistant xylan fractions.

The fitted CHF parameters in Table 1 also indicate that the proposed model effectively described xylan hydrolysis in both DES systems. The CHF model gave R^2 values of 0.969 for ChCl:LA and 0.996 for ChCl:Gly:$FeCl_3$, confirming good agreement between experimental and predicted residual xylan fractions. The apparent activation energy for xylan hydrolysis was higher in ChCl:Gly:$FeCl_3$ (69.87 kJ/mol) than in ChCl:LA (49.54 kJ/mol), indicating that xylan removal in the $FeCl_3$-containing DES was more strongly governed by temperature. This finding is consistent with the broader CHF range observed in ChCl:Gly:$FeCl_3$ and supports the interpretation that Fe^{3+} intensifies hemicellulose hydrolysis at elevated temperatures, as reported in metal chloride-assisted pretreatment systems [34,73,74]. In contrast, the lower activation energy in ChCl:LA suggests that xylan removal can proceed more readily under milder Brønsted-acidic conditions, although the overall extent of xylan removal was lower than that obtained using ChCl:Gly:$FeCl_3$.

The fitted fast- and slow-fraction parameters provide additional insight into the heterogeneous nature of OPEFB fractionation. For lignin removal, the slow-removing fraction represents lignin that remains difficult to solubilize after the more labile lignin domains have been extracted. For xylan hydrolysis, the slow-hydrolyzing fraction represents xylan that remains protected within the biomass matrix. Therefore, the biphasic behavior observed for both L_{res} and X_{res} reflects the heterogeneous distribution and accessibility of lignin and hemicellulose in OPEFB, consistent with previous kinetic interpretations of lignocellulosic fractionation using severity-based descriptors [58,59,63]. The comparison between ChCl:LA and ChCl:Gly:$FeCl_3$ further indicates that

Table 1
Fitted parameters for CDF and CHF models on delignification and xylan hydrolysis for each DES system.

Model	Parameter	Unit	Fitted value	Parameter	Unit	Fitted value
	ChCl:LA			ChCl:Gly:$FeCl_3$		
CDF	$E_{a,L,LA}$	kJ/mol	63.47	$E_{a,L,Fe}$	kJ/mol	87.84
	$\theta_{L,LA}$	–	0.20	$\theta_{L,Fe}$	–	0.23
	$f_{L,LA}$	–	0.02	$f_{L,Fe}$	–	0.01
	$\alpha_{L,LA}$	–	2.71	$\alpha_{L,Fe}$	–	28.01
	$\beta_{L,LA}$	L/mol	3.12	$\beta_{L,Fe}$	L/mol	1.41
	R^2	–	0.996	R^2	–	0.977
CHF	$E_{a,X,LA}$	kJ/mol	49.54	$E_{a,X,Fe}$	kJ/mol	69.87
	$\theta_{X,LA}$	–	0.43	$\theta_{X,Fe}$	–	0.24
	$f_{X,LA}$	–	0.10	$f_{X,Fe}$	–	0.05
	$\alpha_{X,LA}$	–	15.42	$\alpha_{X,Fe}$	–	23.29
	$\beta_{X,LA}$	L/mol	−1.37	$\beta_{X,Fe}$	L/mol	0.69
	R^2	–	0.969	R^2	–	0.996

Ea is expressed in kJ/mol. C_i is the concentration of the dominant active component in the DES system, expressed in mol/L: C_{LA} for ChCl:LA and C_{FeCl_3} for ChCl:Gly:$FeCl_3$. The coefficient β_i is expressed in L/mol so that $\beta_i C_i$ is dimensionless. All CDF and CHF values were calculated using temperature in K, pretreatment time in h, and active component concentration in mol/L. Because the active component concentration was fixed within each DES system, β_i represents an empirical acid/catalyst contribution for the selected DES formulation.

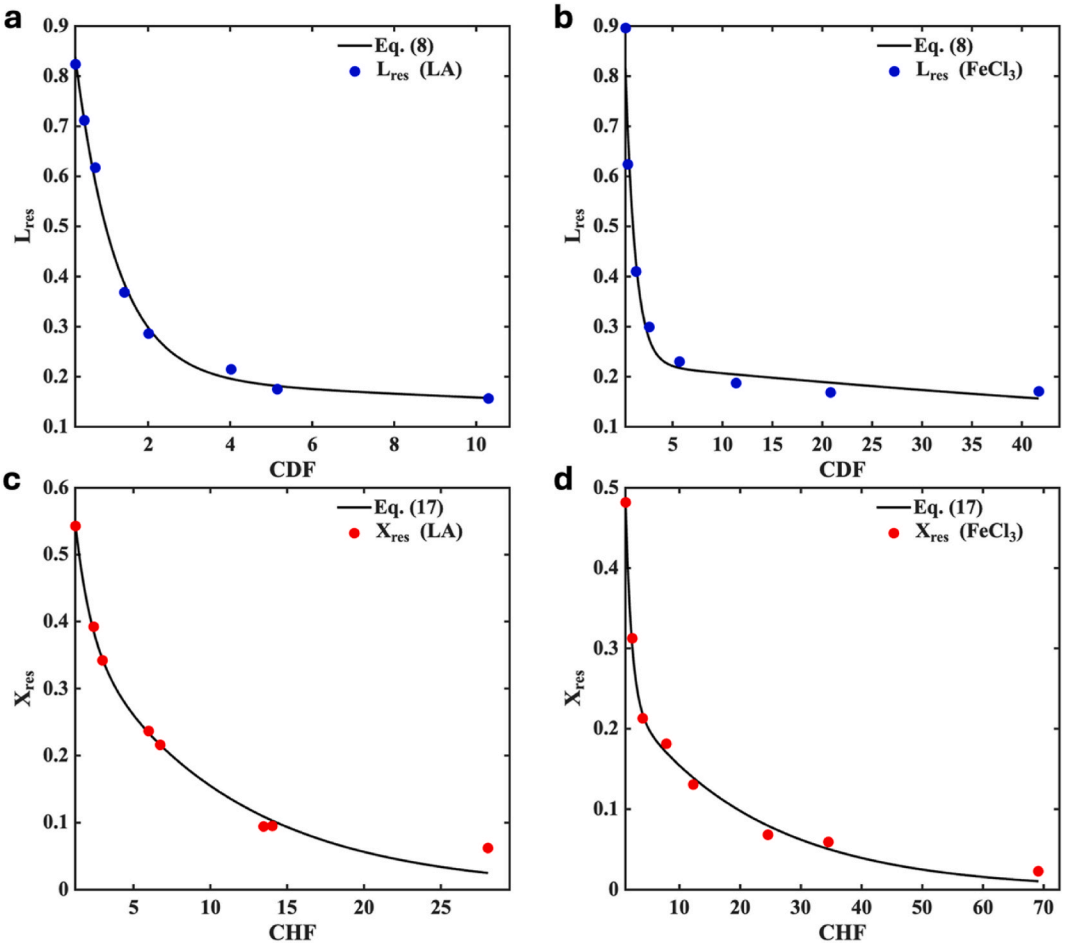

Fig. 2. Correlation of residual lignin and xylan with modified severity factors during DES pretreatment. Residual lignin content, L_{res}, as a function of CDF for (a) ChCl:LA and (b) ChCl:Gly:$FeCl_3$, and residual xylan content, X_{res}, as a function of CHF for (c) ChCl:LA and (d) ChCl:Gly:$FeCl_3$.

the two DES systems deconstruct OPEFB through different dominant pathways. ChCl:LA favors efficient lignin solubilization, which is consistent with previous reports showing that lactic acid-based acidic DESs promote cleavage of lignin–carbohydrate linkages, xylan elimination, and lignin dissolution through Brønsted acidity and hydrogen-bonding interactions [23,25,26]. In contrast, ChCl:Gly:$FeCl_3$ more strongly promotes xylan hydrolysis, in agreement with studies showing that Fe^{3+} or metal chloride-assisted pretreatment enhances hemicellulose depolymerization through Lewis acid-catalyzed cleavage of glycosidic linkages [30,31,74].

Overall, the CDF and CHF models successfully described the severity-dependent fractionation behavior of OPEFB during DES pretreatment. The high fitting accuracy obtained for both descriptors confirms that lignin removal and xylan hydrolysis can be represented separately using response-specific severity factors. ChCl:LA promoted effective delignification within a relatively narrow CDF range, supporting the strong lignin-solubilizing ability commonly reported for ChCl:LA and other organic acid-based DES systems [23,25,26]. Meanwhile, ChCl:Gly:$FeCl_3$ generated stronger xylan hydrolysis over a broader CHF range, reflecting the hydrolytic contribution of Fe^{3+} in the DES matrix [73–75]. These findings demonstrate that the effective severity of DES pretreatment depends not only on temperature and residence time, but also on the acid type and catalytic mechanism of the solvent system. Therefore, CHF and CDF provide useful empirical descriptors for comparing Brønsted-acidic and Lewis acid-assisted DES pretreatments of OPEFB. By unifying temperature, residence time, and acid or catalytic contribution into response-specific severity parameters, these descriptors can support process comparison, operating-window selection, and future scale-up evaluation of DES pretreatment systems. This agrees with previous studies applying combined or modified severity factors to interpret carbohydrate hydrolysis, delignification, and enzymatic digestibility [55,59,63,76].

3.2. *Effect of DES pretreatment variables on OPEFB biomass and lignin recovery*

The effect of DES pretreatment severity on OPEFB fractionation is presented in Fig. 3. The pretreatment conditions were primarily arranged according to the actual operating variables, namely temperature and residence time, while the corresponding CHF and CDF values were included as severity descriptors to support comparison between the two DES systems. In this figure, the upper axis denotes the actual pretreatment condition, whereas CHF and CDF provide unified severity values that reflect the combined influence of temperature, time, and acid or catalytic contribution. The use of severity descriptors is beneficial because it allows different pretreatment conditions to be interpreted through a common scale, facilitates comparison between solvent systems, and supports the identification of an effective operating window for future process development and scale-up evaluation [36,52,53,55]. Fig. 3a and b shows the chemical composition of the recovered solid fractions, while Fig. 3c and d presents hemicellulose removal, cellulose recovery, delignification, and lignin yield. These responses are important because an effective pretreatment should remove non-cellulosic barriers, preserve sufficient cellulose for enzymatic hydrolysis, and recover lignin as a useable product stream.

The untreated OPEFB initially contained approximately 38.6%

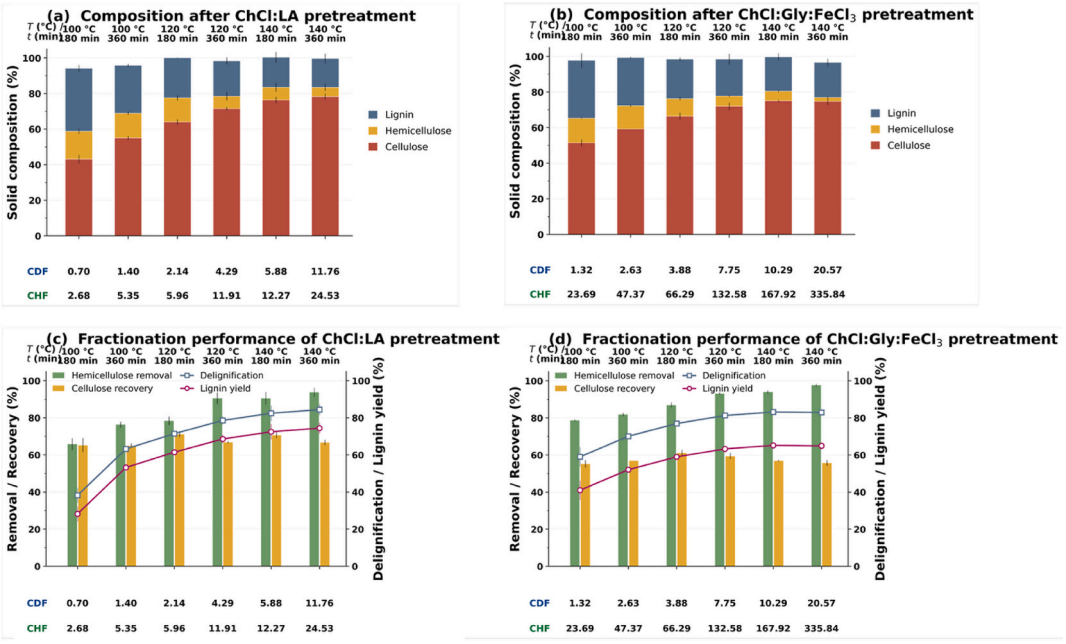

Fig. 3. Severity-dependent compositional and fractionation responses of two DES systems. (a,b) Chemical composition of the recovered solid fraction after pretreatment with ChCl:LA & ChCl:Gly:$FeCl_3$. (c,d) Hemicellulose removal, cellulose recovery, delignification and lignin yield of ChCl:LA & ChCl:Gly:$FeCl_3$ system.

cellulose, 26.8% hemicellulose, and 33.2% lignin. After DES pretreatment, the relative composition of the recovered solid shifted substantially, reflecting the selective removal of non-cellulosic components. For the ChCl:LA system, the cellulose proportion in the recovered solid increased markedly with increasing pretreatment severity, from approximately 43% to 78%. In parallel, the hemicellulose fraction decreased from approximately 16% to below 6%, while the lignin fraction decreased from approximately 35% to 16%. This compositional shift indicates that ChCl:LA effectively removed both hemicellulose and lignin, resulting in a cellulose-enriched solid residue. The most pronounced cellulose enrichment and lignin removal were obtained at the highest tested condition of 140 °C for 6 h, indicating that the ChCl:LA system continued to respond positively to increased temperature and residence time within the investigated range. This trend is consistent with previous reports on ChCl:LA and other organic acid-based DES systems, where increasing pretreatment severity enhanced lignin dissolution, xylan removal, and cellulose enrichment [23,26,77,78]. The increase in cellulose content should be interpreted as an enrichment effect caused by the preferential solubilization of non-cellulosic components rather than the formation of additional cellulose. Such cellulose enrichment is favorable for enzymatic hydrolysis because hemicellulose and lignin removal can open the cell wall structure, reduce physical shielding, and improve enzyme accessibility [53,79–81].

A similar cellulose enrichment trend was observed in the ChCl:Gly:$FeCl_3$ system. The cellulose content increased from approximately 51% to 75%, while the hemicellulose content decreased from approximately 14% to below 3%. This result confirms that ChCl:Gly:$FeCl_3$ was highly effective in removing hemicellulose from OPEFB. However, compared with ChCl:LA, the lignin fraction in the recovered solid remained slightly higher, particularly at high severity. This indicates that the $FeCl_3$-containing DES promoted stronger hemicellulose hydrolysis but was comparatively less selective for lignin solubilization [31,33]. The strong hemicellulose removal can be attributed to the Lewis acidity of Fe^{3+}, which can catalyze glycosidic bond cleavage in xylan, as commonly reported for metal chloride-assisted pretreatment systems [30,33]. In contrast, lignin recovery is governed not only by bond cleavage but also by lignin solvation, precipitation behavior, and the accessibility of lignin within the biomass matrix [26,82]. This distinction is important because ChCl:LA and other organic acid-based DESs are often reported to be particularly effective for lignin solubilization through Brønsted acidity and hydrogen-bonding interactions, whereas $FeCl_3$-containing systems may exert stronger hydrolytic effects toward hemicellulose [33,75,83].

The fractionation performance of ChCl:LA is shown in Fig. 3c. Hemicellulose removal increased from approximately 66% to more than 90% as CHF increased, confirming the hydrolytic effect of the lactic acid-based DES on the hemicellulose fraction. Delignification also increased from approximately 39% to around 85% with increasing CDF, indicating that ChCl:LA effectively promoted lignin solubilization [84,85]. This behavior is consistent with previous studies showing that organic acid-based DESs, particularly ChCl:LA, can promote lignin dissolution and xylan elimination through Brønsted acidity, hydrogen-bonding interactions, and cleavage of lignin–carbohydrate linkages [23,29,39]. Therefore, ChCl:LA appears to provide a balanced fractionation environment in which both hemicellulose and lignin are removed while cellulose is relatively preserved.

Cellulose recovery in the ChCl:LA system remained relatively high, ranging from approximately 64% to 72% across the tested conditions. Although increasing temperature and residence time enhanced delignification and hemicellulose removal, cellulose recovery did not increase proportionally. This indicates that the most suitable operating window should balance three competing outcomes: extensive hemicellulose removal, high delignification, and sufficient cellulose preservation [86–88]. In this context, CHF and CDF are useful because these helps distinguish whether the improvement in fractionation is mainly associated with hydrolytic severity or delignification severity, rather than relying only on temperature and time as independent variables [55,63]. Within the tested range, the highest temperature and longest residence time provided the most favorable fractionation outcome for ChCl:LA, especially when lignin recovery was considered.

For the ChCl:Gly:$FeCl_3$ system, hemicellulose removal was already high at the lowest severity and increased further to approximately 95–97% at higher CHF values, as shown in Fig. 3d. This confirms that the $FeCl_3$-containing DES exerted stronger hydrolytic activity toward hemicellulose than ChCl:LA. The high CHF range of ChCl:Gly:$FeCl_3$ supports the role of Fe^{3+} as a Lewis acid catalyst that facilitates xylan cleavage [33,43,53]. Similar behavior has been reported in metal chloride-assisted pretreatment systems, where Fe^{3+} or other metal ions enhanced hemicellulose depolymerization and improved subsequent

enzymatic digestibility [33,34].

In contrast, delignification in ChCl:Gly:$FeCl_3$ increased from approximately 60% to around 83%, but the improvement became less pronounced at higher CDF. This trend agrees with the CDF-based model in Subsection 3.1, where residual lignin decreased rapidly at low CDF and then approached a plateau at higher severity. Notably, increasing the residence time from 3 h to 6 h at 140 °C did not produce a substantial additional improvement in the ChCl:Gly:$FeCl_3$ system. This indicates that the fractionation response of the $FeCl_3$-containing DES approached an effective plateau at high temperature, where the easily removable lignin fraction had been solubilized, and the remaining lignin was more resistant to be removed.

Lignin yield increased with pretreatment severity in both DES systems, confirming that higher severity promoted lignin solubilization and subsequent precipitation from the DES liquor. In ChCl:LA, lignin yield increased from approximately 29% to around 75%, whereas in ChCl:Gly:$FeCl_3$ it increased from approximately 41% to around 65%. The higher final lignin yield in ChCl:LA indicates that this system was more favorable for lignin recovery, likely because lactic acid-based DESs provide strong lignin solvation and facilitate lignin dissolution through Brønsted acidity and hydrogen-bonding interactions. Recent studies also reported high lignin extraction and recovery from ChCl:LA-based systems, supporting the suitability of this solvent for lignin-focused fractionation [23,25,26,39]. Although ChCl:Gly:$FeCl_3$ achieved strong hemicellulose removal and relatively high delignification, its lower final lignin yield suggests that part of the lignin may have remained in the solid residue or been less efficiently recovered from the DES liquor.

Overall, Fig. 3 demonstrates that the two acidic DES systems produced distinct fractionation profiles. ChCl:LA provided more balanced fractionation, combining high delignification, high lignin yield, and good cellulose enrichment. In contrast, ChCl:Gly:$FeCl_3$ showed stronger hemicellulose removal and higher hydrolytic severity, producing a cellulose-rich solid that is favorable for enzymatic hydrolysis, but with comparatively lower lignin recovery. These differences confirm that the pretreatment outcome depends not only on severity level but also on the acid type and catalytic mechanism of the DES system. The severity-factor approach is therefore valuable because it converts multiple operational variables into comparable response-oriented descriptors, helping to identify whether additional severity still improves fractionation or whether the system has approached a plateau. This is particularly relevant for process scale-up, where increasing temperature or residence time is only beneficial if it produces meaningful gains in component separation and product recovery. Therefore, ChCl:LA is more suitable when lignin recovery is prioritized, particularly because the highest temperature and longest residence time still improved its fractionation outcome. Conversely, ChCl:Gly:$FeCl_3$ is more effective when extensive hemicellulose removal and cellulose accessibility are the main targets, although extending the treatment from 3 h to 6 h at 140 °C provides limited additional benefit.

3.3. Solid characterization of pretreated OPEFB

Structural characterization of untreated and DES-pretreated OPEFB was conducted using SEM, XRD, and FTIR to verify whether the fractionation behavior observed in Section 3.2 was reflected in the physical morphology, cellulose crystallinity, and functional group characteristics of the recovered solids. In Section 3.2, ChCl:LA was shown to increase the cellulose proportion while decreasing both hemicellulose and lignin contents, whereas ChCl:Gly:$FeCl_3$ produced stronger hemicellulose removal but retained a comparatively higher lignin fraction in the recovered solid. These compositional trends indicate that the two DES systems deconstructed OPEFB through different dominant pathways. However, compositional changes alone do not fully describe biomass recalcitrance because enzymatic accessibility also depends on fiber morphology, cellulose ordering, and the persistence of lignin- or hemicellulose-associated functional groups. Therefore, SEM, XRD, and FTIR were used as complementary techniques to evaluate whether the chemical fractionation trends were accompanied by structural disruption and cellulose enrichment. Similar combined characterization approaches have been used to connect biomass composition, crystallinity, functional groups, and enzymatic accessibility after pretreatment [79,89].

To compare temperature-dependent structural changes under a consistent residence-time basis, SEM, XRD, and FTIR analyses were conducted on OPEFB solids pretreated at 100, 120, and 140 °C for 3 h. The SEM images of untreated and DES-pretreated OPEFB are shown in Fig. S1, where panels a–c correspond to ChCl:LA-pretreated samples, panels d–f correspond to ChCl:Gly:$FeCl_3$-pretreated samples, and panel g represents untreated OPEFB. The untreated OPEFB showed a relatively compact and covered surface, suggesting that the native fiber structure was still protected by the lignin–hemicellulose matrix and other amorphous components. After DES pretreatment, both DES systems altered the OPEFB surface morphology, as indicated by surface roughening, partial fiber exposure, localized surace disruption, and erosion. These features suggest that DES pretreatment weakened the compact lignocellulosic architecture and increased the exposure of the pretreated fiber surface. Similar morphological changes have been reported after acidic DES pretreatment, where removal of lignin and hemicellulose opened the biomass structure and improved cellulose accessibility [25,86]. Comparable surface disruption has also been observed after metal salt-assisted pretreatment, where catalytic hydrolysis of hemicellulose weakens the cell-wall matrix [90].

For ChCl:LA-pretreated OPEFB, the surface morphology became rougher and more irregular after pretreatment. At 100 °C for 3 h, surface roughening was already observed, while the sample treated at 140 °C for 3 h showed more visible fiber exposure and fibrillation. This morphology is consistent with the compositional data in Section 3.2, where ChCl:LA produced substantial cellulose enrichment together with high delignification and lignin yield. The enhanced surface opening can be attributed to the combined effects of Brønsted acidity and hydrogen-bonding interactions in the lactic acid-based DES. Liu et al. [26] reported that acidic DES can promote cleavage of lignin–carbohydrate complexes, while H. Li et al. (2021) showed that acidic DES pretreatment enhances bamboo delignification and lignin fractionation. More recently, Rodrigues et al. [43] also demonstrated that ChCl:LA-based pretreatment can enhance lignin extraction and cellulose-to-glucose conversion. In the ChCl:Gly:$FeCl_3$ system, the pretreated OPEFB also showed clear surface modification. The samples treated at 100 and 120 °C for 3 h showed surface disruption and localized pits, whereas the sample treated at 140 °C for 3 h exhibited stronger erosion and a more porous structure. This is consistent with the composition and removal data in Section 3.2, where ChCl:Gly:$FeCl_3$ produced extensive hemicellulose removal. Fe^{3+}-assisted Lewis acidity can intensify xylan hydrolysis and weaken the polysaccharide matrix. Kamireddy et al. [31] described the role of metal chloride salts in improving lignocellulosic deconstruction, while Tang et al. [34] showed that metallic chlorides can alter lignin structure and improve enzymatic hydrolysis. Yang et al. [91] further demonstrated that metal-salt coordinated ChCl:Gly DES systems can promote lignocellulosic pretreatment through coordinated acidity and hydrogen-bond interactions.

The XRD patterns and crystallinity index (CrI) values of untreated and DES-pretreated OPEFB are shown in Fig. S2. Untreated OPEFB showed a CrI of 65.6%. After ChCl:LA pretreatment, the CrI increased markedly to 82.0%, 80.8%, and 81.0% at 100, 120, and 140 °C, respectively. The increase in CrI indicates that ChCl:LA preferentially removed amorphous components, mainly hemicellulose and lignin, thereby enriching the crystalline cellulose fraction in the recovered solid. This interpretation agrees with Section 3.2 composition data, where the cellulose proportion increased while hemicellulose and lignin contents decreased. The relatively stable CrI values at higher temperatures further suggest that the crystalline cellulose structure was largely preserved during ChCl:LA pretreatment, even though non-cellulosic

components were extensively removed. Li et al. [92] similarly reported that acidic DES pretreatment can enhance apparent crystallinity by removing lignin and hemicellulose. Da Costa Lopes et al. [93] also associated selective hemicellulose/lignin degradation with improved enzymolysis efficiency. The broader role of DES pretreatment in removing amorphous barriers and improving cellulose accessibility has also been highlighted in recent reviews [43]. A different crystallinity trend was observed for ChCl:Gly:$FeCl_3$-pretreated OPEFB. The CrI remained almost unchanged at 100 °C (65.5%), increased to 70.2% at 120 °C, and then decreased to 63.3% at 140 °C. The initial increase can be attributed to the preferential removal of amorphous components, particularly hemicellulose and part of the lignin fraction, which enriched the cellulose-rich solid. Similar increases in apparent crystallinity after pretreatment have been associated with the removal of amorphous lignin and hemicellulose fractions [43,79,92]. However, the decrease in CrI at 140 °C suggests that the $FeCl_3$-assisted DES treatment did not simply enrich crystalline cellulose. Instead, the stronger Lewis-acid-assisted deconstruction may have partially altered the ordering of the cellulose-rich solid or increased the relative contribution of less ordered cellulose domains. Since CrI calculated using the Segal method is an apparent crystallinity index, this result should not be interpreted alone as direct evidence of cellulose degradation. Rather, it should be considered together with compositional analysis, SEM morphology, FTIR spectra, and enzymatic hydrolysis results, as biomass digestibility is influenced by multiple structural and chemical features rather than crystallinity alone ([81,89]. In this context, the lower apparent CrI at high ChCl:Gly:$FeCl_3$ severity may contribute to improved cellulase accessibility by exposing less ordered or more accessible cellulose domains. Nevertheless, excessive severity must still be controlled because metallic chloride pretreatment can alter lignin and carbohydrate structures under severe conditions, which may reduce cellulose recovery or increase carbohydrate loss during pretreatment [25,34,94].

The FTIR spectra of untreated and DES-pretreated OPEFB are shown in Fig. S3. The main bands observed in the spectra were located at approximately 3333, 2907, 1729, 1603, 1509, 1371, 1327, 1238, 1110, and 1030 cm^{-1}. The broad band around 3333 cm^{-1}, corresponding to O–H stretching vibrations, decreased after DES pretreatment. This change indicates disruption of the hydrogen-bonding network among cellulose, hemicellulose, and lignin, which is consistent with the removal of matrix-forming amorphous components discussed in Section 3.2. The peak around 2907 cm^{-1}, assigned to C–H stretching vibrations in polysaccharides and lignin, also decreased after pretreatment, suggesting partial removal or structural alteration of carbohydrate and lignin components. These changes confirm that both DES systems modified the chemical environment of the OPEFB solid fraction. Similar changes in O–H and C–H stretching bands have been used to indicate hydrogen-bond disruption and biomass matrix deconstruction after DES pretreatment [23]. In the carbonyl region, the band around 1729 cm^{-1}, commonly attributed to C=O stretching of acetyl and ester groups in hemicellulose, became weaker after DES pretreatment. This decrease supports the removal of hemicellulose, consistent with the high hemicellulose removal shown in Fig. 3. The reduction of bands in the 1238–1371 cm^{-1} region, including peaks around 1371, 1327, and 1238 cm^{-1}, further indicates disruption and solubilization of hemicellulose- and lignin-associated structures. Meanwhile, the bands around 1110 and 1030 cm^{-1} are associated mainly with polysaccharide C–O–C and C–O stretching vibrations, reflecting changes in the carbohydrate-rich solid after pretreatment. H. Li et al. [25] reported similar FTIR changes after acidic DES delignification of bamboo. Huo et al. [23] also linked the reduction of hemicellulose- and lignin-associated bands with improved enzymolysis after DES pretreatment. For ChCl:LA-based pretreatment, Rodríguez-Rebelo et al. [83] further associated lignin extraction and hemicellulose removal with improved cellulose conversion. The lignin-related aromatic skeletal vibration bands around 1603 and 1509 cm^{-1} were also reduced after pretreatment. The decrease was more evident in the ChCl:LA-pretreated solid, supporting the stronger lignin solubilization and higher lignin yield obtained with the lactic acid-based DES. This agrees with the fractionation results in Section 3.2, where ChCl:LA showed more balanced hemicellulose removal and delignification. The efficient lignin removal by acidic DESs has been attributed to the ability of organic acid-based DES systems to disrupt lignin-associated linkages and improve lignin solvation [27,92]. In contrast, the persistence of lignin-related bands in ChCl:Gly:$FeCl_3$-pretreated solids suggests that part of the lignin remained associated with the recovered solid fraction. This observation is consistent with the comparatively lower lignin recovery of ChCl:Gly:$FeCl_3$, despite its strong hemicellulose removal. Tang et al. [34] also showed that metallic chloride pretreatment can strongly affect biomass deconstruction while modifying lignin structure. Therefore, FTIR analysis supports the interpretation that ChCl:LA was more favorable for lignin removal, whereas ChCl:Gly:$FeCl_3$ primarily promoted hemicellulose-directed deconstruction.

Overall, SEM, XRD, and FTIR analyses confirmed that the two DES systems modified OPEFB through different structural pathways. ChCl:LA effectively disrupted the lignin–hemicellulose matrix, reduced lignin-associated FTIR bands, and preserved high apparent cellulose crystallinity, explaining the cellulose enrichment and high lignin recovery observed in the fractionation data. This behavior is consistent with previous reports showing that organic acid-based DESs promote lignin solubilization, lignin–carbohydrate complex cleavage, and cellulose enrichment [23,26,28]. In contrast, ChCl:Gly:$FeCl_3$ produced stronger hemicellulose-directed disruption, surface erosion, and partial reduction in apparent CrI at high temperature. These changes suggest that the $FeCl_3$-containing DES increased cellulose accessibility not only by removing hemicellulose but also by opening the cell-wall structure and exposing less ordered cellulose domains. Similar effects of Fe^{3+} or metallic chloride-assisted pretreatment on hemicellulose disruption, lignocellulose deconstruction, and enzymatic digestibility have been reported previously [33,34,95]. Therefore, ChCl:LA is more favorable for balanced delignification, lignin recovery, and cellulose enrichment, whereas ChCl:Gly:$FeCl_3$ is more effective for generating a highly digestible cellulose-rich solid through hemicellulose removal and structural accessibility improvement. This integrated structural interpretation provides the basis for the enzymatic hydrolysis behavior discussed in the next section.

3.4. Effect of pretreatment on OPEFB saccharification

The effect of DES pretreatment on OPEFB saccharification was evaluated by correlating enzymatic hydrolysis yield (Y_{EH}) with CHF and CDF, as shown in Fig. 4. CHF represents the severity of xylan hydrolysis, while CDF represents the severity of delignification. Therefore, both factors were used to determine whether hemicellulose removal and lignin removal contributed to the improvement of enzymatic digestibility after ChCl:LA and ChCl:Gly:$FeCl_3$ pretreatment.

For the ChCl:LA system, Y_{EH} increased with increasing CHF, as shown in Fig. 4a. The enzymatic hydrolysis yield increased from 46.6% at low CHF to 75.8% at the highest CHF. The increase was rapid at low-to-moderate CHF and then approached a plateau at higher CHF values. This trend indicates that xylan removal strongly improved cellulose accessibility during the early stage of pretreatment. However, after most accessible hemicellulose had been removed, further increase in CHF only slightly improved enzymatic hydrolysis. The fitted model showed a good correlation between CHF and Y_{EH}, with $R^2 = 0.883$ and RMSE = 3.20%, confirming that CHF can describe the contribution of hemicellulose hydrolysis to enzymatic digestibility. A similar trend was observed when Y_{EH} was correlated with CDF for ChCl:LA, as shown in Fig. 4b. The hydrolysis yield increased with increasing CDF and reached a plateau at higher delignification severity. The correlation between CDF and Y_{EH} gave a slightly higher fitting accuracy, with $R^2 = 0.924$ and

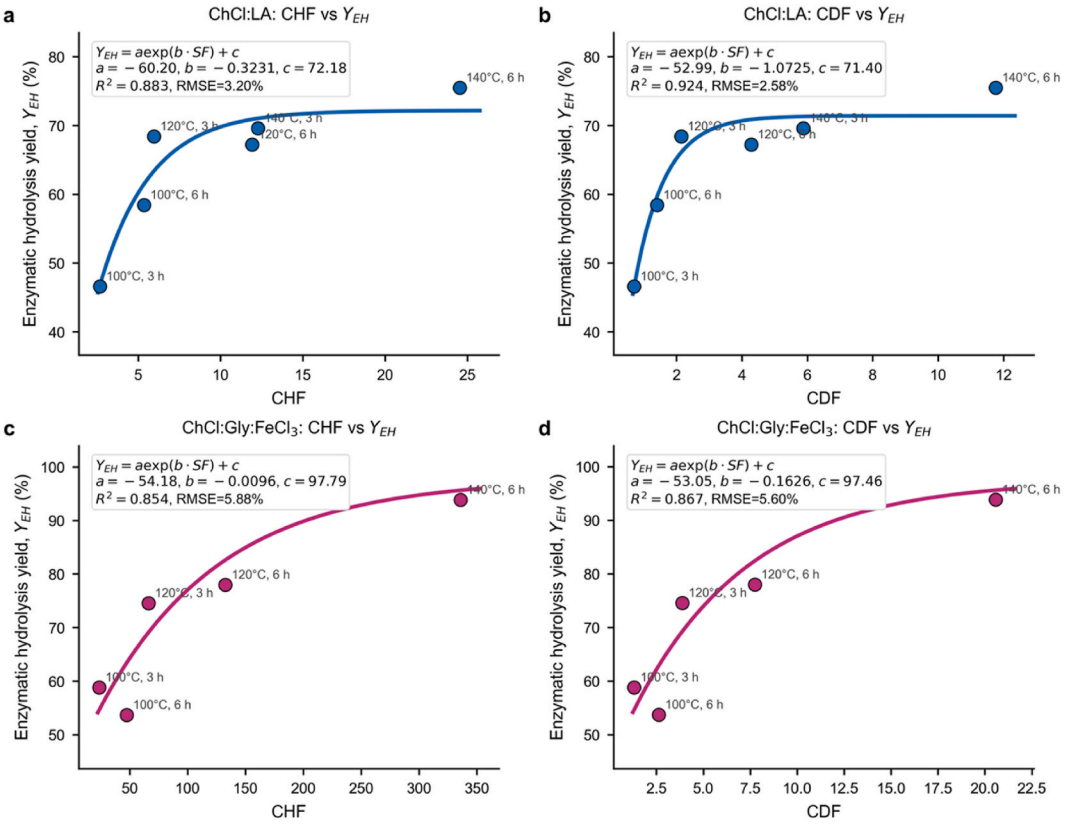

Fig. 4. Effects of modified severity factors on enzymatic hydrolysis yield of DES-pretreated OPEFB. Correlation of Y_{EH} with (a) CHF and (b) CDF for ChCl:LA, and with (c) CHF and (d) CDF for ChCl:Gly:$FeCl_3$.

RMSE = 2.58%. This suggests that, in the ChCl:LA system, lignin removal had a strong contribution to enzymatic hydrolysis improvement. This result is consistent with the fractionation data, where ChCl:LA showed effective delignification and lignin recovery. The removal of lignin likely reduced the physical barrier around cellulose and decreased non-productive enzyme binding, resulting in higher cellulose digestibility [82,96].

For the ChCl:Gly:$FeCl_3$ system, Y_{EH} also increased with increasing CHF, as shown in Fig. 4c. The hydrolysis yield increased from approximately 54–59% at low CHF to 93.8% at the highest CHF. Compared with ChCl:LA, ChCl:Gly:$FeCl_3$ reached a much broader CHF range and achieved a higher final Y_{EH}. This confirms that the $FeCl_3$-containing DES strongly enhanced OPEFB digestibility, mainly through extensive hemicellulose removal and improved cellulose accessibility. The Lewis acidity of Fe^{3+} can promote cleavage of glycosidic linkages in xylan, thereby reducing the hemicellulose barrier surrounding cellulose microfibrils and increasing cellulase access to the cellulose-rich solid [25,33]. The CHF–Y_{EH} model gave $R^2 = 0.854$ and RMSE = 5.88%, indicating a reasonable correlation, although the deviation was higher than that of the ChCl:LA model. This relatively larger deviation suggests that the hydrolysis behavior of ChCl:Gly:$FeCl_3$-pretreated OPEFB was not governed by hemicellulose removal alone, but also by additional structural and compositional factors.

The high enzymatic hydrolysis yield of ChCl:Gly:$FeCl_3$-pretreated OPEFB should also be interpreted together with the structural characterization results. Although the apparent CrI decreased at 140 °C, this decrease does not contradict the high hydrolysis yield. Enzymatic digestibility of lignocellulosic biomass is not governed by crystallinity alone, but by the combined effects of hemicellulose removal, lignin removal, cellulose exposure, accessible surface area, pore formation, and enzyme accessibility [82,97]. In the ChCl:Gly:$FeCl_3$ system, extensive hemicellulose removal reduced the xylan barrier surrounding cellulose microfibrils, while partial delignification and surface erosion decreased physical shielding and improved cellulase penetration into the recovered solid. The lower apparent CrI may also indicate partial deordering of the cellulose-rich fraction, which can increase the proportion of less ordered or more accessible cellulose domains. Therefore, the 93.8% hydrolysis yield was likely caused by the combined effects of hemicellulose removal, partial lignin removal, surface disruption, and increased cellulose accessibility, rather than by a single structural factor.

The relationship between CDF and Y_{EH} for ChCl:Gly:$FeCl_3$ is shown in Fig. 4d. The hydrolysis yield increased with increasing CDF and gradually approached a high plateau. The CDF–Y_{EH} model showed $R^2 = 0.867$ and RMSE = 5.60%, slightly better than the CHF-based correlation for the same DES system. This indicates that delignification also contributed to enzymatic hydrolysis improvement in ChCl:Gly:$FeCl_3$, although the effect was less direct than in ChCl:LA. This may be because ChCl:Gly:$FeCl_3$ primarily promoted hemicellulose removal, while part of the lignin remained in the recovered solid or may have undergone condensation or redeposition at higher severity. Such residual or modified lignin may still affect enzymatic hydrolysis through physical shielding or non-productive enzyme adsorption [7,23]. Therefore, the saccharification behavior of ChCl:Gly:$FeCl_3$ should be interpreted as a combined result of xylan removal, partial delignification, surface disruption, apparent cellulose deordering, and improved cellulose accessibility.

The different behavior between the two DES systems shows that enzymatic digestibility was controlled by multiple structural and compositional factors rather than by CHF or CDF alone. In ChCl:LA, the stronger CDF–hydrolysis relationship suggests that lignin removal played a major role in improving saccharification by reducing physical shielding and non-productive enzyme adsorption. Similar effects of lignin removal on improved enzymatic digestibility have been reported in previous lignocellulosic pretreatment studies [7,96,98]. In ChCl:Gly:

$FeCl_3$, the high final hydrolysis yield was mainly associated with stronger hydrolytic severity, extensive hemicellulose removal, surface disruption, and increased cellulose accessibility, although delignification still contributed to the overall improvement. These results agree with previous reports showing that enzymatic hydrolysis increases after pretreatment because enhances cellulose exposure, lignin removal reduces physical shielding and non-productive adsorption, and structural disruption increases enzyme-accessible surface area [81,82,99].

Overall, DES pretreatment significantly improved the enzymatic hydrolysis of OPEFB. ChCl:LA increased the hydrolysis yield up to 75.8%, while ChCl:Gly:$FeCl_3$ achieved a higher maximum yield of 93.8%. The results confirm that modified severity factors can be used to describe saccharification performance, but they should be interpreted together with compositional and structural changes. CHF mainly reflects the contribution of xylan hydrolysis to cellulose accessibility, whereas CDF reflects the contribution of lignin removal to reducing biomass recalcitrance, consistent with previous severity-based interpretations of enzymatic digestibility [55,58,63]. Therefore, the highest enzymatic hydrolysis yield was obtained when hemicellulose and lignin barriers were sufficiently disrupted, the cell-wall structure was opened, and the cellulose-rich solid became more accessible to cellulase.

The enzyme loading used in this study should also be considered when interpreting the saccharification results. A cellulase dosage of 20 FPU/g dry substrate was selected to evaluate the digestibility potential of raw and DES-pretreated OPEFB under enzyme-sufficient conditions, rather than to optimize enzyme economy. Reported cellulase loadings in lignocellulosic hydrolysis studies vary widely depending on biomass type, pretreatment method, enzyme formulation, substrate loading, and the denominator used for enzyme dosage. Low cellulase loadings of approximately 2–5 FPU/g have been reported in some optimized or assisted hydrolysis systems [100,101], whereas broader optimization studies have evaluated higher loadings extending to 40 FPU/g or above [102–104]. Intermediate loadings around 15–30 FPU/g are also frequently used in laboratory-scale lignocellulosic hydrolysis studies, including dry-matter- or substrate-based enzyme dosage [105–108]. Therefore, the 20 FPU/g dry substrate used in this work is within the commonly reported laboratory-scale range for evaluating biomass digestibility.

Nevertheless, enzyme-loading bases reported in the literature are not always directly interchangeable. Some studies express cellulase loading as FPU/g dry matter or FPU/g substrate, whereas others use FPU/g glucan or FPU/g cellulose [101–103]. These bases can lead to different apparent enzyme dosages because they depend on the cellulose or glucan content of the substrate. Therefore, the enzyme loading in the present study should be interpreted specifically as a dry-substrate-based comparative condition. Under this enzyme-sufficient condition, differences in hydrolysis yield mainly reflect pretreatment-induced changes in substrate accessibility, including hemicellulose removal, delignification, surface disruption, cellulose exposure, and reduced biomass recalcitrance. Thus, the high hydrolysis yield obtained for ChCl:Gly:$FeCl_3$--pretreated OPEFB indicates that this pretreatment produced a highly digestible cellulose-rich solid.

From a practical perspective, however, the enzyme dosage used here should not be regarded as an optimized industrial dosage. Enzyme loading is an important contributor to the operating cost of lignocellulosic sugar production, and enzyme-reduction strategies such as enzyme recycling, high-solids hydrolysis, optimized enzyme cocktails, and process additives have been widely explored to improve process feasibility [100,104,109]. Therefore, future work should evaluate lower cellulase dosages, enzyme recycling, higher-solid hydrolysis, and enzyme–substrate interactions after DES pretreatment to determine the minimum enzyme requirement for economically favorable glucose production.

The stability of cellulase during the 72 h hydrolysis period should also be considered when interpreting the saccharification data. The hydrolysis condition used in this study, 50 °C and pH 4.8 for 72 h, is commonly applied in laboratory-scale lignocellulosic hydrolysis studies, including studies using pretreated lignocellulosic biomass and empty fruit bunch substrates (Yang et al., 2017; Luo et al., 2019; Fabbrizi et al., 2022). Nevertheless, cellulase is a protein catalyst, and partial activity loss may occur during prolonged incubation because of thermal denaturation, product inhibition, non-productive adsorption on residual lignin, and enzyme binding to insoluble biomass solids ([104]; Chen et al., 2016; Santos et al., 2026). Therefore, the 72-h hydrolysis yield should be interpreted as a standardized endpoint digestibility measurement rather than a direct measurement of intrinsic cellulase stability.

In the present work, all raw and DES-pretreated OPEFB samples were hydrolyzed under identical enzyme loading, temperature, pH, agitation, and incubation time. Therefore, any gradual enzyme deactivation would be expected to affect all treatments under the same experimental protocol, allowing the hydrolysis results to remain valid for comparative evaluation among pretreatment conditions. The relatively lower R^2 values observed in some severity–hydrolysis correlations, especially for ChCl:Gly:$FeCl_3$, should not be attributed solely to cellulase instability. They may also reflect the heterogeneous nature of pretreated OPEFB, differences in residual lignin, non-productive enzyme adsorption, cellulose accessibility, surface morphology, crystallinity, and the nonlinear relationship between severity descriptors and enzymatic digestibility [37,55,63]. However, the possible contribution of enzyme deactivation during prolonged hydrolysis is now acknowledged as a limitation. Future work should include time-course hydrolysis analysis, residual cellulase activity measurement, protein adsorption analysis, glucose and cellobiose monitoring, and enzyme-recycling or enzyme-stability evaluation to better separate substrate accessibility effects from enzyme deactivation effects.

3.5. Recovered lignin characterization and fabrication of CMC-lignin film

3.5.1. Recovered lignin characterization

The recovered DES lignins were further characterized to evaluate their suitability as functional additives for CMC-based composite films. As shown in Table 2, both DES systems produced lignin with high purity, reaching 91.7% for ChCl:LA lignin and 93.1% for ChCl:Gly:$FeCl_3$ lignin. These values indicate that the DES pretreatment not only promoted lignin solubilization from OPEFB but also enabled the recovery of lignin with relatively low carbohydrate contamination. High lignin purity is important for film applications because residual polysaccharides and inorganic impurities may reduce compatibility with the polymer matrix and weaken the contribution of lignin to hydrophobicity, mechanical reinforcement, and antioxidant functionality. Similar observations have been reported for DES-extracted lignins, where high purity, lower molecular weight, and more homogeneous structure improved compatibility with CMC and enhanced the physicochemical performance of CMC–lignin films [47].

The molecular weight distribution of the recovered lignin also differed between the two DES systems. ChCl:LA lignin showed higher Mn and Mw values of 1998 and 2541 g/mol, respectively, with a dispersity of 1.591. In contrast, ChCl:Gly:$FeCl_3$ lignin exhibited lower Mn and Mw values of 1344 and 2139 g/mol, respectively, with a narrower dispersity of 1.272. The lower molecular weight and narrower distribution of ChCl:Gly:$FeCl_3$ lignin suggest that the Lewis-acid-assisted DES system promoted more extensive lignin depolymerization or selective solubilization of lower-molecular-weight lignin fragments. This behavior may be associated with the catalytic role of Fe^{3+} in cleaving ether linkages and disrupting lignin–carbohydrate interactions during

Table 2
Molecular weight and purity of recovered DES lignin.

DES Lignin	Purity	Mn	Mw	Mw/Mn
ChCl:LA	91.7%	1998	2541	1.591
ChCl:Gly:$FeCl_3$	93.1%	1344	2139	1.272

pretreatment [33]. Lower-molecular-weight lignin can be beneficial for film formation because it may disperse more easily in the CMC matrix and form more uniform intermolecular interactions. However, excessive depolymerization may also increase the amount of phenolic hydroxyl groups and polar functionalities, which can influence surface wettability and water vapor transport [40,45].

The FTIR spectra of the recovered lignins are presented in Fig. S4. Both ChCl:LA and ChCl:Gly:$FeCl_3$ lignins exhibited typical lignin absorption bands, confirming that the recovered fractions retained the main aromatic lignin structure. The broad band at around 3200–3400 cm^{-1} corresponds to O–H stretching vibrations from phenolic and aliphatic hydroxyl groups, while the bands near 2920 cm^{-1} are associated with C–H stretching of methyl and methylene groups [110]. The characteristic aromatic skeletal vibrations of lignin were observed around 1600, 1510, and 1420 cm^{-1}, indicating the preservation of the aromatic backbone after DES pretreatment [111]. In addition, bands in the region of 1260–1210 cm^{-1} and 1120–1030 cm^{-1} can be assigned to guaiacyl/syringyl-related C–O vibrations and ether linkages, suggesting the presence of typical lignin units in both recovered samples [50]. These results support the successful isolation of lignin from the DES filtrate and are consistent with the high lignin purity values obtained from compositional analysis. The presence of hydroxyl- and aromatic-related bands is also important for the subsequent CMC–lignin film application, because phenolic hydroxyl groups contribute to antioxidant activity, while the aromatic structure of lignin contributes to hydrophobicity, UV-absorbing capability, and barrier performance [40,47]. Similar FTIR features have been reported for DES lignin incorporated into CMC films, where preserved aromatic and hydroxyl functionalities contributed to improved physicochemical and antioxidant properties of the resulting films [46,47].

The structural features of the recovered DES lignins were further evaluated by 2D-HSQC NMR, as shown in Fig. S5, and the semi-quantitative structural indicators are summarized in Table S1. In the aromatic region, signals at approximately δ_C/δ_H 103–106/6.4–6.8 ppm were assigned to syringyl $S_{2,6}$ correlations, signals around 110–120/6.7–7.3 ppm were assigned to guaiacyl aromatic correlations, and signals near 127–132/7.2–7.8 ppm were assigned cautiously to H-type or p-coumarate-related aromatic structures because this region may overlap with other phenolic aromatic signals in grass-type lignins [47,112–114]. Semi-quantitative integration showed that both recovered lignins were S-rich. ChCl:LA lignin showed 45.9% S, 23.2% G, and 30.9% H/p-coumarate-related units, with an S/G ratio of 1.98, whereas ChCl:Gly:$FeCl_3$ lignin showed 53.4% S, 24.4% G, and 22.2% H/p-coumarate-related units, with an S/G ratio of 2.19. These aromatic correlations indicate that both DES systems recovered lignin fractions that still retained the main aromatic lignin framework.

The side-chain region provides clearer evidence for the difference between preserved structure and depolymerization. ChCl:LA lignin showed a higher β-O-4-related signal, estimated at 22.9 per 100 aromatic units, compared with 16.7 per 100 aromatic units for ChCl:Gly:$FeCl_3$ lignin. Because β-O-4 aryl ether linkages are major native lignin interunit linkages, their higher relative abundance in ChCl:LA lignin suggests that the Brønsted-acidic ChCl:LA system solubilized lignin while preserving more of the native-like side-chain framework. In contrast, the lower β-O-4-related signal in ChCl:Gly:$FeCl_3$ lignin indicates stronger cleavage of aryl ether-type linkages, supporting lignin depolymerization under Fe^{3+}-assisted Lewis acidic conditions. This interpretation is consistent with previous studies showing that $FeCl_3$ and other metal chloride-assisted systems can promote lignocellulose deconstruction, oxygen-containing bond cleavage, and lignin structural modification [29,32,34,70]. The β–5-related and β–β/overlapped oxygenated linkage regions were also estimated, but these values were interpreted cautiously because technical lignins often show weak or overlapping contours in the side-chain region ([47,112].

This structural difference is consistent with the GPC/SEC results, where ChCl:Gly:$FeCl_3$ lignin exhibited lower molecular weight and narrower dispersity than ChCl:LA lignin. The lower molecular weight of ChCl:Gly:$FeCl_3$ lignin suggests that $FeCl_3$-assisted DES pretreatment promoted more extensive lignin fragmentation. Such depolymerization can increase the accessibility of phenolic hydroxyl groups, explaining the stronger antioxidant activity of the CMC–ChCl:Gly:$FeCl_3$ lignin film, as reflected by its lower IC_{50} value[46,47]. Meanwhile, the relatively more preserved aromatic framework and higher molecular weight of ChCl:LA lignin may contribute to better hydrophobicity and moisture-barrier behavior, as shown by its higher water contact angle and lower WVTR. Therefore, Fig. S5 supports the conclusion that the pretreatment chemistry controlled not only lignin extraction but also the downstream functional performance of the recovered lignin in CMC-based packaging films.

3.5.2. *Characterization of CMC-Lignin film*

FTIR spectra of the CMC–DES lignin films is shown in Fig. 5. The spectra confirmed the successful incorporation of recovered lignin into the CMC matrix. The broad absorption band around 3200–3400 cm^{-1} can be assigned to O–H stretching vibrations from hydroxyl groups in CMC, glycerol, and lignin. The bands near 2920 cm^{-1} are associated with C–H stretching of aliphatic groups, while the absorption bands around 1590–1600 cm^{-1} and 1410–1420 cm^{-1} are related to carboxylate groups of CMC and aromatic skeletal vibrations of lignin. The presence of lignin-related bands in the composite films indicates that the recovered DES lignin was successfully incorporated into the CMC network. In addition, possible shifts or intensity changes in the O–H and carboxylate regions suggest intermolecular hydrogen bonding between hydroxyl groups of CMC and phenolic/aliphatic hydroxyl groups of lignin. Such interactions are important because they can improve matrix cohesion, reduce free volume, and contribute to the enhanced mechanical and barrier properties of the films. Previous studies on CMC–DES lignin films similarly attributed improved film performance to the compatibility and intermolecular interactions between DES lignin and CMC [46,47].

The antioxidant, physical, and mechanical properties of CMC-DES lignin films were summarized In Table 3. The incorporation of DES lignin improved the antioxidant activity of the CMC films, as indicated by the decrease in IC_{50} values from 50.3 g/mL for neat CMC to 20.8 g/mL for CMC–ChCl:LA lignin and 12.6 g/mL for CMC–ChCl:Gly:$FeCl_3$ lignin. Since a lower IC_{50} value indicates stronger radical scavenging ability, the ChCl:Gly:$FeCl_3$ lignin film showed the highest antioxidant performance among the tested films. This enhancement can be attributed to the aromatic and phenolic structures of lignin, which can donate hydrogen atoms or electrons to neutralize free radicals [40,45]. The

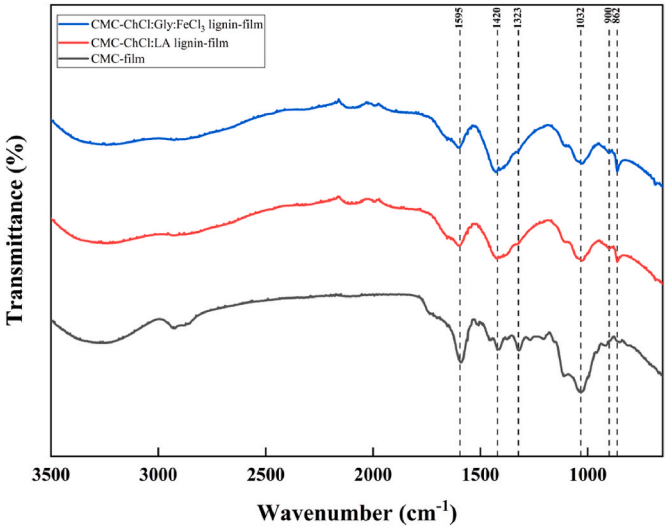

Fig. 5. FTIR Spectra of CMC-lignin film.

Table 3
Antioxidant, physical, and mechanical properties of CMC-DES lignin films.

CMC-lignin film	Antioxidant (IC_{50}) (μg/mL)	Water contact angle (°)	WVTR (g/m^{2}h)	Thickness (mm)	Tensile strength (MPa)	Elongation at break (%)
CMC	50.3	68.5 ± 0.3	19.95 ± 0.74	0.1	8.05	39
CMC-ChCl-LA lignin	20.8	70.7 ± 0.2	13.94 ± 0.16	0.12	12.13	21.83
CMC-ChCl-Gly-$FeCl_3$	12.6	65.8 ± 0.7	15.84 ± 0.72	0.13	13.08	20.67

stronger antioxidant activity of the ChCl:Gly:$FeCl_3$ lignin film may be related to its lower molecular weight and higher purity, which could increase the accessibility of phenolic hydroxyl groups within the film matrix. This interpretation agrees with previous reports showing that lignin-containing films exhibit improved antioxidant activity due to phenolic hydroxyl groups from syringyl, guaiacyl, and p-hydroxyphenyl units ([115]; [41]). In food packaging applications, this antioxidant function is valuable because it may help reduce oxidative deterioration, lipid oxidation, and quality loss during storage.

The surface wettability of the films was also affected by lignin incorporation. The neat CMC film showed a water contact angle of 68.5°, confirming its hydrophilic nature. After lignin addition, the contact angle increased slightly to 70.7° for CMC–ChCl:LA lignin, indicating improved surface hydrophobicity. This increase can be attributed to the aromatic and hydrophobic domains of lignin, which reduce the exposure of hydrophilic CMC groups at the film surface. In contrast, the CMC–ChCl:Gly:$FeCl_3$ lignin film showed a lower contact angle of 65.8°, despite having higher purity and stronger antioxidant activity. This result suggests that the ChCl:Gly:$FeCl_3$ lignin may contain a greater proportion of accessible polar groups, particularly phenolic hydroxyl groups generated through lignin depolymerization [47]. Therefore, while lignin generally contributes hydrophobic aromatic domains, the final wettability of the composite film depends on the balance between hydrophobic aromatic structures and exposed polar functionalities. A similar trend has been reported in lignin-based films, where the incorporation of lignin can increase hydrophobicity, but the extent depends strongly on lignin structure, purity, molecular weight, and phenolic hydroxyl content (Syahidah et al., 2025).

The WVTR results further demonstrate the role of DES lignin in improving the moisture barrier properties of CMC films. The neat CMC film showed the highest WVTR of 19.95 g/m^{2}h, reflecting the water-sensitive nature of the CMC matrix. Incorporation of ChCl:LA lignin reduced the WVTR to 13.94 g/m^{2}h, while ChCl:Gly:$FeCl_3$ lignin reduced it to 15.84 g/m^{2}h. These reductions indicate that recovered DES lignin can hinder water vapor diffusion through the CMC film. The improved barrier performance can be explained by two complementary mechanisms. First, the hydrophobic aromatic structure of lignin can decrease water affinity within the film matrix. Second, lignin particles or domains can create a more tortuous diffusion pathway, thereby slowing water vapor transport across the film [46,116]. The slightly better WVTR reduction observed for CMC–ChCl:LA lignin may be consistent with its higher contact angle, suggesting a more hydrophobic surface and stronger resistance to water vapor transmission. Previous studies have also shown that lignin incorporation can reduce water vapor permeability in biopolymer films by improving matrix compactness and introducing hydrophobic domains [47,117].

Mechanical testing showed that DES lignin incorporation improved the tensile strength of the CMC films. The tensile strength increased from 8.05 MPa for neat CMC to 12.13 MPa for CMC–ChCl:LA lignin and 13.08 MPa for CMC–ChCl:Gly:$FeCl_3$ lignin. This enhancement indicates that lignin acted as a reinforcing component within the CMC matrix. The improvement may result from hydrogen bonding and physical interactions between CMC chains and lignin functional groups, which strengthen the composite network and improve stress transfer during tensile loading. The slightly higher tensile strength of the ChCl:Gly:$FeCl_3$ lignin film may be associated with its lower molecular weight and narrower dispersity, which could promote more uniform dispersion and stronger interfacial interaction with CMC. However, the elongation at break decreased from 39% for neat CMC to 21.83% and 20.67% for the ChCl:LA and ChCl:Gly:$FeCl_3$ lignin films, respectively. This reduction suggests that lignin increased film rigidity and restricted CMC chain mobility (Syahidah et al., 2025)[118,119]. Therefore, DES lignin improved strength but reduced flexibility, reflecting a typical reinforcement effect in biopolymer composite films.

Overall, the recovered DES lignins from OPEFB demonstrated strong potential as functional additives for CMC-based films. Both lignins improved antioxidant activity, reduced WVTR, and increased tensile strength compared with neat CMC. ChCl:LA lignin gave better surface hydrophobicity and moisture barrier performance, while ChCl:Gly:$FeCl_3$ lignin provided stronger antioxidant activity and higher tensile strength. These differences indicate that the pretreatment chemistry not only affects lignin recovery and enzymatic glucose production but also determines the downstream functionality of recovered lignin in packaging materials. Thus, the DES fractionation strategy developed in this work supports an integrated OPEFB biorefinery concept, in which the cellulose-rich solid fraction is converted into glucose and the recovered lignin is valorized as an active reinforcing component for biodegradable CMC-based packaging films.

3.6. Process mass balance analysis of DES-enzymatic hydrolysis process

Process mass balance analysis was conducted to evaluate the integrated performance of DES pretreatment and enzymatic hydrolysis on the basis of 100 g raw OPEFB. While the previous sections separately discussed fractionation behavior, structural modification, enzymatic digestibility, and lignin-based film performance, the mass balance provides a more practical assessment of how effectively the initial biomass was converted into two major product streams: glucose from the cellulose-rich solid and recovered lignin from the DES liquor. This evaluation is important because a pretreatment condition with high enzymatic hydrolysis yield does not necessarily provide the highest overall glucose recovery on a raw biomass basis, particularly if excessive solid loss or cellulose degradation occurs during pretreatment. Similarly, high delignification is only beneficial for lignin valorization when the solubilized lignin can be effectively recovered.

The glucose and lignin yields obtained from the ChCl:LA and ChCl:Gly:$FeCl_3$ systems are shown in Fig. 6. In the ChCl:LA system, increasing pretreatment severity generally improved both enzymatic glucose production and lignin recovery. The best-performing ChCl:LA condition within the investigated range was 140 °C for 6 h, producing approximately 21.6 g glucose and 24.7 g recovered lignin per 100 g raw OPEFB. This result is consistent with the fractionation behavior discussed in Section 3.2, where ChCl:LA promoted strong delignification, high lignin yield, and cellulose enrichment at higher severity. Although the enzymatic hydrolysis yield of ChCl:LA-pretreated solid was lower than that of the ChCl:Gly:$FeCl_3$ system, its higher lignin recovery demonstrates the advantage of ChCl:LA when lignin valorization is considered as an important output of the process. In contrast, the ChCl:Gly:$FeCl_3$ system produced slightly higher glucose recovery, reaching approximately 21.7 g glucose per 100 g raw OPEFB, while the recovered lignin yield was approximately 23.1 g per 100 g raw OPEFB. The higher glucose production agrees with the stronger enzymatic hydrolysis performance observed in Section 3.4, where ChCl:Gly:$FeCl_3$-pretreated OPEFB achieved the highest enzymatic hydrolysis yield. This behavior can be

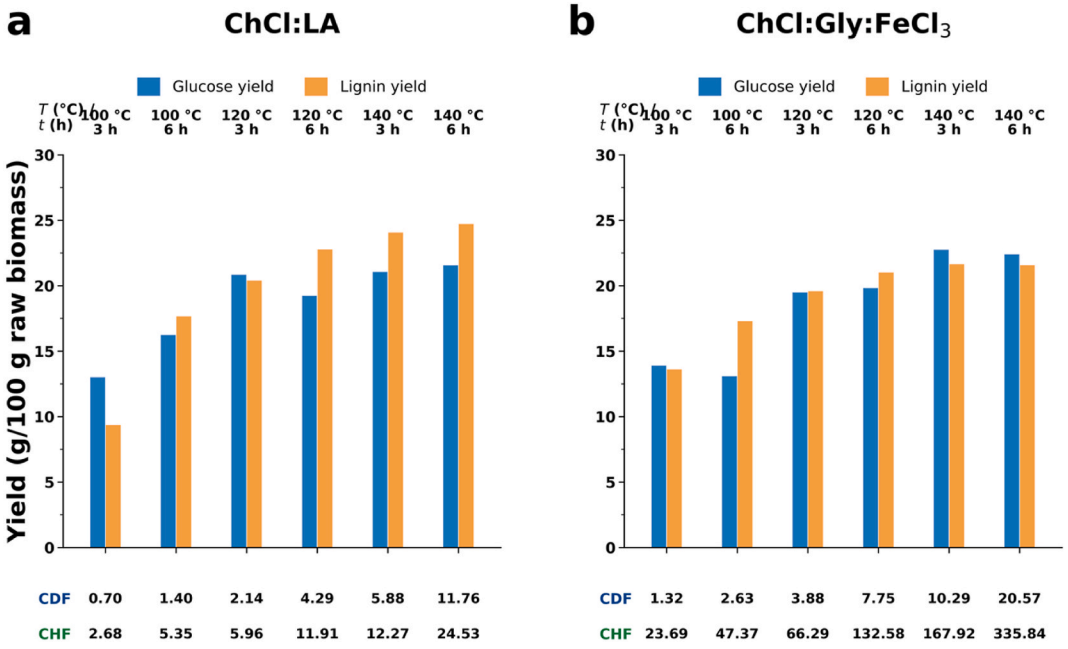

Fig. 6. Glucose and lignin yield on a 100 g raw OPEFB basis (a) ChCl:LA system + Enzymatic hydrolysis & (b) ChCl:Gly:$FeCl_3$+enzymatic hydrolysis.

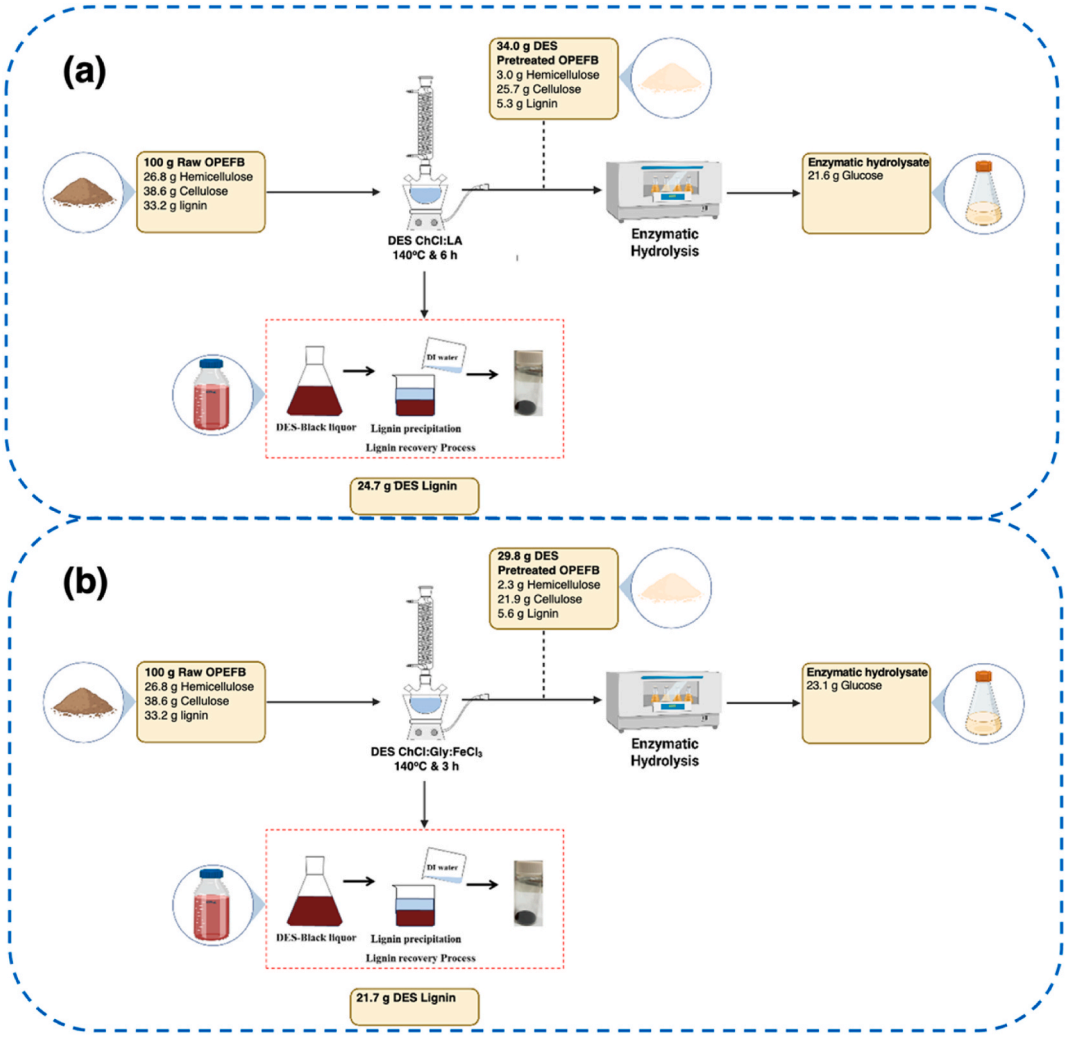

Fig. 7. Process mass balances of highest total glucose and lignin in (a) ChCl:LA DES and (b) ChCl:Gly:$FeCl_3$ DES with basis 100 g raw OPEFB.

attributed to the strong hydrolytic effect of Fe^{3+}, which promoted extensive hemicellulose removal and improved cellulose accessibility [33,95]. However, the lignin yield was slightly lower than that obtained using ChCl:LA, confirming that the $FeCl_3$-containing DES was more favorable for carbohydrate accessibility than for maximizing lignin recovery.

It should also be noted that the glucose recoveries reported in this mass balance were calculated from the standardized 72 h enzymatic hydrolysis endpoint used for all samples. Therefore, these values are suitable for comparing the relative digestibility of the two DES-pretreated solids under identical hydrolysis conditions, although future time-course and residual-enzyme-activity analyses would be needed to evaluate the contribution of enzyme stability to absolute glucose yield.

The detailed process mass balances for the best-performing conditions of both DES systems are presented in Fig. 7. This analysis further confirms that evaluating pretreatment performance only from enzymatic hydrolysis yield may be misleading, because the final glucose recovery also depends on solid recovery, cellulose preservation, and the amount of cellulose remaining in the pretreated solid. For ChCl:LA pretreatment, the highest integrated product recovery was obtained at 140 °C for 6 h. Under this condition, the process generated 21.6 g glucose and 24.7 g recovered lignin from 100 g raw OPEFB. This result indicates that ChCl:LA provided a balanced fractionation route, where a substantial portion of lignin was solubilized and recovered while the cellulose-rich residue remained sufficiently digestible for glucose production. The higher recovered lignin mass agrees with the stronger delignification and lignin yield discussed in Section 3.2, confirming the suitability of ChCl:LA for lignin-oriented OPEFB fractionation. For ChCl:Gly:$FeCl_3$, the best-performing mass balance within the investigated range was obtained at 140 °C for 3 h, producing 21.7 g glucose and 23.1 g recovered lignin per 100 g raw OPEFB. Although this DES system achieved the highest enzymatic hydrolysis yield, the raw-biomass-based glucose recovery was only slightly higher than that of ChCl:LA. This indicates that the strong hydrolytic action of Fe^{3+} improved cellulose accessibility, but the overall glucose recovery was also constrained by the amount of cellulose retained in the solid fraction after pretreatment [33,70]. Therefore, the mass balance highlights an important distinction between enzymatic digestibility and overall glucose recovery. A highly digestible solid does not necessarily give proportionally higher glucose production if pretreatment also causes greater solid loss or partial carbohydrate degradation.

Comparison of the two mass balances shows that both DES systems converted OPEFB into similar amounts of glucose, but through different mechanistic routes. ChCl:LA produced slightly lower glucose but higher recovered lignin, whereas ChCl:Gly:$FeCl_3$ produced slightly higher glucose but lower recovered lignin. This difference should not be attributed to a single factor such as delignification, hemicellulose removal, or crystallinity alone. Instead, glucose recovery on a raw-biomass basis depends on the combined effects of solid recovery, cellulose preservation, cellulose enrichment, hemicellulose removal, lignin removal, cellulose accessibility, and enzymatic hydrolysis efficiency. In the ChCl:Gly:$FeCl_3$ system, strong Lewis-acid-assisted hemicellulose removal, surface disruption, and partial reduction in apparent CrI produced a highly digestible cellulose-rich solid, consistent with the highest enzymatic hydrolysis yield. Similar effects of $FeCl_3$ or metal chloride-assisted pretreatment on xylan disruption and enzymatic digestibility have been reported previously [30,33,95]. However, its glucose recovery on a 100 g raw OPEFB basis was only slightly higher than that of ChCl:LA because total glucose production was also constrained by the amount of cellulose retained after pretreatment. In contrast, ChCl:LA provided a more balanced fractionation route, combining strong delignification, high lignin recovery, cellulose enrichment, and sufficient cellulose preservation. Therefore, the mass balance highlights the distinction between digestibility of the recovered solid and total glucose recovery from the initial biomass.

As shown in Table 4, previous OPEFB pretreatment studies achieved different balances between enzymatic sugar production and lignin recovery. The peracetic acid–sulfuric acid pretreatment produced a higher recalculated enzymatic glucose yield than the present DES systems, indicating its strong effectiveness in improving cellulose digestibility. However, lignin was not recovered as an isolated product stream in that process; therefore, its contribution was mainly sugar-oriented [42]. Similarly, the ionosolv pretreatment using [DMBA][HSO_4] generated relatively high glucose release and recovered lignin, but the estimated recovered lignin yield was substantially lower than that obtained in the present DES systems [44]. In the sequential hydrothermal–organosolv process, both lignin and reducing sugar were recovered, but the lignin yield and enzymatic sugar recovery on a raw OPEFB basis were lower than those obtained in the present DES-based process [65].

In comparison, the present ChCl:LA and ChCl:Gly:$FeCl_3$ pretreatments produced similar glucose recovery, 21.6 and 21.7 g/100 g raw OPEFB, respectively, while also recovering 24.7 and 23.1 g lignin/100 g raw OPEFB. Although the glucose recovery was lower than that reported for peracetic acid–sulfuric acid pretreatment, the present process provided a more balanced product distribution because both the carbohydrate and lignin fractions were recovered as useable streams. This distinction is important for biorefinery development, where the economic and environmental value of pretreatment depends not only on sugar production but also on the valorization of lignin as a co-product [109].

Although the present DES pretreatment demonstrated effective OPEFB fractionation and dual recovery of glucose and lignin, DES loading and solvent recyclability remain important considerations for scale-up. In this study, the OPEFB-to-DES ratio was fixed at 1:15 (w/w), which was selected as a laboratory-scale comparative condition to ensure sufficient wetting, mixing, heat transfer, and contact between biomass and the DES phase. Relatively high solvent loading is frequently applied in laboratory-scale DES pretreatment to reduce mass-transfer limitations and provide sufficient solvent capacity for lignin solubilization and lignocellulose deconstruction [32,49,51,114]. However, direct translation of this solvent loading to industrial scale may increase solvent inventory, reactor volume, heating requirement, downstream separation load, and overall operating cost. Previous techno-economic and process-design studies have emphasized that solvent recovery efficiency, solvent-to-biomass ratio, energy demand, and recycling stability are key

Table 4
Previous fractionation study of OPEFB.

Process	Conditions	Recovered Lignin (per 100 g raw OPEFB)	EH Glucose (per 100 g raw OPEFB)	References
Ionosolv pretreatment coupled EH	[DMBA][HSO_4]: H_2O = 80:20 wt%, biomass/solvent ratio 1:10, 170 °C, 1 h & EH	8	25	[44]
PA– H_2SO_4 pretreatment coupled EH	PA 200 mM, H_2SO_4 100 mM, 140 °C, 5 min	-	28.4	[42]
Sequential HT &H_2SO_4 -organosolv pretreatment	HT: 180 °C, 30 min, 10 mM H_2SO_4, Organosolv: EtOh 80%, 185 °C,	9.1	12.6	[65]
DES pretreatment & EH	ChCl:LA (1:2) 140 °C & 6 h	24.7	21.6	This study
DES pretreatment & EH	ChCl:Gly:$FeCl_3$ 140 °C & 3 h	23.1	21.7	This study

HT: hydrothermal; DES: deep eutectic solvent; DMBA: N,N,N-dimethylbutylamine; EH: enzymatic hydrolysis; PA: paracetic acid.

determinants of the feasibility of DES-based lignocellulose pretreatment [19,120,121]. Therefore, the 1:15 ratio used in this work should be interpreted as a laboratory-scale solvent loading rather than an optimized industrial solvent-to-biomass ratio.

DES recovery is also a critical factor because lignin regeneration was performed by adding water to the DES filtrate. Water addition reduces DES solvent strength and promotes lignin precipitation, but it also dilutes the DES phase and creates an additional requirement for water removal before solvent reuse [29,49,51]. In our previous study on coconut husk fractionation using hydrothermal and ChCl:LA DES pretreatment, DES recycling was performed after lignin recovery by removing ethanol and water through rotary evaporation at approximately 50 °C, and the recovered DES was directly reused in subsequent pretreatment cycles without additional purification. The recycled DES remained effective over multiple cycles, but its performance gradually decreased. Hemicellulose removal declined from 79.96% in the first cycle to 68.0% in the fourth cycle, lignin removal decreased from 64.18% to 49.7%, and lignin yield decreased from 50.2% to 37.4% [49]. Similar decreases in recycled DES performance have been associated with solvent dilution, reduced acidity, impurity accumulation, and saturation by solubilized lignocellulosic fragments [29,32]. This decline may reduce the ability of recycled DES to disrupt lignin–carbohydrate complexes and maintain consistent lignin solubilization across repeated cycles.

These findings indicate that DES recycling is feasible but requires further optimization to maintain pretreatment efficiency across repeated cycles. For the present OPEFB system, the current study should therefore be regarded as a laboratory-scale proof of concept rather than an industrially optimized process. Future work should evaluate lower DES-to-biomass ratios, high-solids pretreatment, DES recycling over multiple cycles, solvent make-up requirements, impurity accumulation, ethanol and water recovery, and the energy demand for DES reconcentration [19,121,122]. These evaluations are necessary to improve the economic and practical feasibility of DES-based lignocellulose fractionation.

Beyond solvent loading and recyclability, the practical comparison between ChCl:LA and ChCl:Gly:$FeCl_3$ should also consider residence time, solvent formulation, catalyst requirement, apparent activation energy, solvent recovery, and process-energy implications, because these parameters strongly influence the economic feasibility of DES-based lignocellulose pretreatment [19,120–122]. Based on the fitted CDF and CHF models, ChCl:Gly:$FeCl_3$ showed higher apparent activation energies than ChCl:LA for both lignin removal and xylan hydrolysis. The apparent activation energy for lignin removal was 87.84 kJ/mol in ChCl:Gly:$FeCl_3$ and 63.47 kJ/mol in ChCl:LA, while that for xylan hydrolysis was 69.87 kJ/mol in ChCl:Gly:$FeCl_3$ and 49.54 kJ/mol in ChCl:LA. These values indicate that fractionation in the $FeCl_3$-containing DES was more temperature-sensitive, which is consistent with the broader CDF and CHF ranges observed for ChCl:Gly:$FeCl_3$. In contrast, the lower apparent activation energies of ChCl:LA suggest that lignin solubilization and xylan removal can proceed more readily within a narrower Brønsted-acidic severity window.

The best-performing conditions for both DES systems used the same pretreatment temperature of 140 °C, but different residence times. ChCl:LA required 6 h and produced 21.6 g glucose and 24.7 g recovered lignin per 100 g raw OPEFB, whereas ChCl:Gly:$FeCl_3$ required only 3 h and produced 21.7 g glucose and 23.1 g recovered lignin per 100 g raw OPEFB. Therefore, although ChCl:Gly:$FeCl_3$ had higher apparent activation energies, its Lewis-acid-assisted catalytic effect allowed comparable glucose recovery at a shorter holding time. This may offer an advantage in terms of reducing the energy associated with maintaining the reactor at the target temperature. However, apparent activation energy should not be directly equated with total process-energy consumption. Total process energy also depends on DES heat capacity, viscosity, mixing requirement, solvent-to-biomass ratio, heat recovery, ethanol and water removal, DES reconcentration, solvent loss, and solvent reuse efficiency [19,49,122].

In addition, the incorporation of $FeCl_3$ introduces additional process considerations, including catalyst cost, salt recovery, possible corrosion control, impurity accumulation during recycling, and potential effects of residual metal species on downstream lignin and hydrolysate applications. Although Lewis-acid-mediated DES systems can intensify lignocellulose fractionation by promoting hemicellulose disruption, lignin cleavage, and cellulose accessibility, metal chloride addition may also increase process complexity through catalyst handling and recovery requirements [29,30,34,50,70]. Therefore, ChCl:LA may be more attractive when simpler solvent formulation and lignin recovery are prioritized, whereas ChCl:Gly:$FeCl_3$ may be more suitable when shorter pretreatment time and enzymatic glucose production are emphasized [19,120]. Nevertheless, this comparison should be regarded as a preliminary feasibility interpretation rather than a complete techno-economic or energy analysis. A rigorous comparison would require quantitative data on solvent cost, DES heat capacity, viscosity, heating duty, evaporation duty, solvent loss, catalyst make-up, DES recycling stability, equipment compatibility, corrosion risk, wastewater generation, and product purification requirements [19,70,120].

Considering these process-level trade-offs, ChCl:LA showed a stronger advantage for lignin-oriented fractionation because it produced the highest recovered lignin yield, used a simpler Brønsted-acidic DES formulation, and later gave better moisture-barrier performance in the CMC–lignin film. Conversely, ChCl:Gly:$FeCl_3$ gave slightly higher glucose recovery and produced lignin that contributed stronger antioxidant activity and tensile reinforcement. Therefore, the present DES pretreatment route is not merely a saccharification-enhancement strategy, but a dual-product OPEFB valorization approach in which the cellulose-rich fraction is converted into glucose and the recovered lignin is further upgraded into functional CMC-based packaging material.

4. Conclusions

This study demonstrated an integrated OPEFB valorization strategy through DES pretreatment, enzymatic glucose production, lignin recovery, and CMC–lignin composite film development. The two DES systems exhibited distinct fractionation behaviors: ChCl:LA promoted stronger lignin solubilization and higher lignin recovery, whereas ChCl:Gly:$FeCl_3$ enhanced hemicellulose removal and enzymatic hydrolysis through Lewis acid-assisted deconstruction. The CDF and CHF models successfully described the severity-dependent delignification and xylan hydrolysis behavior, confirming that pretreatment performance was governed by the combined effects of temperature, residence time, and the acidic or catalytic nature of the DES. On a 100 g raw OPEFB basis, ChCl:LA pretreatment at 140 °C for 6 h produced 21.6 g glucose and 24.7 g recovered lignin, while ChCl:Gly:$FeCl_3$ pretreatment at 140 °C for 3 h produced 21.7 g glucose and 23.1 g recovered lignin. The recovered DES lignins were successfully incorporated into CMC-based films, where ChCl:LA lignin provided better water resistance and moisture-barrier performance, while ChCl:Gly:$FeCl_3$ lignin contributed stronger antioxidant activity and tensile reinforcement. Overall, this work confirms that OPEFB can be converted through a multiproduct biorefinery pathway, in which the cellulose-rich fraction is utilized for glucose production and the recovered lignin is upgraded into functional biodegradable packaging films. Future studies should focus on DES recyclability, solvent recovery, techno-economic assessment, life-cycle evaluation, and scale-up validation to further assess the industrial feasibility and sustainability of this integrated process.

CRediT authorship contribution statement

Candra Wijaya: Conceptualization, Data curation, Formal analysis, Investigation, Methodology, Visualization, Writing – original draft. **Andika Prastika:** Data curation, Formal analysis, Investigation. **Olivia Izzati Atiqa:** Data curation, Formal analysis, Investigation. **Tabina**

Raissa Apol: Data curation, Formal analysis, Investigation. **Urania Noor Lintang Pertiwi:** Data curation, Formal analysis, Investigation. **Lieke Riadi:** Supervision, Writing – review & editing. **Maktum Muharja:** Methodology, Supervision, Writing – review & editing. **Arief Widjaja:** Conceptualization, Funding acquisition, Methodology, Project administration, Supervision, Writing – review & editing.

Declaration of competing interest

The authors declare that they have no known competing financial interests or personal relationships that could have appeared to influence the work reported in this paper.

Acknowledgments

This research is funded by the Indonesian Endowment Fund for Education (LPDP) under the EQUITY Program (Contract No. 4299/B3/DT.03.08/2025)

Appendix A. Supplementary data

Supplementary data to this article can be found online at https://doi.org/10.1016/j.biombioe.2026.109859.

Data availability

Data will be made available on request.

References

[1] C.P. Bosah, S. Li, G.K.M. Ampofo, I. Sangare, A continental and global assessment of the role of energy consumption, total natural resource rent, and economic growth as determinants of carbon emissions, Sci. Total Environ. 892 (2023) 164592, https://doi.org/10.1016/J.SCITOTENV.2023.164592.
[2] H. Chen, C. Sun, Y. Hu, C. Xia, F. Sun, Z. Zhang, Reaction characteristics of metal-salt coordinated deep eutectic solvents during lignocellulosic pretreatment, J. Environ. Chem. Eng. 11 (2023) 109531, https://doi.org/10.1016/J.JECE.2023.109531.
[3] R. Li, Y. Zheng, X. Zhao, Q. Yong, X. Meng, A. Ragauskas, C. Huang, Recent advances in biomass pretreatment using biphasic solvent systems, Green Chem. 25 (2023) 2505–2523, https://doi.org/10.1039/D3GC00271C.
[4] K. Mishra, S. Singh Siwal, A. Kumar Saini, V.K. Thakur, Recent update on gasification and pyrolysis processes of lignocellulosic and algal biomass for hydrogen production, Fuel 332 (2023), https://doi.org/10.1016/j.fuel.2022.126169.
[5] M. Wang, X. Fu, Y. Chang, J. Wei, H. Cui, Recent advancements in deep eutectic solvent (DES) pretreatment: applications, mechanisms, and integration with emerging technologies for biorefinery, Ind. Crops Prod. 229 (2025) 121028, https://doi.org/10.1016/j.indcrop.2025.121028.
[6] Z. Chen, Y. Wang, H. Cheng, H. Zhou, Hemicellulose degradation: an overlooked issue in acidic deep eutectic solvents pretreatment of lignocellulosic biomass, Ind. Crops Prod. 187 (2022) 115335, https://doi.org/10.1016/J.INDCROP.2022.115335.
[7] M. Li, B. Jiang, W. Wu, S. Wu, Y. Yang, J. Song, M. Ahmad, Y. Jin, Current understanding and optimization strategies for efficient lignin-enzyme interaction: a review, Int. J. Biol. Macromol. 195 (2022) 274–286, https://doi.org/10.1016/J.IJBIOMAC.2021.11.188.
[8] E.J. Panakkal, K. Cheenkachorn, S. Chuetor, P. Tantayotai, N. Raina, Y.S. Cheng, M. Sriariyanun, Optimization of deep eutectic solvent pretreatment for bioethanol production from napier grass, Sustain. Energy Technol. Assessments 54 (2022) 102856, https://doi.org/10.1016/J.SETA.2022.102856.
[9] H.A. Ruiz, M. Galbe, G. Garrote, D.M. Ramirez-Gutierrez, E. Ximenes, S.-N. Sun, D. Lachos-Perez, R.M. Rodríguez-Jasso, R.-C. Sun, B. Yang, M.R. Ladisch, Severity factor kinetic model as a strategic parameter of hydrothermal processing (steam explosion and liquid hot water) for biomass fractionation under biorefinery concept, Bioresour. Technol. 342 (2021) 125961, https://doi.org/10.1016/j.biortech.2021.125961.
[10] S. Suhartini, N.A. Rohma, E. Mardawati, Kasbawati, N. Hidayat, L. Melville, Biorefining of oil palm empty fruit bunches for bioethanol and xylitol production in Indonesia: a review, Renew. Sustain. Energy Rev. 154 (2022) 111817, https://doi.org/10.1016/j.rser.2021.111817.
[11] W. Fatriasari, W. Ulwan, T. Aminingsih, F.P. Sari, Fitria, L. Suryanegara, A. H. Iswanto, M. Ghozali, L.N. Kholida, M.H. Hussin, A. Fudholi, E. Hermiati, Optimization of maleic acid pretreatment of oil palm empty fruit bunches (OPEFB) using response surface methodology to produce reducing sugars, Ind. Crops Prod. 171 (2021), https://doi.org/10.1016/j.indcrop.2021.113971.
[12] D. Ouyang, T. Liu, A.A. Astimar, H.L.N. Lau, S.S. Teh, J. Nursyairah, D. Liu, X. Zhao, Model-based process intensification of dilute acid pre-hydrolysis of oil palm empty fruit bunch biomass for pretreatment and furfural production, Bioresour. Technol. 372 (2023), https://doi.org/10.1016/j.biortech.2023.128626.
[13] C. Wijaya, U.N.L. Pertiwi, T.R. Apol, I.P.N. Rohmah, M. Muharja, T. Widjaja, L. Riadi, A. Widjaja, Enhancing enzymatic digestibility and lignin production of oil palm empty fruit bunch (OPEFB) by green deep eutectic solvent, Bull. Chem. React. Eng. Catal. 21 (2026) 412–427, https://doi.org/10.9767/bcrec.20526.
[14] E.F. Ahmad, P. Lestari, K. Oginawati, Y. Yulizar, J. Sianturi, M.M. Munir, A. Adawiah, Soda-anthraquinone-catalyzed delignification of coconut husk waste, Bull. Chem. React. Eng. Catal. 21 (2026) 128–136, https://doi.org/10.9767/bcrec.20537.
[15] C. Huang, X. Zhao, Y. Zheng, W. Lin, C. Lai, Q. Yong, A.J. Ragauskas, X. Meng, Revealing the mechanism of surfactant-promoted enzymatic hydrolysis of dilute acid pretreated bamboo, Bioresour. Technol. 360 (2022), https://doi.org/10.1016/j.biortech.2022.127524.
[16] M.M. Kininge, P.R. Gogate, Intensification of alkaline delignification of sugarcane bagasse using ultrasound assisted approach, Ultrason. Sonochem. 82 (2022) 105870, https://doi.org/10.1016/j.ultsonch.2021.105870.
[17] A. Ovejero-Pérez, V. Rigual, J.C. Domínguez, M.V. Alonso, M. Oliet, F. Rodriguez, Organosolv and ionosolv processes for autohydrolyzed poplar fractionation: lignin recovery and characterization, Int. J. Biol. Macromol. 197 (2022) 131–140, https://doi.org/10.1016/j.ijbiomac.2021.12.079.
[18] B.B. Hansen, S. Spittle, B. Chen, D. Poe, Y. Zhang, J.M. Klein, A. Horton, L. Adhikari, T. Zelovich, B.W. Doherty, B. Gurkan, E.J. Maginn, A. Ragauskas, M. Dadmun, T.A. Zawodzinski, G.A. Baker, M.E. Tuckerman, R.F. Savinell, J. R. Sangoro, Deep eutectic solvents: a review of fundamentals and applications, Chem. Rev. 121 (2021) 1232–1285, https://doi.org/10.1021/acs.chemrev.0c00385.
[19] J. Peng, H. Xu, W. Wang, Y. Kong, Z. Su, B. Li, Techno-economic analysis of bioethanol preparation process via deep eutectic solvent pretreatment, Ind. Crops Prod. 172 (2021) 114036, https://doi.org/10.1016/J.INDCROP.2021.114036.
[20] B. Soares, A.M. da Costa Lopes, A.J.D. Silvestre, P.C. Rodrigues Pinto, C.S. R. Freire, J.A.P. Coutinho, Wood delignification with aqueous solutions of deep eutectic solvents, Ind. Crops Prod. 160 (2021), https://doi.org/10.1016/j.indcrop.2020.113128.
[21] H. Yu, Z. Xue, R. Shi, F. Zhou, T. Mu, Lignin dissolution and lignocellulose pretreatment by carboxylic acid based deep eutectic solvents, Ind. Crops Prod. 184 (2022), https://doi.org/10.1016/j.indcrop.2022.115049.
[22] X. Liang, Y. Zhu, B. Qi, S. Li, J. Luo, Y. Wan, Structure-property-performance relationships of lactic acid-based deep eutectic solvents with different hydrogen bond acceptors for corn stover pretreatment, Bioresour. Technol. 336 (2021) 125312, https://doi.org/10.1016/j.biortech.2021.125312.
[23] D. Huo, Y. Sun, Q. Yang, F. Zhang, G. Fang, H. Zhu, Y. Liu, Selective degradation of hemicellulose and lignin for improving enzymolysis efficiency via pretreatment using deep eutectic solvents, Bioresour. Technol. 376 (2023), https://doi.org/10.1016/j.biortech.2023.128937.
[24] S. Kumar, S. Sharma, S.M. Arumugam, C. Miglani, S. Elumalai, Biphasic separation approach in the DES biomass fractionation facilitates lignin recovery for subsequent valorization to phenolics, ACS Sustain. Chem. Eng. 8 (2020) 19140–19154, https://doi.org/10.1021/acssuschemeng.0c07747.
[25] H. Li, X. Li, T. You, D. Li, H. Nawaz, X. Zhang, F. Xu, Insights into alkaline choline chloride-based deep eutectic solvents pretreatment for populus deltoides: lignin structural features and modification mechanism, Int. J. Biol. Macromol. 193 (2021) 319–327, https://doi.org/10.1016/J.IJBIOMAC.2021.10.134.
[26] Q. Liu, T. Yuan, Q. Fu, jin Bai, Y. yuan, F. Peng, C. li Yao, Choline chloride-lactic acid deep eutectic solvent for delignification and nanocellulose production of moso bamboo, Cellulose 26 (2019) 9447–9462, https://doi.org/10.1007/s10570-019-02726-0.
[27] S. Hong, X.J. Shen, B. Pang, Z. Xue, X.F. Cao, J.L. Wen, Z.H. Sun, S.S. Lam, T. Q. Yuan, R.C. Sun, In-depth interpretation of the structural changes of lignin and formation of diketones during acidic deep eutectic solvent pretreatment, Green Chem. 22 (2020) 1851–1858, https://doi.org/10.1039/d0gc00006j.
[28] W.X. Li, W.Z. Xiao, Y.Q. Yang, Q. Wang, X. Chen, L.P. Xiao, R.C. Sun, Insights into bamboo delignification with acidic deep eutectic solvents pretreatment for enhanced lignin fractionation and valorization, Ind. Crops Prod. 170 (2021), https://doi.org/10.1016/j.indcrop.2021.113692.
[29] Y. Bai, X.F. Zhang, Z. Wang, T. Zheng, J. Yao, Deep eutectic solvent with bifunctional brønsted-lewis acids for highly efficient lignocellulose fractionation, Bioresour. Technol. 347 (2022), https://doi.org/10.1016/j.biortech.2022.126723.
[30] L. Chen, R. Chen, S. Fu, FeCl3 pretreatment of three lignocellulosic biomass for ethanol production, ACS Sustain. Chem. Eng. 3 (2015) 1794–1800, https://doi.org/10.1021/acssuschemeng.5b00377.
[31] S.R. Kamireddy, J. Li, M. Tucker, J. Degenstein, Y. Ji, Effects and mechanism of metal chloride salts on pretreatment and enzymatic digestibility of corn stover, Ind. Eng. Chem. Res. 52 (2013) 1775–1782, https://doi.org/10.1021/ie3019609.
[32] Z.K. Wang, S. Hong, J. long Wen, C.Y. Ma, L. Tang, H. Jiang, J.J. Chen, S. Li, X. J. Shen, T.Q. Yuan, Lewis acid-facilitated deep eutectic solvent (DES) pretreatment for producing high-purity and antioxidative lignin, ACS Sustain. Chem. Eng. 8 (2020) 1050–1057, https://doi.org/10.1021/acssuschemeng.9b05846.
[33] X. Chen, H. Yang, L. Zhang, Z. Li, Y. Xue, R. Wang, X. Fan, S. Sun, Green construction and release mechanism of lignin-based double-layer coated urea,

Biotechnol. Biofuels Bioprod. 16 (2023) 97, https://doi.org/10.1186/s13068-023-02355-7.
[34] W. Tang, X. Wu, C. Huang, Z. Ling, C. Lai, Q. Yong, Revealing the influence of metallic chlorides pretreatment on chemical structures of lignin and enzymatic hydrolysis of waste wheat straw, Bioresour. Technol. 342 (2021) 125983, https://doi.org/10.1016/J.BIORTECH.2021.125983.
[35] Q. Wei, C. Shi, D. Wang, J. Yang, Z. Shi, J.-L. Wen, H.-Y. Yang, Metal chloride mediated choline chloride-lactic acid deep eutectic solvent pretreatment of bamboo for improved cellulose saccharification and lignin recovery, Int. J. Biol. Macromol. 305 (2025) 141107, https://doi.org/10.1016/j.ijbiomac.2025.141107.
[36] A.R. Abouelela, P.Y.S. Nakasu, J.P. Hallett, Influence of pretreatment severity factor and hammett acidity on softwood fractionation by an acidic protic ionic liquid, ACS Sustain. Chem. Eng. 11 (2023) 2404–2415, https://doi.org/10.1021/acssuschemeng.2c06076.
[37] C. Wijaya, N.L. Sangadji, M. Muharja, T. Widjaja, L. Riadi, E. Elaine, R. Lau, A. Widjaja, Prediction by a modified severity factor in $FeCl_3$-catalyzed hydrothermal fractionation of coconut husk: enhancing hemicellulose hydrolysis and enzymatic digestibility of cellulose, Bioresour. Technol. Rep. (2025) 102282, https://doi.org/10.1016/j.biteb.2025.102282.
[38] A. Varilla-Mazaba, J.A. Raggazo-Sánchez, M. Calderón-Santoyo, J. Gómez-Rodríguez, M.G. Aguilar-Uscanga, Optimization of lignin extraction by response surface methodology from sugarcane bagasse using deep eutectic solvents (DES), Ind. Crops Prod. 184 (2022) 115040, https://doi.org/10.1016/J.INDCROP.2022.115040.
[39] Y. Zhang, Y. Guo, X. Xie, V.M. Chernyshev, Y. Liu, W. Qi, Effects of phosphoric acid/hydrogen peroxide, ammonia/hydrogen peroxide and deep eutectic solvent pretreatments on component separation and enzymatic saccharification of Glycyrrhiza residue, Ind. Crops Prod. 196 (2023) 116525, https://doi.org/10.1016/J.INDCROP.2023.116525.
[40] M. Michelin, A.M. Marques, L.M. Pastrana, J.A. Teixeira, M.A. Cerqueira, Carboxymethyl cellulose-based films: effect of organosolv lignin incorporation on physicochemical and antioxidant properties, J. Food Eng. 285 (2020) 110107, https://doi.org/10.1016/J.JFOODENG.2020.110107.
[41] M. Zubair, Z. Rauf, S. Fatima, A. Ullah, Lignin-derived bionanocomposites as functional food packaging materials, Sustain. Food Technol. 2 (2024) 945–966, https://doi.org/10.1039/D4FB00105B.
[42] L. Darus, S. Susana, H. Sihombing, A.R.I. Utami, M. Mel, Enzymatic hydrolysis enhancement of oil palm empty fruit bunch by Peracetic-sulfuric acid pretreatment, Chem. Eng. J. 429 (2022), https://doi.org/10.1016/j.cej.2021.132452.
[43] B.G. Rodrigues, Á.H.M. José, C.A. Prado, D. Rodrigues, R.C.L.B. Rodrigues, Optimizing corncob pretreatment with eco-friendly deep eutectic solvents to enhance lignin extraction and cellulose-to-glucose conversion, Int. J. Biol. Macromol. 283 (2024) 137432, https://doi.org/10.1016/J.IJBIOMAC.2024.137432.
[44] S.M.S.N. Shikh Zahari, Y. Liu, P. Yao, M.S. Ideris, H.H. Azman, J.P. Hallett, OPEFB pretreatment using the low-cost N,N,N-dimethylbutylammonium hydrogen sulfate ionic liquid under varying conditions, Sci. Rep. 13 (2023), https://doi.org/10.1038/s41598-023-48722-0.
[45] M.T. Haqiqi, W. Bankeeree, P. Lotrakul, P. Pattananuwat, H. Punnapayak, R. Ramadhan, T. Kobayashi, R. Amirta, S. Prasongsuk, Antioxidant and UV-Blocking properties of a carboxymethyl cellulose–lignin composite film produced from oil palm empty fruit bunch, ACS Omega 6 (2021) 9653–9666, https://doi.org/10.1021/ACSOMEGA.1C00249.
[46] Y. He, H.C. Ye, T.T. You, F. Xu, Sustainable and multifunctional cellulose-lignin films with excellent antibacterial and UV-shielding for active food packaging, Food Hydrocoll. 137 (2023) 108355, https://doi.org/10.1016/J.FOODHYD.2022.108355.
[47] Y. Zhu, H. Li, Q.S. Zhao, B. Zhao, Effect of DES lignin incorporation on physicochemical, antioxidant and antimicrobial properties of carboxymethyl cellulose-based films, Int. J. Biol. Macromol. 263 (2024) 130294, https://doi.org/10.1016/J.IJBIOMAC.2024.130294.
[48] B. Hames, R. Ruiz, C. Scarlata, A. Sluiter, J. Sluiter, D. Templeton, Preparation of Samples for Compositional Analysis: Laboratory Analytical Procedure (LAP); Issue Date 08/08/2008, 2008.
[49] C. Wijaya, N.L. Sangadji, M. Muharja, T. Widjaja, L. Riadi, A. Widjaja, An integrated green fractionation of coconut husk: hydrothermal and deep eutectic solvent pretreatment for enhanced sugar and lignin production, Bioresour. Technol. Rep. 29 (2025) 102078, https://doi.org/10.1016/j.biteb.2025.102078.
[50] C. He, Feiyue Shen, D. Tian, M. Huang, L. Zhao, Q. Yu, Fei Shen, Lewis acid/base mediated deep eutectic solvents intensify lignocellulose fractionation to facilitate enzymatic hydrolysis and lignin nanosphere preparation, Int. J. Biol. Macromol. 254 (2024) 127853, https://doi.org/10.1016/j.ijbiomac.2023.127853.
[51] C. Alvarez-Vasco, R. Ma, M. Quintero, M. Guo, S. Geleynse, K.K. Ramasamy, M. Wolcott, X. Zhang, Unique low-molecular-weight lignin with high purity extracted from wood by deep eutectic solvents (DES): a source of lignin for valorization, Green Chem. 18 (2016) 5133–5141, https://doi.org/10.1039/c6gc01007e.
[52] R. Wang, K. Wang, M. Zhou, J. Xu, J. Jiang, Efficient fractionation of moso bamboo by synergistic hydrothermal-deep eutectic solvents pretreatment, Bioresour. Technol. 328 (2021) 124873, https://doi.org/10.1016/J.BIORTECH.2021.124873.
[53] Y. Guo, J. Zhang, C. Wang, M. Liu, J. You, L. Yin, M. Shi, Green pretreatment of lignocellulosic biomasses via deep eutectic solvents, Sustain. Chem. Pharm. 39 (2024) 101569, https://doi.org/10.1016/J.SCP.2024.101569.
[54] G. Wan, Q. Zhang, M. Li, Z. Jia, C. Guo, B. Luo, S. Wang, D. Min, How pseudo-lignin is generated during dilute sulfuric acid pretreatment, J. Agric. Food Chem. 67 (2019) 10116–10125, https://doi.org/10.1021/acs.jafc.9b02851.
[55] X. Jiang, R. Zhai, H. Li, C. Li, Q. Deng, M. Jin, Understanding acid hydrolysis of corn stover during densification pretreatment for quantitative predictions of enzymatic hydrolysis efficiency using modified pretreatment severity factor, Bioresour. Technol. 386 (2023) 129487, https://doi.org/10.1016/j.biortech.2023.129487.
[56] H. Zhou, J.Y. Zhu, X. Luo, S.Y. Leu, X. Wu, R. Gleisner, B.S. Dien, R.E. Hector, D. Yang, X. Qiu, E. Horn, J. Negron, Bioconversion of beetle-killed lodgepole pine using SPORL: process scale-up design, lignin coproduct, and high solids fermentation without detoxification, Ind. Eng. Chem. Res. 52 (2013) 16057–16065, https://doi.org/10.1021/ie402873y.
[57] L. Zhu, W. Tang, C. Ma, Y.-C. He, Efficient co-production of reducing sugars and xylooligosaccharides via clean hydrothermal pretreatment of rape straw, Bioresour. Technol. 388 (2023) 129727, https://doi.org/10.1016/j.biortech.2023.129727.
[58] Q. Ma, J. Zhu, R. Gleisner, R. Yang, J.Y. Zhu, Valorization of wheat straw using a recyclable hydrotrope at low temperatures (≤90 °c), ACS Sustain. Chem. Eng. 6 (2018) 14480–14489, https://doi.org/10.1021/acssuschemeng.8b03135.
[59] Q. Gao, Z. Tang, Y.C. He, Valorization of wheat straw through enhancement of cellulose accessibility, xylan elimination and lignin removal by choline chloride: p-toluenesulfonic acid pretreatment, Int. J. Biol. Macromol. 301 (2025), https://doi.org/10.1016/j.ijbiomac.2025.140335.
[60] Q. Yuan, S. Liu, M.G. Ma, X.X. Ji, S.E. Choi, C. Si, The kinetics studies on hydrolysis of hemicellulose, Front. Chem. 9 (2021) 781291, https://doi.org/10.3389/FCHEM.2021.781291/FULL.
[61] L. Schoofs, H. Hilker, N. Conen, A. Jupke, H. Klose, P.M. Grande, Time-resolved analysis of lignocellulose extraction in a biphasic, acid-catalyzed flow-through system, ACS Sustain. Chem. Eng. 14 (2026) 7099–7108, https://doi.org/10.1021/acssuschemeng.5c05534.
[62] Z. Tang, C. Wu, W. Tang, M. Huang, C. Ma, Y.C. He, Enhancing enzymatic saccharification of sunflower straw through optimal tartaric acid hydrothermal pretreatment, Bioresour. Technol. 385 (2023), https://doi.org/10.1016/j.biortech.2023.129279.
[63] H. Ji, Y. Song, X. Zhang, T. Tan, Using a combined hydrolysis factor to balance enzymatic saccharification and the structural characteristics of lignin during pretreatment of hybrid poplar with a fully recyclable solid acid, Bioresour. Technol. 238 (2017) 575–581, https://doi.org/10.1016/j.biortech.2017.04.092.
[64] A. Sluiter, B. Hames, R. Ruiz, C. Scarlata, J. Sluiter, D. Templeton, Determination of Ash in Biomass: Laboratory Analytical Procedure (LAP); Issue Date: 7/17/2005, 2008.
[65] N.L. Sangadji, C. Wijaya, M. Muharja, E. Elaine, H.F. Sangian, R. Lau, A. Widjaja, Two step fractionation of oil palm empty fruit bunches integrating hydrothermal-organosolv pretreatment for enhanced lignin extraction and enzymatic hydrolysis efficiency, Case Stud. Chem. Environ. Eng. (2025) 101275, https://doi.org/10.1016/j.cscee.2025.101275.
[66] P.D. Sutrisna, R.P. Hadi, C. Wijaya, J. Liliani, C. Robby, Cellulose acetate-based mixed matrix membrane for methylene blue wastewater treatment, in: AIP Conference Proceedings, American Institute of Physics Inc, 2023, https://doi.org/10.1063/5.0112184.
[67] A. Mittal, T.B. Vinzant, R. Brunecky, S.K. Black, H.M. Pilath, M.E. Himmel, D. K. Johnson, Investigation of the role of lignin in biphasic xylan hydrolysis during dilute acid and organosolv pretreatment of corn stover, Green Chem. 17 (2015) 1546–1558, https://doi.org/10.1039/c4gc02258k.
[68] Y. Zhu, B. Qi, X. Liang, J. Luo, Y. Wan, Comparison of corn stover pretreatments with lewis acid catalyzed choline chloride, glycerol and choline chloride-glycerol deep eutectic solvent, Polymers 13 (2021), https://doi.org/10.3390/POLYM13071170. Page 1170 13, 1170.
[69] C. He, Feiyue Shen, D. Tian, M. Huang, L. Zhao, Q. Yu, Fei Shen, Lewis acid/base mediated deep eutectic solvents intensify lignocellulose fractionation to facilitate enzymatic hydrolysis and lignin nanosphere preparation, Int. J. Biol. Macromol. 254 (2024) 127853, https://doi.org/10.1016/J.IJBIOMAC.2023.127853.
[70] Feiyue Shen, S. Wu, M. Huang, L. Zhao, J. He, Y. Zhang, S. Deng, J. Hu, D. Tian, Fei Shen, Integration of lignin microcapsulated pesticide production into lignocellulose biorefineries through FeCl3-mediated deep eutectic solvent pretreatment, Green Chem. 24 (2022) 5242–5254, https://doi.org/10.1039/D2GC01255C.
[71] T.M. Curry, M.J. Peña, B.R. Urbanowicz, An update on xylan structure, biosynthesis, and potential commercial applications, Cell Surf. (2023), https://doi.org/10.1016/j.tcsw.2023.100101.
[72] H. Wei, X. Chen, J. Shekiro, E. Kuhn, W. Wang, Y. Ji, E. Kozliak, M.E. Himmel, M. P. Tucker, Kinetic modelling and experimental studies for the effects of fe2+ ions on xylan hydrolysis with dilute-acid pretreatment and subsequent enzymatic hydrolysis, Catalysts 8 (2018), https://doi.org/10.3390/catal8010039.
[73] I. Romero, J.C. López-Linares, M. Moya, E. Castro, Optimization of sugar recovery from rapeseed straw pretreated with FeCl3, Bioresour. Technol. 268 (2018) 204–211, https://doi.org/10.1016/j.biortech.2018.07.112.
[74] X. Wu, Chen Huang, W. Tang, Caoxing Huang, C. Lai, Q. Yong, Use of metal chlorides during waste wheat straw autohydrolysis to overcome the self-buffering effect, Bioresour. Technol. 268 (2018) 259–265, https://doi.org/10.1016/J.BIORTECH.2018.07.132.
[75] W. Tang, X. Wu, C. Huang, Z. Ling, C. Lai, Q. Yong, Comprehensive understanding of the effects of metallic cations on enzymatic hydrolysis of humic acid-pretreated waste wheat straw, Biotechnol. Biofuels 14 (2021) 25, https://doi.org/10.1186/s13068-021-01874-5.

[76] W. Zhu, C.J. Houtman, J.Y. Zhu, R. Gleisner, K.F. Chen, Quantitative predictions of bioconversion of aspen by dilute acid and SPORL pretreatments using a unified combined hydrolysis factor (CHF), Process Biochem. 47 (2012) 785–791, https://doi.org/10.1016/j.procbio.2012.02.012.
[77] Y. Li, Z. Lin, X. Wang, Z. Duan, P. Lu, S. Li, D. Ji, Z. Wang, G. Li, D. Yu, W. Liu, High-hydrophobic ZIF-8@PLA composite aerogel and application for oil-water separation, Sep. Purif. Technol. 270 (2021) 118794, https://doi.org/10.1016/J.SEPPUR.2021.118794.
[78] B. Zhang, C. Peng, S. Zhang, M. Zhang, D. Li, X. Wang, B. Mao, Comprehensive analysis of the combined flocculation and filtration process for microalgae harvesting at various operating parameters, Sci. Total Environ. 857 (2023), https://doi.org/10.1016/j.scitotenv.2022.159658.
[79] R. Kumar, G. Mago, V. Balan, C.E. Wyman, Physical and chemical characterizations of corn stover and poplar solids resulting from leading pretreatment technologies, Bioresour. Technol. 100 (2009) 3948–3962, https://doi.org/10.1016/j.biortech.2009.01.075.
[80] H. Li, X. Li, D. Li, J. Zhang, H. Nawaz, T. You, F. Xu, Highly-efficient pretreatment using alkaline enhanced aqueous deep eutectic solvent to unlock poplar for high yield of fermentable sugars: synergistic removal of lignin and mannan, Bioresour. Technol. 351 (2022) 126993, https://doi.org/10.1016/J.BIORTECH.2022.126993.
[81] Y. Su, P. Wang, C. Lai, C. Huang, Z. Ling, Q. Yong, Revealing key factors influencing enzymatic digestibility of hydrothermally pretreated poplar in comparison with corn stover, Ind. Crops Prod. 194 (2023), https://doi.org/10.1016/j.indcrop.2023.116297.
[82] S.L. Sunar, R.K. Oruganti, D. Bhattacharyya, D. Shee, T.K. Panda, Deep eutectic solvent pretreatment of sugarcane bagasse for efficient lignin recovery and enhanced enzymatic hydrolysis, J. Ind. Eng. Chem. 139 (2024) 539–553, https://doi.org/10.1016/j.jiec.2024.05.030.
[83] F. Rodríguez-Rebelo, B. Rodríguez-Martínez, P.G. Del-Río, M.N. Collins, G. Garrote, B. Gullón, Assessment of deep eutectic solvents (DES) to fractionate paulownia wood within a biorefinery scheme: cellulosic bioethanol production and lignin isolation, Ind. Crops Prod. 216 (2024) 118761, https://doi.org/10.1016/j.indcrop.2024.118761.
[84] S.O. Anuchi, K.L.S. Campbell, J.P. Hallett, Effective pretreatment of lignin-rich coconut wastes using a low-cost ionic liquid, Sci. Rep. 12 (1 12) (2022) 1–11, https://doi.org/10.1038/s41598-022-09629-4, 2022.
[85] A.R. Mankar, A. Pandey, K.K. Pant, Microwave-assisted extraction of lignin from coconut coir using deep eutectic solvents and its valorization to aromatics, Bioresour. Technol. 345 (2022) 126528, https://doi.org/10.1016/J.BIORTECH.2021.126528.
[86] C. Ji, R. Weng, C. Yu, Y. Fan, J. Ouyang, Insights into acidic deep eutectic solvent-mediated softwood pretreatment for high fermentable sugar yield and efficient lignin recovery, Ind. Crops Prod. 227 (2025), https://doi.org/10.1016/j.indcrop.2025.120779.
[87] G. Miao, F. Ge, Y. Hu, H. Li, S. Yu, Y. He, S. Chen, F. Xu, Z. Chen, J. Xu, Mechanisms and mass-transfer kinetics of hemicellulose and lignin dissolution during deep eutectic solvent pretreatment, AIChE J. (2025), https://doi.org/10.1002/aic.70116.
[88] M.F. Syakir Bahazin, N.I. Amalin Mohd Isa, N.A. Natasha Mohd Azlan, M. R. Anuar, K.F. Pa'ee, T.L. Kelly Yong, Valorization of oil palm biomass: investigating chcl:lactic acid deep eutectic solvents for efficient furfural production, Biomass Bioenergy 200 (2025) 107971, https://doi.org/10.1016/J.BIOMBIOE.2025.107971.
[89] J. Yan, O. Oyedeji, J.H. Leal, B.S. Donohoe, T.A. Semelsberger, C. Li, A.N. Hoover, E. Webb, E.A. Bose, Y. Zeng, C.L. Williams, K.D. Schaller, N. Sun, A.E. Ray, D. Tanjore, Characterizing variability in lignocellulosic biomass: a review, ACS Sustain. Chem. Eng. (2020), https://doi.org/10.1021/acssuschemeng.9b06263.
[90] S.C. Sun, Y. Xu, C.Y. Ma, C. Zhang, C. Zuo, D. Sun, J.L. Wen, T.Q. Yuan, Green and efficient fractionation of bamboo biomass via synergistic hydrothermal-alkaline deep eutectic solvents pretreatment: valorization of carbohydrates, Renew. Energy 217 (2023) 119175, https://doi.org/10.1016/J.RENENE.2023.119175.
[91] B. Yang, B. Fan, Y.C. He, Metal salt-assisted hydrogen peroxide-malonic acid pretreatment for effectively enhancing delignification and saccharification of rapeseed straw, Ind. Crops Prod. 230 (2025), https://doi.org/10.1016/j.indcrop.2025.121076.
[92] P. Li, W. Qian, S. Wu, Y. Liu, Acidic deep eutectic solvents for lignocellulose pretreatment: insights into lignin extraction efficiency and structural transformation, ACS Sustain. Chem. Eng. 13 (2025) 9987–10018, https://doi.org/10.1021/acssuschemeng.5c02184.
[93] A.M. Da Costa Lopes, J.R.B. Gomes, J.A.P. Coutinho, A.J.D. Silvestre, Novel insights into biomass delignification with acidic deep eutectic solvents: a mechanistic study of β-O-4 ether bond cleavage and the role of the halide counterion in the catalytic performance, Green Chem. 22 (2020) 2474–2487, https://doi.org/10.1039/C9GC02569C.
[94] P. Moodley, Y. Sewsynker-Sukai, E.B. Gueguim Kana, Progress in the development of alkali and metal salt catalysed lignocellulosic pretreatment regimes: potential for bioethanol production, Bioresour. Technol. 310 (2020) 123372, https://doi.org/10.1016/j.biortech.2020.123372.
[95] H. Zhang, W. Chen, X. Han, Y. Zeng, J. Zhang, Z. Gao, J. Xie, Intensification of sugar production by using tween 80 to enhance metal-salt catalyzed pretreatment and enzymatic hydrolysis of sugarcane bagasse, Bioresour. Technol. 339 (2021), https://doi.org/10.1016/j.biortech.2021.125522.
[96] Z. Zhao, X. Chen, M.F. Ali, A.A. Abdeltawab, S.M. Yakout, G. Yu, Pretreatment of wheat straw using basic ethanolamine-based deep eutectic solvents for improving enzymatic hydrolysis, Bioresour. Technol. 263 (2018) 325–333, https://doi.org/10.1016/J.BIORTECH.2018.05.016.
[97] Y. Yuan, B. Jiang, H. Chen, W. Wu, S. Wu, Y. Jin, H. Xiao, Recent advances in understanding the effects of lignin structural characteristics on enzymatic hydrolysis, Biotechnol. Biofuels 14 (1 14) (2021) 1–20, https://doi.org/10.1186/S13068-021-02054-1, 2021.
[98] S. Hou, B. Shen, D. Zhang, R. Li, X. Xu, K. Wang, C. Lai, Q. Yong, Understanding of promoting enzymatic hydrolysis of combined hydrothermal and deep eutectic solvent pretreated poplars by tween 80, Bioresour. Technol. 362 (2022), https://doi.org/10.1016/j.biortech.2022.127825.
[99] H. Zhang, M. Fan, X. Li, A. Zhang, J. Xie, Enhancing enzymatic hydrolysis of sugarcane bagasse by ferric chloride catalyzed organosolv pretreatment and tween 80, Bioresour. Technol. 258 (2018) 295–301, https://doi.org/10.1016/j.biortech.2018.03.004.
[100] X. Shi, L. Wang, L. Sun, H. Chen, Sufficient premixing enhances enzymatic hydrolysis efficiency of lignocellulose at high-solids loading, Chem. Eng. J. 444 (2022) 136612, https://doi.org/10.1016/j.cej.2022.136612.
[101] J. Yang, X. Zhang, Q. Yong, S. Yu, Three-stage enzymatic hydrolysis of steam-exploded corn stover at high substrate concentration, Bioresour. Technol. 102 (2011) 4905–4908, https://doi.org/10.1016/j.biortech.2010.12.047.
[102] D.H. Fockink, M.B. Urio, J.H. Sánchez, L.P. Ramos, Enzymatic hydrolysis of steam-treated sugarcane bagasse: effect of enzyme loading and substrate total solids on its fractal kinetic modeling and rheological properties, Energy Fuel. 31 (2017) 6211–6220, https://doi.org/10.1021/acs.energyfuels.7b00818.
[103] M.G. Ganter de Moura, T.A. da Silva, A.Z. Filho, M.L. Corazza, L.P. Ramos, Fed-batch enzymatic hydrolysis of steam-exploded sugarcane bagasse, Bioresources 18 (2023) 3160–3177, https://doi.org/10.15376/biores.18.2.3160-3177.
[104] J.K. Kim, J. Yang, S.Y. Park, J.-H. Yu, K.H. Kim, Cellulase recycling in high-solids enzymatic hydrolysis of pretreated empty fruit bunches, Biotechnol. Biofuels 12 (2019) 138, https://doi.org/10.1186/s13068-019-1476-x.
[105] D. Ludwig, B. Michael, T. Hirth, S. Rupp, S. Zibek, High solids enzymatic hydrolysis of pretreated lignocellulosic materials with a powerful stirrer concept, Appl. Biochem. Biotechnol. 172 (2014) 1699–1713, https://doi.org/10.1007/s12010-013-0607-2.
[106] M.H. Sipponen, M. Österberg, Aqueous ammonia pre-treatment of wheat straw: process optimization and broad spectrum dye adsorption on nitrogen-containing lignin, Front. Chem. 7 (2019), https://doi.org/10.3389/fchem.2019.00545.
[107] F. Xin, H. Zhang, W. Wong, Bioethanol production from horticultural waste using crude fungal enzyme mixtures produced by solid state fermentation, Bioenergy Res. 6 (2013) 1030–1037, https://doi.org/10.1007/s12155-013-9330-7.
[108] V.P. Zambare, A.V. Zambare, D. Barh, L.P. Christopher, Optimization of enzymatic hydrolysis of prairie cordgrass for improved ethanol production, J. Renew. Sustain. Energy 4 (2012), https://doi.org/10.1063/1.4729587.
[109] A.K. Chandel, V.K. Garlapati, A.K. Singh, F.A.F. Antunes, S.S. da Silva, The path forward for lignocellulose biorefineries: bottlenecks, solutions, and perspective on commercialization, Bioresour. Technol. 264 (2018) 370–381, https://doi.org/10.1016/j.biortech.2018.06.004.
[110] Y. Xiao, J. Qi, Z. Yu, W. Zhao, W. Shao, N. Li, Y. Kong, L. Li, W. Wei, Pretreatment of corncob powder by choline chloride-urea-ethanolamine to co-produce glucose, xylose and lignin nanospheres, Ind. Crops Prod. 206 (2023) 117695, https://doi.org/10.1016/J.INDCROP.2023.117695.
[111] Y. Guo, L. Xu, F. Shen, J. Hu, M. Huang, J. He, Y. Zhang, S. Deng, Q. Li, D. Tian, Insights into lignocellulosic waste fractionation for lignin nanospheres fabrication using acidic/alkaline deep eutectic solvents, Chemosphere 286 (2022) 131798, https://doi.org/10.1016/j.chemosphere.2021.131798.
[112] Z. Guo, Z. Ling, C. Wang, X. Zhang, F. Xu, Integration of facile deep eutectic solvents pretreatment for enhanced enzymatic hydrolysis and lignin valorization from industrial xylose residue, Bioresour. Technol. 265 (2018) 334–339, https://doi.org/10.1016/j.biortech.2018.06.027.
[113] M. Karlsson, J. Romson, T. Elder, Å. Emmer, M. Lawoko, Lignin structure and reactivity in the organosolv process studied by NMR spectroscopy, mass spectrometry, and density functional theory, Biomacromolecules 24 (2023) 2314–2326, https://doi.org/10.1021/acs.biomac.3c00186.
[114] X.J. Shen, J.L. Wen, Q.Q. Mei, X. Chen, D. Sun, T.Q. Yuan, R.C. Sun, Facile fractionation of lignocelluloses by biomass-derived deep eutectic solvent (DES) pretreatment for cellulose enzymatic hydrolysis and lignin valorization, Green Chem. 21 (2019) 275–283, https://doi.org/10.1039/c8gc03064b.
[115] Syahidah, A.S.R.D. Lestari, A. Arif, I. Taskirawati, Fardhatillah Makkarennu, R. Zhafira, M.R.A. Pratama, S. Sulaeha, S.H. Anita, M. Ghozali, F.P. Sari, A. D. Martino, W. Fatriasari, Lignin from the sugar palm's fiber (Arenga pinnata merr.) as a potential active compound in packaging, Case Stud. Chem. Environ. Eng. 11 (2025), https://doi.org/10.1016/j.cscee.2025.101133.
[116] C.E. de A. Padilha, C. da C. Nogueira, B.R.A. Alencar, Í.B.S. de Abreu, E.D. Dutra, J.A.C. Ruiz, D.F. de S. Souza, E.S. dos Santos, Production and application of lignin-based chemicals and materials in the cellulosic ethanol production: an overview on lignin closed-loop biorefinery approaches, Waste Biomass Valor. (2021), https://doi.org/10.1007/s12649-021-01455-5.
[117] H. Mostafa, M. Hamdi, J.O. Airouyuwaa, F. Hamed, Y. Wang, S. Maqsood, Lignin and green solvent extracted phenolic compounds from date palm leaves as functional ingredients for the formulation of soy protein isolate biocomposite packaging materials: a circular packaging concept, Int. J. Biol. Macromol. 279 (2024) 134843, https://doi.org/10.1016/J.IJBIOMAC.2024.134843.
[118] I. Korbag, S. Mohamed Saleh, Studies on the formation of intermolecular interactions and structural characterization of polyvinyl alcohol/lignin film, Int. J. Environ. Stud. 73 (2016) 226–235, https://doi.org/10.1080/00207233.2016.1143700.

[119] A. Wichaphian, P. Yasan, W. Pathom-aree, S. Lumyong, N. Suwannarach, J. Kumla, S. Chaipoot, S. Hoijang, T. Krasian, P. Worajittiphon, W. Punyodom, B. Cheirsilp, G. Wang, S. Srinuanpan, From agricultural waste to active films: enhanced crystallinity of spent mushroom substrate-derived cellulose via deep eutectic solvent-based microwave-assisted pretreatment and its application in reinforcing CMC-Based composite films, J. Agric. Food Res. 20 (2025), https://doi.org/10.1016/j.jafr.2025.101759.

[120] J.F. Leal Silva, P.Y.S. Nakasu, A.C. da Costa, R. Maciel Filho, S.C. Rabelo, Techno-economic analysis of the production of 2G ethanol and technical lignin via a protic ionic liquid pretreatment of sugarcane bagasse, Ind. Crops Prod. 189 (2022), https://doi.org/10.1016/j.indcrop.2022.115788.

[121] P. Li, C. Yang, Z. Jiang, Y. Jin, W. Wu, Lignocellulose pretreatment by deep eutectic solvents and related technologies: a review, J. Bioresour. Bioprod. (2022), https://doi.org/10.1016/j.jobab.2022.11.004.

[122] H.A. Ruiz, W.G. Sganzerla, V. Larnaudie, R.J. Veersma, G. van Erven, Shiva, L. J. Ríos-González, R.M. Rodríguez-Jasso, G. Rosero-Chasoy, M.D. Ferrari, M. A. Kabel, T. Forster-Carneiro, C. Lareo, Advances in process design, techno-economic assessment and environmental aspects for hydrothermal pretreatment in the fractionation of biomass under biorefinery concept, Bioresour. Technol. 369 (2023) 128469, https://doi.org/10.1016/j.biortech.2022.128469.

Biomass and Bioenergy

Supports open access

Volume 217, Part A

In progress (February 2027)

This issue is in progress but contains articles that are final and fully citable.

Research Articles

Biomass and Bioenergy

Spatial separation of hydrogen and oxygen gas in SCP production by hydrogen oxidizing bacteria: a theoretical energy-efficiency assessment

Carlos Serrano-Fajardo, Giuseppe Olivieri, René H. Wijffels, Ruud A. Weusthuis

Article 109760

View PDF Article preview

Research article Full text access

Enhanced removal of Cu(II) and Ni(II) from binary systems by Ca-modified low-temperature pine bark biochar

Eun-Chae Im, Jae-In Lee, Seong-Jik Park, Chang-Gu Lee

Article 109741

View PDF Article preview

Research article Full text access

Influence of light source and intensity on the biochemical profile of *Chlorella vulgaris* and the plasmonic properties of biosynthesized silver nanoparticles

Hui Ying Teh, Man Kee Lam, Yee Ho Chai, Voon-Loong Wong, ... Wai Hong Leong

Article 109758

View PDF Article preview

Research article Full text access

Enhanced degradation of bamboo shoot shells via a two-step process: Sodium chlorite pretreatment and xylanase hydrolysis for xylooligosaccharides production

Menghan Zhang, Qiang Li, Chao Teng, Chunyan Huo, ... Siting Li

Article 109767

View PDF Article preview

Research article Full text access

Phosphorus recovery as struvite from hydrothermally treated manure digestate:optimization of operating parameters and life cycle assessment

Qiao Xiong, Yujie Zhou, Yinqiu Li, Xiao Ma, ... Chang Chen

Article 109765

View PDF Article preview

Research article Full text access

Performance on carboxylates extraction from dark acid fermentation of agroresidual wastes

María de Lourdes Mendoza, Luis Vaca, Pablo Villa

Article 109791

View PDF Article preview

Research article Full text access

Synthesis and in-depth characterization of hydrochars derived from cellulose and nanocellulose

Antônio J.R. Castro, Gilberto D. Saraiva, Franciso H. Soares Junior, Alessandra A. Aquino, ... Odair P. Ferreira

Article 109783

Biomass and Bioenergy

Research article Full text access

Dual effects of granular activated carbon on methane enhancement of distillers' grains in solid-state anaerobic digestion: Restructuring microbial consortia and adsorbing methanogenic substrates

Jiaxing Zhang, Suyue Fan, Ruilin Jiang, Qiuxia Meng, ... Guoxue Li

Article 109790

View PDF Article preview

Research article *Open access*

Optimization of almond shell cellulose phosphorylation using Box–Behnken design: Structural and thermal characterization of functionalized cellulose

Yassine EL Khayat Driaa, Hafida Maarir, Adama Konaté, Nabil Grimi, ... Nadia Boussetta

Article 109781

View PDF Article preview

Research article *Open access*

Fiber fractionation and oxygen delignification pretreatments of Old Corrugated Container (OCC) pulp for controlled rheological spinnability in [DBNH][OAc] ionic liquid systems

Autumn M. Reynolds, Anibal Moran, Syed Mohammad Baqir, Inge Schlapp-Hackl, ... Richard A. Venditti

Article 109786

View PDF Article preview

Research article *Open access*

Optimization and characterization of biochars from biogenic residues for application in self-reducing pellets for direct reduction ironmaking

Rafiandy Dwi Putra, Andreas Schedl, Özge Mutlu, Andreas Siegfried Braeuer, Volker Herdegen

Article 109784

View PDF Article preview

Research article Full text access

Effect of pyrolysis temperature and milling treatment on wheat straw biochar for crystal violet adsorption

Corinna Maria Grottola, Paola Giudicianni, Raffaele Ragucci, Elena Lamberti, ... Gianluca Viscusi

Article 109788

View PDF Article preview

Research article Full text access

Synergistic engineering of sustainable COF-biochar-Al_2O_3 ternary hybrids composite for elite simultaneous capture of divalent lead and cadmium from groundwater: Mechanisms, energetics, and structural resilience

Eslam A. Mohamed, Ali M. Hassan, Mahmoud F. Mubarak

Article 109782

View PDF Article preview

Biomass and Bioenergy

Research article *Open access*

UK bioenergy policies and implications for global land use change

Jalil Yesufu, Patricia Thornley

Article 109794

View PDF Article preview

Research article Full text access

Ammonia-nitrogen removal enhancement from rare earth elements wastewater using self-flocculating *Spirulina platensis* CMB-02: Pre-pilot-scale evaluation of photobioreactor systems and metabolic mechanisms

Mingmin Zheng, Dandan Che, Qiang Wang, Guanglu Huang, ... Mingzi Wang

Article 109789

View PDF Article preview

Research article *Open access*

Ethanol quenching in fast-pyrolysis of sugarcane bagasse and straw: Implications for bio-oil hydrodeoxygenation

Mariana M. Campos Fraga, Danilo E. Hirayama, Renata Moreira, Naiara R. Telis, ... Nicolaus Dahmen

Article 109774

View PDF Article preview

Research article Full text access

Biochar-immobilized *Phanerochaete chrysosporium* for accelerated lignocellulose bioconversion in green waste composting

Zejin Li, Zhipeng Feng, Lu Zhang

Article 109787

View PDF Article preview

Research article *Open access*

Integrated valorization of hop vine chaff silage by steam pulping and explosive decompression enabling coupled fiber production, methane generation and viroid mitigation

Leonhard Lenz, Benedikt Hülsemann, Hans Oechsner, Sven Schneider, ... Andreas Lemmer

Article 109797

View PDF Article preview

Research article Full text access

Synergistic enhancement of syngas production from vinegar residue via air-steam co-gasification: Performance and life cycle assessment

Feng Tan, Qi Wang, Ding Jiang, Pengyu Lu, ... Anqing Zheng

Article 109776

View PDF Article preview

Research article *Open access*

Reactivity-guided experimental design and severity factor development for optimizing the chemical activation of hydrolysis lignin into CO_2-adsorbing carbons

Chamseddine Guizani, Virpi Siipola, Fanni Hakanen, Mikko Mäkelä

Biomass and Bioenergy

Article 109775

View PDF Article preview

Research article Full text access

Dual-functional biochar with Mg-Zn-Fe LDH and phosphate groups: A versatile adsorbent for RhB, MO, and OTC in water

Yingying Zhu, Zhong Wang, Jinze Li, Yumeng Ren, ... Geng Chen

Article 109798

View PDF Article preview

Research article Full text access

A multi-scale approach to hydrothermal liquefaction of two-phase olive mill waste: From laboratory test to regional biorefinery in Andalusia

A. Ronda, S. Moreno, G. Blázquez, C. Moliner, ... P. Haro

Article 109793

View PDF Article preview

Research article *Open access*

Nitrogen upcycling and carbon capture from food waste through dark fermentation coupled with microalgae and hydrogen oxidising bacteria cultivation

Raffaele Manzo, Stefano Papirio, Giovanni Esposito, José de Jesús Montoya Rosales, ... Raúl Muñoz Torre

Article 109792

View PDF Article preview

Research article *Open access*

Catalytically graphitized carbon derived from biorefinery hydrolysis lignin as a sustainable anode for lithium-ion batteries

Sherif Hegazy, Hossein Rostami, Tao Hu, Rafal Sliz, Ulla Lassi

Article 109795

View PDF Article preview

Research article Full text access

Alkaline resistant tunable superaerophobic bio-based chitosan/dialdehyde starch hydrogels

Vojtěch Škopek, Ewa Olewnik-Kruszkowska, Magdalena Gierszewska, Iztok Dogsa, ... Ilja Gasan Osojnik Črnivec

Article 109799

View PDF Article preview

Research article Full text access

Renewable peak shaving via integrated biomass gasification, fuel cell, and storage systems: Biomass selection, life cycle assessment-driven exergoenvironmental analysis, and machine-learning optimization

Manwen Tian, Ali Basem, Yonghui Li, Hyder H. Abed Balla, ... Ibrahim Mahariq

Article 109772

View PDF Article preview

Biomass and Bioenergy

Research article Full text access

Enhancement of humification and heavy metal stabilization in chicken manure compost: Comparative effects of adding zeolite and peat separately

Jiali Wang, Siyi Yang, Yongbing Li, Guiyuan Yu, ... Liejin Guo

Article 109803

View PDF Article preview

Research article *Open access*

Sugarcane filter cake-derived humic acid modulates phosphorus acquisition and transporter response in tomato under low-phosphorus conditions

Keiji Jindo, Luciano Pasqualoto Canellas, Lázaro Eustáquio Pereira Peres, Natália Oliveira Aguiar Canellas, ... Jean Luiz Simoes-Araujo

Article 109806

View PDF Article preview

Research article *Open access*

Structural characterization and biochar potential of *Spirulina* sp. LEB 18

Laiz Helena Soares Falchetto, Larissa Chivanski Lopes, Gabriel Martins Rosa, Thaisa Duarte Santos, ... Jorge Alberto Vieira Costa

Article 109808

View PDF Article preview

Research article Full text access

Efficient synthesis of ethyl levulinate from furfuryl alcohol using several biomass-based carbon

Kongde Li, Qikai Si, Guangyu Wu, Guijing Liu, ... Bin He

Article 109807

View PDF Article preview

Research article Full text access

Unveiling the thermodynamic and kinetic mechanisms of acaiomass pyrolysis for Fe-N Co-doped biochar

Shouzhi Li, Haolin He, Haoyu Yao, Linghui Yu, ... Wei Chen

Article 109804

View PDF Article preview

Research article Full text access

Photocatalytic conversion of biomass derived furfural into fuel and fragrance precursors over CdS quantum dots under visible-light irradiation

Mina Shafiee-Nattaj, Kimia Ghazipoor, Mona Hosseini-Sarvari

Article 109802

View PDF Article preview

Research article Full text access

Pre-carboxylation modification of lignin toward high-efficiency bifunctional oxygen electrocatalysis of nitrogen-doped porous carbon

Yuping Zhu, Yiming Liu, Guoli Pang, Tingzhou Lei, ... Suxia Ren

Biomass and Bioenergy

View PDF Article preview

Research article Full text access

Valorization of reed bamboo as a torrefied energy crop for coal co-processing: contrasting responses of co-combustion and co-grinding behavior

Quan Tang, Zipeng Xiao, Erwei Leng, Yuanwang Deng, Jiaqiang E

Article 109819

View PDF Article preview

Research article *Open access*

From wastewater to value: Techno-Economic and life-cycle assessment of a continuous microalgae biorefinery for high-value metabolites and bioenergy

Abdullah M. Alsalal, Salem Alkanaimsh, Fares Almomani

Article 109818

View PDF Article preview

Research article Full text access

Development of Chitosan@ZnO@Ghassoul clay biohybrid beads for photocatalytic dye degradation and Cu(II) photoreduction

Soukaina El Bourachdi, Yassine Ballout, Ali Raza Ayub, Abdelhay El Amri, ... Amal Lahkimi

Article 109821

View PDF Article preview

Research article Full text access

Surfactants in hydrothermal carbonization of tangerine peel tailor pore characteristics of hydrochar-derived activated carbon

Shuaizhi Man, Yuchen Jiang, Chao Li, Shu Zhang, ... Xun Hu

Article 109825

View PDF Article preview

Research article Full text access

Microbially activated coal gangue for remediation of aeolian sandy soil: Nutrient release from clay minerals and soil property enhancement

Xiaoli Zhu, Jiayi Ji, Zhizhong Ren, Ziye Zhang, ... Shengguo Xue

Article 109827

View PDF Article preview

Research article Full text access

Beyond pristine biochar: A comparative study on environmental sustainability and tetracycline adsorption performance of pristine, activated, and iron-nitrogen co-doped hardwood waste-derived biochar

Subhash Chandra, Isha Medha, Chandra Sekhar Tiwary, Nabisab Mujawar Mubarak

Article 109830

View PDF Article preview

Biomass and Bioenergy

Research article Full text access

Engineering of N-enriched muscovite/hydrochar composite through hydrothermal treatment for RB5 remediation: Adsorption performance in distilled water and tap water matrices

Yahia Saghir, Asma Amjlef, Nadya Douihi, Ayoub Chaoui, ... Mohamed Ez-Zahery

Article 109832

View PDF Article preview

Research article Full text access

Sustainable fabrication of 3D rGO/NiS composites from peanut shell biomass residue for dye-sensitized solar cell counter electrodes

Kasempong Srisawad, Pornchanok Ngaophithaksinlapin, Nattakan Kanjana, Nuchjarin Sangwong, ... Wasan Maiaugree

Article 109834

View PDF Article preview

Research article Full text access

Sustainable valorization of rice husks into silicon carbide for high performance anti-corrosion coatings

Junjie Li, Peng Gao, Jie Li, Wenrui Hu, ... Jianqiang Chen

Article 109835

View PDF Article preview

Research article Full text access

Valorization of fish scale biowaste into activated carbon for multi-contaminant removal from water: kinetic, isotherm, thermodynamics and techno-economic studies

Yogesh Dangoliya, Nabendu Paul, M.M. Malik, Rupak Kishor

Article 109836

View PDF Article preview

Research article *Open access*

A novel synthetic fungal–bacterial anodic consortium for multifunctional microbial fuel cells under simulated hydroponic conditions

Ignacio Baquedano, Daniel González-García, Alicia Prieto, Jorge Barriuso

Article 109842

View PDF Article preview

Research article Full text access

Mechanistic understanding of carbon–hydrogen conversion during rice straw supercritical water gasification through Taguchi–RSM-guided optimization and liquid-phase intermediate evolution

Tianrong Li, Lei Yi, Lanlan Fan, Zhimin Wang, ... Bin Chen

Article 109839

View PDF Article preview

Research article Full text access

Modeling and optimization of premix burner utilizing low calorific value gaseous fuels for industrial applications

Biomass and Bioenergy

Wahyu Setiawan, Siska Nuri Fadilah, Subriyer Nasir, Muhammad Said, ... Fakhili Gulo
Article 109844

View PDF Article preview

Research article Full text access

Oxone synergized with microorganisms for enhanced sludge reduction: Promotion effects and mechanisms
Chenhao Wang, Junfeng Su, Shuyu Liu, Shicheng Xie, ... Jingting Feng
Article 109841

View PDF Article preview

Research article Full text access

Porous loofah sponge meets bimetallic MOF: Synergistic effect for efficient tetracycline removal
Lei She, Yuan Zhao, Mei-Jin Li, Jing-Yi Zhao, ... Tao Chen
Article 109846

View PDF Article preview

Research article Full text access

A multi-scale kinetic-thermal framework for scaling continuous screw torrefaction: Bridging laboratory kinetics and industrial design for rubberwood biomass
Jannisa Kasawapat, Wipawee Dechapanya, Attaso Khamwichit
Article 109845

View PDF Article preview

Research article Full text access

AI driven integrated approach of microalgae Chlorella vulgaris AK and amine functionalized multi-walled carbon nanotubes (AF-MWCNT) for sewage wastewater treatment with improved biodiesel and anti-fungal activity
Anwesha Dey, Juhi Saxena, Prince Jain, Jaivik Pathak, ... Shakeel Ahmad Khan
Article 109851

View PDF Article preview

Research article Full text access

High temperature drives a thermophilic microbial communities reconstruction with high metabolic potential for achieving higher methane production via hydrogenotrophic methanogenesis
Weimin Wu, Heng Wu, Zhilin Xing, Yunzhu Chen, Zhaoqin Liu
Article 109852

View PDF Article preview

Research article Full text access

Synergistic mechanisms in co-pyrolysis of lignin and polystyrene: A comprehensive study integrating experiments, ReaxFF-MD simulations, and kinetics
Fang Xu, Mingjun Liu, Wenxiao Wang, Mohan Zhao, ... Qing Wang
Article 109854

View PDF Article preview

Biomass and Bioenergy

Integrated valorization of oil palm empty fruit bunch (OPEFB) by deep eutectic solvent pretreatment: Glucose production enhancement and lignin-CMC composite for sustainable packaging

Candra Wijaya, Andika Prastika, Olivia Izzati Atiqa, Tabina Raissa Apol, ... Arief Widjaja

Article 109859

View PDF Article preview

Research article Full text access

Hydrothermal-assisted *Trametes versicolor* pretreatment as a pore-engineering strategy for biomass-derived hierarchical porous carbon toward supercapacitor electrodes

Jinhang Yu, Yu Jiang, Kunjie Chen, Chao Li, ... Qing Dong

Article 109858

View PDF Article preview

Research article Full text access

Low-dosage thiourea-assisted *p*-toluenesulfonic acid pretreatment of bamboo for lignin condensation suppression and residue valorization

Wenjun Ying, Xudong Li, Sisi Wang, Junhua Zhang, Qiang Yong

Article 109867

View PDF Article preview

Research article Full text access

Biomass pyrolysis over ZIF-67 catalyst: thermogravimetric, pyrolysis vapors, kinetics, thermodynamics and artificial neural network modelling

Samy Yousef, Vilmantė Kudelytė, Nerijus Striūgas, Mohammed Ali Abdelnaby

Article 109868

View PDF Article preview

Research article Full text access

Integrated multi-stage valorization of distiller's grains for co-production of feed protein and biomethane: A techno-economic assessment

Xueke Bai, Shilei Wang, Yue Zhang, Xi Wang, ... Hanjie Ying

Article 109870

View PDF Article preview

Research article *Open access*

Electrocatalytic hydrogenation of pyrolysis bio-oil: Effect of pulsed electrolysis on the conversion of carbohydrate-derived oxygenates

Saartjie M. Gouws, Hein W.J.P. Neomagus, Clarissa Booysen, Robbie H. Venderbosch, John R. Bunt

Article 109861

View PDF Article preview

Research article Full text access

Combustion performance and burnout characteristics of a 600 MW opposed wall-fired boiler under high ratio biomass co-firing

Biomass and Bioenergy

Jiapei Li, Yehua Shen, Yanan Li, Tinglong Zhang, ... Chen Chen
Article 109873

View PDF Article preview

Research article *Open access*

Anaerobic immersed side-stream membrane bioreactor for single-stage cyclic recovery of volatile fatty acids from food waste

O. Kanine, A.R. Fleitas García, M. Reynaud, M. Gonçalves, ... J.S. Guez
Article 109879

View PDF Article preview

Research article Full text access

Structural characteristics of corn stover char at different pyrolysis temperatures and kinetics of pressurized CO_2 gasification

Xinmin Wang, Zhuangzhuang Song, Qi Liu, Jingru Bai, ... Qing Wang
Article 109871

View PDF Article preview

Research article *Open access*

Engineering biochar–polymer interactions for sustainable composite applications: A review

Mohammad Mezbah Ul Hoque, Muhammad Khusairy Bin Bakri, Avishek Chanda, Manuel Garcia-Perez, Vikram Yadama
Article 109878

View PDF Article preview

Research article *Open access*

Understanding the influence of phosphate salts on supercritical water gasification of acetic acid over Raney nickel catalyst

Julie Michel, Hary Demey, Alban Chappaz
Article 109888

View PDF Article preview

Research article *Open access*

Leaching and drying of herbaceous bales with different density to improve their combustion performance

Miguel J. Fernández-Llorente, Ruth Barro, Raquel Bados
Article 109876

View PDF Article preview

Research article Full text access

Integrated experimental and machine learning study of pyrolysis oil and model waste cooking oil co-hydrotreating over NiMo/γ-Al_2O_3

Peerawat Wongsurakul, Nutchapon Chotigkrai, Worapon Kiatkittipong, Manish Sakhakarmy, ... Sushil Adhikari
Article 109880

View PDF Article preview

Research article Full text access

Biomass and Bioenergy

Unveiling the role of dissolved organic matter in nano-biochar/PMS system for antibiotic degradation: The critical interaction with environmentally persistent free radicals

Jing Zhao, Yanzhuo Zhang, Jiaqi Xu, Xiaozhuan Zhang, Alexandr V. Bildyukevich

Article 109885

View PDF Article preview

Research article Full text access

Alkali pretreatment enables enhanced levoglucosan production from catalytic pyrolysis of waste cellulose acetate

Hengbin Zhang, Rui Shan, Ying Liu, Chengyu Li, ... Haoran Yuan

Article 109891

View PDF Article preview

Research article *Open access*

Optimizing MaxEnt to project habitat shifts of *Idesia polycarpa var. vestita* Diels, a bioenergy tree, in China under climate change scenarios

Yixuan Peng, Longcheng Jiang, Jin Wang, Rou Ma, ... Yuan Li

Article 109889

View PDF Article preview

Research article *Open access*

Optimizing wheat straw bioconversion: Sequential H_2O_2-$NaClO_2$ pretreatment for enhanced bioethanol production

Ayesha Aslam, Rabia Liaquat, Midhat Naveed, Hassan Waseem, Zeshan Sheikh

Article 109893

View PDF Article preview

Research article Full text access

All softwood components deconstruction into chemicals in semi-continuous plug flow reactor: unraveling acid versus base catalysed mechanisms in SC MeOH

A.A. Komenan, M. Eternot, N. Essayem

Article 109887

View PDF Article preview

Research article Full text access

Machine learning–driven efficient optimization for conversion of cellulose to glucose over sulfonated biochar solid acid

Genmao Guo, Hongmin Zhang, Xiaoyu Shi, Renjie Yang, ... Fangming Jin

Article 109892

View PDF Article preview

Research article Full text access

Biochar-mediated microbial interactions enhance start-up of anaerobic digestion for high-strength wastewater

Wantanasak Suksong, Saowaluk Krainara, Varunee Kongduan, Nasrul Hudayah, ... Benjaphon Suraraksa

Article 109894

View PDF Article preview

Biomass and Bioenergy

Research article Full text access

Identifying the optimal harvest stage for forage and biogas production from sweet sorghum under semi-arid Mediterranean conditions

Recep Irfan Nazli, Burak Beyaz, Asiye Sena Cavdar, Hasan Beytullah Donmez, Muhammad Azhar Nadeem

Article 109926

View PDF Article preview

Research article Full text access

Magnesium oxide induces orthophosphate over polyphosphate formation during pyrolysis of potassium phosphate-enriched cassava waste

Sreypov Yoem, Kaewta Jetsrisuparb, Khanita Kamwilaisak, Jesper T.N. Knijnenburg

Article 109895

View PDF Article preview

Research article *Open access*

Batch refreshment and bacterial strain: Key factors for sustained biohydrogen production from organic substrates

Larissa Desordi Bortoli, Gabriela Aparecida Santos Mendonça, Fabiana Regina Xavier Batista, Vicelma Luiz Cardoso, Miriam Maria de Resende

Article 109899

View PDF Article preview

Review Articles

Review article *Open access*

Mechanistic insights into lignin reduction and methane enhancement: A systematic review of pretreatment technologies for lignocellulosic biomass (2005–2025)

Mylena Kellyn de Paula Rosetti, Laercio Mantovani Frare, Helton José Alves, Leandro S. Herculano, ... Joel Gustavo Teleken

Article 109805

View PDF Article preview

Review article Full text access

Diversity, ecology, and electrogenic mechanism of electrochemically active bacteria

Yanyu Xiao, Shicheng Wang, Shuang Zhang, Xinxin Fan, ... Lei Yan

Article 109850

View PDF Article preview

Review article Full text access

Eichhornia crassipes as a sustainable aquatic biomass: valorization, bioactive compounds, and bioenergy potential

Mano Magdalin Rubella Kennedy, Aleyamma Alexander, Israel V.M.V. Enoch

Article 109860

View PDF Article preview

Biomass and Bioenergy

Review article Full text access

Biomass-derived biochar for CO_2 adsorption: Physicochemical design, adsorption kinetics, isotherm modeling, and carbon-management perspectives

Baala H. Anandapadmanaban, Shu-Hui Liu, Chi-Wen Lin, Tzung-Han Chou, Rabia Tasaduq Hussain

Article 109897

View PDF Article preview

Previous vol/issue Next vol/issue

About this publication

ISSN: 0961-9534

Biomass and Bioenergy

Supports open access

8.9 CiteScore | 7.0 Impact Factor

Editorial board

Gender diversity of editors and editorial board members

- **64%** man
- **35%** woman
- **2%** prefer not to disclose
- **0%** non-binary or gender diverse

Data represents responses from 93.2% of 59 editors and editorial board members

Editorial board by country/region

59 editors and editorial board members in 21 countries/regions

1 United Kingdom (10)

2 India (8)

3 Italy (7)

See more editors by country/region

Editor-in-Chief

Manuel Garcia Perez

Washington State University, Pullman, Washington, United States

Pyrolysis, Pyrolysis oil chemistry, thermochemical reactions, bio-char chemistry, biorefineries, sustainable aviation fuels

View full biography

Executive Editor

Annie Chimphango

Stellenbosch University, Department of Chemical Engineering, Stellenbosch, South Africa

Biomass conversion, Advanced biomaterials, Biocomposites, Nanomaterials, Integrated biorefineries, Agricultural waste valorization, Sustainability analysis, Circular economy, Postharvest technologies, Bioenergy, Bioproducts, Biomaterials

View full biography

Associate Editors

Sankar Chakma

Indian Institute of Science Education and Research Bhopal, Bhopal, India

Biomass Valorization, Thermochemical Conversion, Engine Performance and Emissions, Wastewater Treatment, Ultrasound, Sonochemistry, Biochar, Biomaterials, Electrochemistry, Pyrolysis

View full biography

Guanyi Chen

Tianjin University of Commerce, Tianjin, China

Thermo-chemical conversion of biomass/wastes, Biological conversion, Environmental pollutants control, Processing modeling, Bioenergy system

View full biography

Isabel Fonts

University of Zaragoza, Department of Chemical Engineering and Environmental Technologies, Zaragoza, Spain

Pyrolysis, Gasification, NH3 production, Phosphorus Recovery, Biochar, Waste Valorization, Gas Adsorption, Biooil upgrading

View full biography

Sun-Mi Lee

Korea University Division of Environmental Science and Ecological Engineering, Seongbuk District, Korea, Republic of

Biomanufacturing, Synthetic biology, Yeast engineering, Lignocellulosic biomass, Bio-upcycling

View full biography

Yan Liu

Michigan State University, East Lansing, Michigan, United States

Solange Mussatto

Technical University of Denmark, Kongens Lyngby, Denmark

Biomass conversion, BioProcess development, Process optimization, Biorefinery, Bioeconomy, Sustainability, Biofuels, Biochemicals, Green technologies, Zero waste, Circular economy, Biomass pre-treatment and hydrolysis, Fermentation, Separation and purification, Techno-economic analysis, Extraction, Enzymes, Food ingredients, Agriculture, Cellulose, Hemicellulose, Lignin, Protein, Antioxidants

View full biography

Frederik Ronsse

Ghent University, Gent, Belgium

Thermochemical conversion of biomass

View full biography

Jhuma Sadhukhan

Global Center for Sustainable Bioproducts at University of Surrey, Guildford, United Kingdom

Circular Bioeconomy Engineering, Life Cycle Assessment, Techno Economic Analysis TEA, CO_2 to Chemicals Innovation, Process Integration &, , Systems Analysis

View full biography

Chunbao Xu

City University of Hong Kong School of Energy and Environment, Hong Kong, Hong Kong

Biorefinery, Fractionation of lignocellulosic biomass into cellulose, hemicellulose and lignin, Production of bio-polymers from cellulose and lignin via chemical modifications, Production of oxygenated bio-chemicals and C5-C18 alkanes from C5/C6 sugars, Production of sustainable aviation fuels SAFs from lignin, biocrude/pyrolysis oils, Hydrothermal reforming HTR technology for green H2 generation from aqueous bio-feedstocks, Chemical hydrogen storage technologies

View full biography

Fabio Minoru Yamaji

Federal University of Sao Carlos - Campus Sorocaba, Sorocaba, Brazil

Biomass, Bioenergy, Biochar, Briquettes, RDF, Pellets, Ash

View full biography

International Editorial Board

Purushothaman Abhilash

Banaras Hindu University Institute of Environment & Sustainable Development, Varanasi, India

Biomass production from marginal and degraded lands, Land restoration, Sustainable agriculture

View full biography

Mustafa Acaroğlu

Selçuk University, Konya, Türkiye

Energy Engineering, Fuel, Biofuel, Renewable Energy sources, Energy policy, Energy crops

View full biography

Anju Arora

ICAR - Indian Agricultural Research Institute, New Delhi, India

Biomass management/ valorisation, Composting, Bioenergy/Biofuels, Bioremediation

View full biography

Marco Baratieri

Free University of Bolzano, Bolzano, Italy

Thermal engineering, Bioenergy, Biofuels, Poly-generation, Biomass gasification

View full biography

Tony Bridgewater

Aston University School of Engineering and Technology, Birmingham, United Kingdom

Enrico Ceotto

Council for Research in Agriculture and Agricultural Economy Analysis Research Centre for Animal Production and Aquaculture, Lodi, Italy

Dedicated energy crops, Nitrogen fertilization and use efficiency, Soil carbon dynamics, Agronomy, Anaerobic digestion

View full biography

Yu-Shen Cheng

National Yunlin University of Science and Technology, Douliu, Taiwan

Biorefinery, Bioprocessing, Applied microbiology

View full biography

David Chiaramonti

Polytechnic of Turin, Turin, Italy

Biofuels, biochar, bioenergy, biomethane, bioeconomy

View full biography

Papita Das

Jadavpur University, Kolkata, India

Adsorption, Wastewater, Environmental Pollution Control, Surface reaction, Circular economy, Biofuel, Chemical, NanoTechnology, Bioenergy, Biodegradation, Waste to wealth

View full biography

Ana Fernando

NOVA University of Lisbon NOVA FCT, Department of Chemistry, Caparica, Portugal

Energy crops, Phytoremediation, Bioenergy and Biofuels, Biobased products

View full biography

Silvia Fiore

Polytechnic of Turin, Department of Environmental Land and Infrastructure Engineering, Turin, Italy

Circular economy, Biorefinery, Biochar, Sustainability, Techno-economic analysis., anaerobic digestion

View full biography

Axel Funke

Karlsruhe Institute of Technology Institute of Catalysis Research and Technology, Eggenstein-Leopoldshafen, Germany

Pyrolysis oil, fast pyrolysis, phase equilibria, auger reactor, process design

Rosana Goldbeck

Campinas, Brazil

Biotechnology

View full biography

Md Sohrab Hossain

Universiti Teknologi PETRONAS Fundamental and Applied Sciences Department, Bandar Seri Iskandar, Malaysia

Biomass to bioenergy, Solid waste management, Wastewater treatment, Supercritical fluids technology, Nanotechnology and Materials characterization

View full biography

Wiebren de Jong

Delft University of Technology, Delft, Netherlands

Electo LORA

Itajubá, Brazil

Biomass energy conversion, Thermochemical conversion, Life cycle analysis, Biofuels, Solar thermal energy, Hydrogen, Biomass gasification

View full biography

Michael Ladisch

Purdue University, Department of Agricultural & Biological Engineering, West Lafayette, Indiana, United States

bioseparations, cellulose conversion, fermentation ethanol, cellulase enzymes, microfluidics, biorector modeling, biomanufacturing

View full biography

Wei Liao

Michigan State University, Department of Biosystems and Agricultural Engineering, East Lansing, Michigan, United States

Guofeng Shen

Peking University, Beijing, China

Sustainable household energy and environment, Indoor air pollution, biomass burning, air pollution

View full biography

Nathan Skillen

Queen's University Belfast, Belfast, United Kingdom

Photocatalysis, reactor design, bioenergy, environmental remediation

View full biography

Vasiliki (Vicky) Skoulou

University of Hull School of Engineering, Hull, United Kingdom

Biomass waste /Waste characterisation, pre-treatments, carbonization-torrefaction-pyrolysis-gasification- clean combustion of non food-woody biomass waste, other waste for waste to energy WtE, bioenergy-biofuels, biochar production, bioenergy systems design, circular economy and industrial symbiosis scenarios based on biomass waste, resilient and sustainable waste to energy generation for industry, transportation and building sectors

View full biography

Raffaele Spinelli

Institute of BioEconomy National Research Council, Sesto Fiorentino, Italy

Surindra Suthar

Doon University, Dehradun, India

Agriculture waste valorization, Anaerobic digestion, Weed biomass utility, Waste-to-Energy, Composting Technology, Biohydrogen, Sewage sludge utility, Biochar application

View full biography

Patricia Thornley

Aston University School of Engineering and Technology, Birmingham, United Kingdom

biomass, bioenergy, bioproducts, life cycle assessment, sustainability

View full biography

Ravikrishnan Vinu

Indian Institute of Technology Madras, Chennai, India

Biomass, Plastics, Coal, Algae, Wastes, Py-GC/MS, Pyrolysis kinetics, Catalytic pyrolysis, Hydrothermal liquefaction, Resource recovery

View full biography

Timothy Volk

SUNY College of Environmental Science and Forestry, Syracuse, New York, United States

short rotation forestry, willow, agroforestry, bioenergy

View full biography

Jonathan Wagner

Loughborough University, Loughborough, United Kingdom

Circular Economy, Hydrothermal Liquefaction, Process Integration, Biorefinery, Biomass conversion, Catalysis

View full biography

Orla Williams

University of Nottingham, Department of Mechanical Materials and Manufacturing Engineering, Nottingham, United Kingdom

biomass processing, critical raw materials, material characterisation, milling, particle size, life cycle analysis, building services, energy management

View full biography

Asheesh Kumar Yadav

Council of Scientific and Industrial Research Institute of Minerals and Materials Technology, Bhubaneswar, India

Bioelectrochemical processes of waste and wastewater treatment, Biomass for energy recovery and value-added products development, Constructed wetlands, and Bioelectrochemical systems

View full biography

Xiaolei Zhang

University of Strathclyde, Glasgow, United Kingdom

Waste valorization for production of fuels and advanced materials, Bioenergy, biofuel, production of high value-added chemicals, Quantum Mechanics QM modelling based on Density Functional Theory DFT, Process design and optimization of energy systems

Early Career Editorial Board

José Luiz Francisco Alves, PhD

Paraiba Federal University, João Pessoa, Brazil

Carbon capture and utilization, bioenergy, low-carbon biofuels, biomass, thermochemical conversion, sustainable development, renewable chemicals, circular economy

View full biography

Bijoy Biswas, PhD

Sardar Swaran Singh National Institute of Bio-Energy, Industrial Area, India

Biomass/Waste, thermochemical process, Lignin, Catalysis, Biochar, Adsorption, Bio-oil upgradation.

View full biography

Leilei Dai, PhD

Southeast University, Nanjing, Jiangsu, China

Thermochemical conversion, Microwave, Biomass, Plastic, Organic solid waste, Circular Economy

View full biography

Sara Fulignati, PhD

University of Pisa, Department of Chemistry and Industrial Chemistry, Pisa, Italy

Biomass fractionation, bio-fuel, hydrolysis, hydrogenation, alcoholysis, catalysis, Green Chemistry, hydrothermal carbonization, waste valorization

View full biography

Busiswa Ndaba, PhD

University of South Africa College of Science Engineering and Technology, Pretoria, South Africa

Biomass valorisation, fermentation, biofuel production, green synthesis, nanoparticles.

View full biography

Alok Kumar Patel, PhD

Luleå University of Technology, Department of Civil Environmental and Natural Resources Engineering, Luleå, Sweden

Bioprocess development, Oleaginous microorganisms, Nutraceuticals and value-added products from microalgae, Renewable energy, Biomass production

View full biography

Yuanting Qiao, PhD

Swansea University, Swansea, United Kingdom

Carbon capture and utilisation, biomass reuse, techno-economic analysis, life cycle assessment, social analysis for the circular economy

View full biography

Shuzhuang Sun, PhD

Zhengzhou University, Zhengzhou, China

Integrated CO2 capture and utilization, Carbon capture, Thermal catalytic conversion of CO2

View full biography

Zhao Sun, PhD

Central South University, Changsha, China

CO2 conversion, Biomass conversion, Chemical looping, Hydrogen production, Advanced energy materials

View full biography

Jiawei Zhong, PhD

South China Agricultural University, Guangzhou, Guangdong, China

Natural gas, methane, reforming, syngas, biogas, biomass

View full biography

All members of the Editorial Board have identified their affiliated institutions or organizations, along with the corresponding country or geographic region. Elsevier remains neutral with regard to any jurisdictional claims.

Source details

Biomass and Bioenergy

Years currently covered by Scopus: from 1991 to 2027

Publisher: Elsevier

ISSN: 0961-9534 E-ISSN: 1873-2909

Subject area: Agricultural and Biological Sciences: Forestry | Agricultural and Biological Sciences: Agronomy and Crop Science | Environmental Science: Waste Management and Disposal | Energy: Renewable Energy, Sustainability and the Environment

Source type: Journal

CiteScore 2025
8.9

SJR 2025
1.132

SNIP 2025
1.308

View all documents > | Set document alert | Save to source list

CiteScore | CiteScore rank & trend | Scopus content coverage

CiteScore 2025

$$8.9 = \frac{14{,}664 \text{ Citations } 2022 - 2025}{1{,}648 \text{ Documents } 2022 - 2025}$$

Calculated on 05 May, 2026

CiteScoreTracker 2026

$$6.5 = \frac{16{,}900 \text{ Citations to date}}{2{,}599 \text{ Documents to date}}$$

Last updated on 05 August, 2026 • Updated monthly

CiteScore rank 2025

Category	Rank	Percentile
Agricultural and Biological Sciences Forestry	#10/181	94th
Agricultural and Biological Sciences Agronomy and Crop Science	#40/422	90th

View CiteScore methodology > | CiteScore FAQ > | Add CiteScore to your site

About Scopus

What is Scopus

Content coverage

Scopus blog

Scopus API

Privacy matters

Language

日本語版を表示する

查看简体中文版本

查看繁體中文版本

Просмотр версии на русском языке

Customer Service

Help

Tutorials

Contact us

Biomass and Bioenergy

United Kingdom | Universities and research institutions | Media Ranking

Country

United Kingdom

SCIMAGO INSTITUTIONS RANKINGS

SCImago Media Rankings

Subject Area and Category

Agricultural and Biological Sciences
- Agronomy and Crop Science
- Forestry

Energy
- Renewable Energy, Sustainability and the Environment

Environmental Science
- Waste Management and Disposal

Publisher

Elsevier Ltd

SJR 2025

1.132

Q1

H-Index

222

Publication type

Journals

ISSN

09619534, 18732909

Coverage

1991-2026

Information

Home

How to publish in this journal

Contact

Scope

Biomass & Bioenergy is an international journal publishing original research papers and short communications, review articles and case studies on biological resources, chemical and biological processes, and biomass products for new renewable sources of energy and materials. The scope of the journal extends to the environmental, management and economic aspects of biomass and bioenergy. Key areas covered by the journal: • Biomass: sources, energy crop production processes, genetic improvements, composition. Please note that research on these biomass subjects must be linked directly to bioenergy generation. • Biological Residues: residues/rests from agricultural production, forestry and plantations (palm, sugar etc), processing industries, and municipal sources (MSW). Papers on the use of biomass residues through innovative processes/technological novelty and/or consideration of feedstock/system sustainability (or unsustainability) are welcomed. However waste treatment processes and pollution control or mitigation which are only tangentially related to bioenergy are not in the scope of the journal, as they are more suited to publications in the environmental arena. Papers that describe conventional waste streams (ie well described in existing literature) that do not empirically address 'new' added value from the process are not suitable for submission to the journal. • Bioenergy Processes: fermentations, thermochemical conversions, liquid and gaseous fuels, and petrochemical substitutes • Bioenergy Utilization: direct combustion, gasification, electricity production, chemical processes, and by-product remediation • Biomass and the Environment: carbon cycle, the net energy efficiency of bioenergy systems, assessment of sustainability, and biodiversity issues.

Quartiles

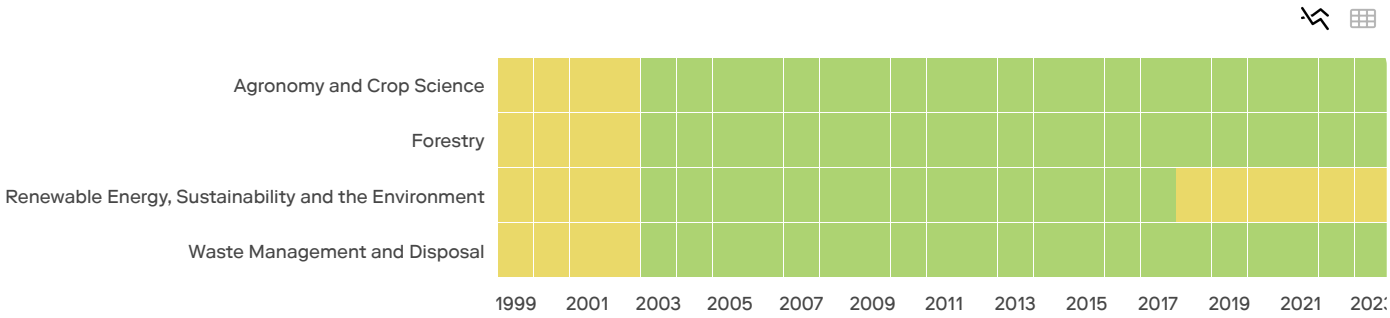

Find similar journals

All quartiles

Download

Only Open Access Journals

1 - Biofuels, Bioproducts and Biorefining

87%

similarity

2 - Bioenergy Research

86%

similarity

3 - Biofuels

82%

similarity

SJR

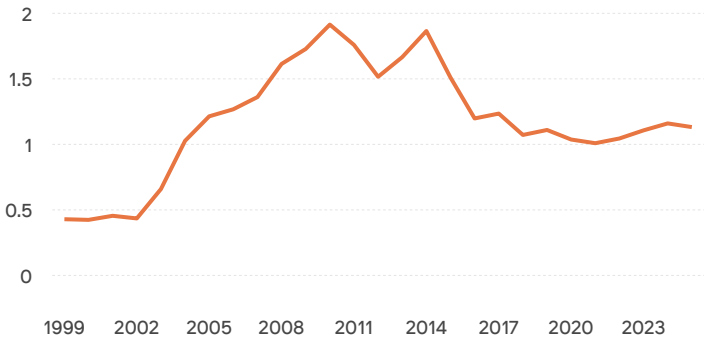

Total Documents

External Cites per Doc Cites per Doc

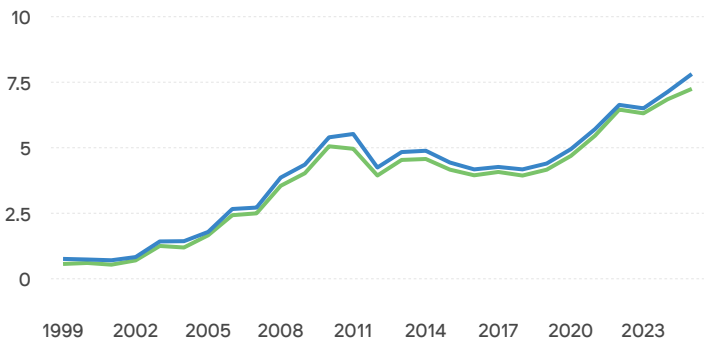

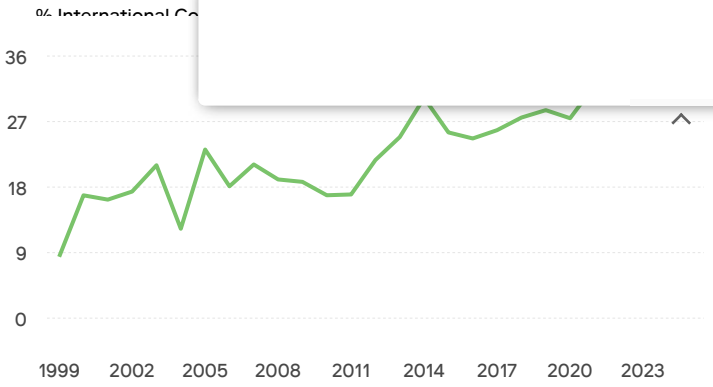

Cited documents Uncited documents

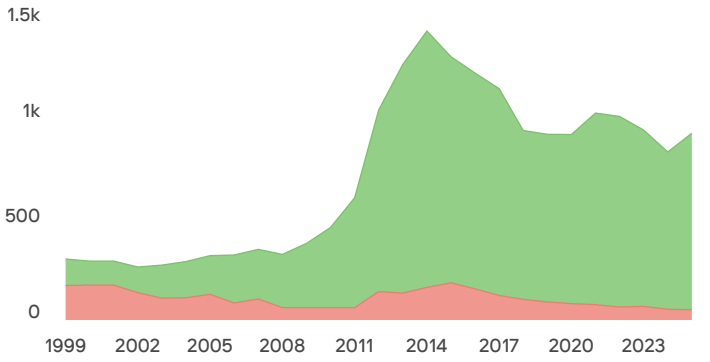

% Female Authors

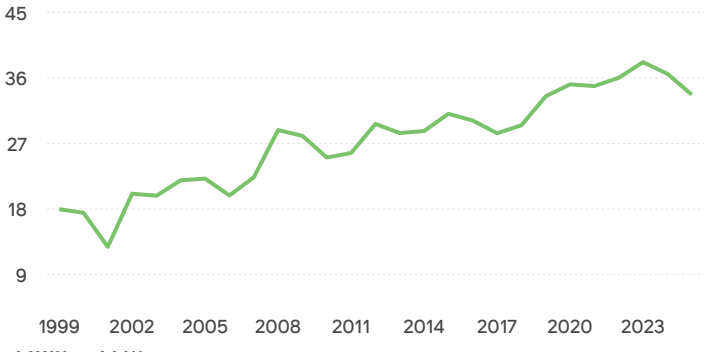

Estimated APC

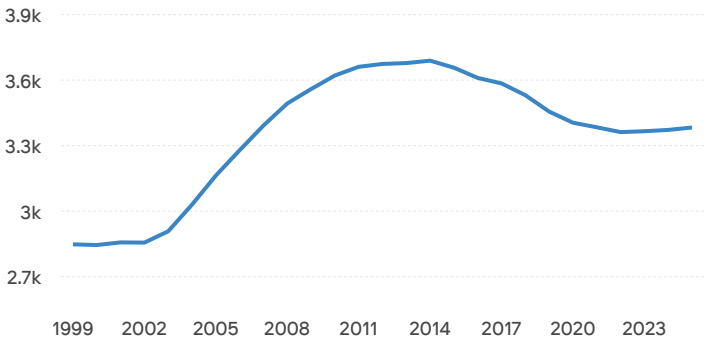

Estimated financial value


9M
6M

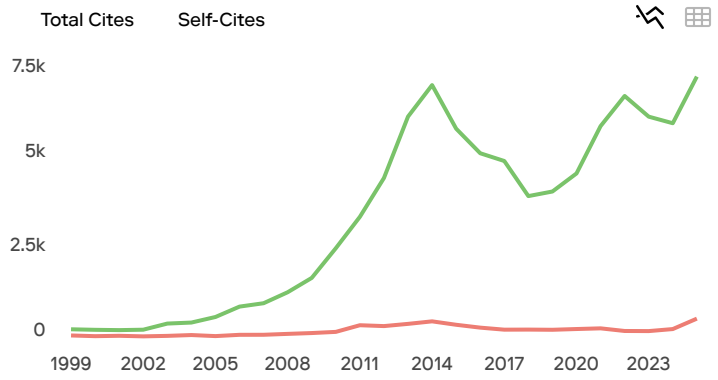
Total Cites
Self-Cites
7.5k
5k
2.5k
0
1999
2002
2005
2008
2011
2014
2017
2020
2023

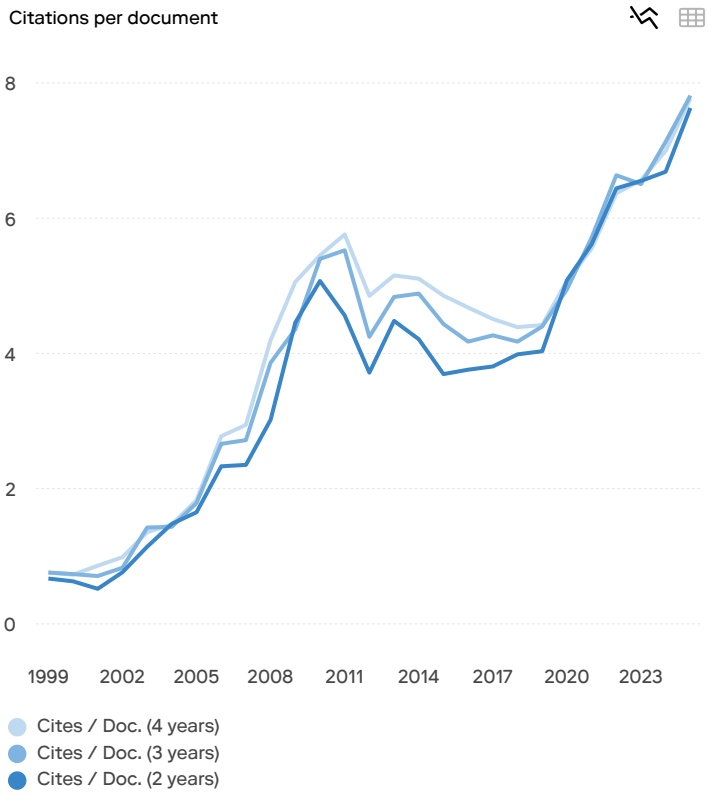
Citations per document
8
6
4
2
0
1999
2002
2005
2008
2011
2014
2017
2020
2023
Cites / Doc. (4 years)
Cites / Doc. (3 years)
Cites / Doc. (2 years)

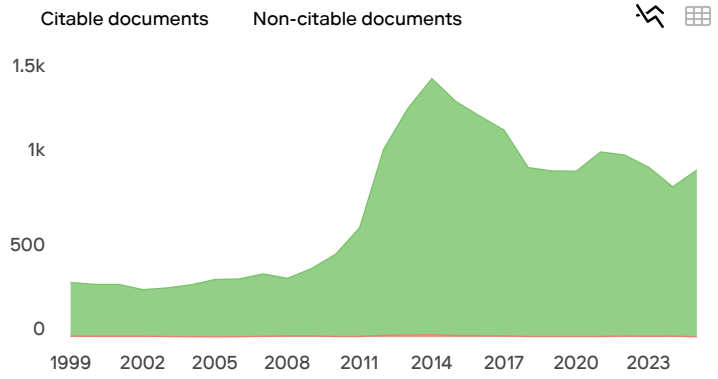
Citable documents
Non-citable documents
1.5k
1k
500
0
1999
2002
2005
2008
2011
2014
2017
2020
2023


Documents cited by public policy (Overton)

Documents related to SDGs (UN)

Coming soon

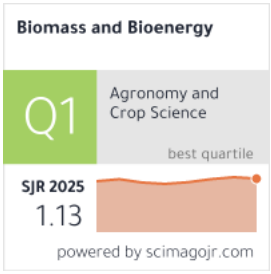

← Show this widget in your own website

Just copy the code below and paste within your html code:

```
<a href="https://www.scimago
```

SCImago Graphica

Explore, visually communicate and make sense of data with our new data visualization tool.

Metrics based on Scopus® data as of March 2026

Loading comments...

Dashboard
Explore SINTA
Mutation History
List Verificator PT
My SINTA

Filter Quartile

- [ ] Quartile 1
- [ ] Quartile 2
- [ ] Quartile 3
- [ ] Quartile 4
- [ ] No Quartile

Filter

Reset

Sort By

Year

Page 1 of 2 | Total Records : 14

Q1 **Synergistic effects of combining ZIF-8 and graphene oxide inside cellulose acetate-based mixed matrix membranes on the removal of methylene blue**
Creator : Sutrisna P.D.
Case Studies in Chemical and Environmental Engineering
Journal publish at **2026**
1 cited

Q1 **Synthesis of dual-fiber cellulose aerogel from oil palm empty fruit bunch and banana petiole combined with graphene oxide for oil spill adsorption**
Creator : Muharja M.
Case Studies in Chemical and Environmental Engineering
Journal publish at **2026**
2 cited

Q1 **Synergistic effect of UV-C mutagenesis and light wavelength on lipid and EPA productivity of Nannochloropsis oculata in POME medium**
Creator : Pratiwi K.A.
Case Studies in Chemical and Environmental Engineering
Journal publish at **2026**
0 cited

Q3 **Enhancing Enzymatic Digestibility and Lignin Production of Oil Palm Empty Fruit Bunch (OPEFB) by Green Deep Eutectic Solvent**
Creator : Wijaya C.
Bulletin of Chemical Reaction Engineering and Catalysis
Journal publish at **2026**
1 cited

Q1 **Integrated valorization of oil palm empty fruit bunch (OPEFB) by deep eutectic solvent pretreatment: Glucose production enhancement and lignin-CMC composite for sustainable packaging**
Creator : Wijaya C.
Biomass and Bioenergy
Journal publish at **2026**
0 cited

Integrated valorization of oil palm empty fruit bunch (OPEFB) by deep eutectic solvent pretreatment: Glucose production enhancement and lignin-CMC composite for sustainable packaging

Biomass and Bioenergy • Review • 2026 • DOI: 10.1016/j.biombioe.2026.109859

Wijaya, Candra [a, b]; Prastika, Andika [a]; Izzati Atiqa, Olivia [a]; Raissa Apol, Tabina [a]; Pertiwi, Urania Noor Lintang [a]; +3 authors

[a] Department of Chemical Engineering, Institut Teknologi Sepuluh Nopember, Kampus ITS Sukolilo, Surabaya, 60111, Indonesia

Abstract

Oil palm empty fruit bunch (OPEFB) is an abundant lignocellulosic residue with potential for integrated biorefinery applications, but its recalcitrant structure limits direct enzymatic conversion and lignin utilization. This study investigated the integrated valorization of OPEFB through deep eutectic solvent (DES) pretreatment using choline chloride–lactic acid (ChCl:LA) and choline chloride–glycerol–$FeCl_3$ (ChCl:Gly:$FeCl_3$) systems for glucose production, lignin recovery, and CMC–lignin composite film development. Modified severity descriptors, namely combined delignification factor (CDF) and combined hydrolysis factor (CHF), were applied to describe severity-dependent lignin removal and xylan hydrolysis. The CDF and CHF models successfully described the severity-dependent fractionation behavior of OPEFB during DES pretreatment. ChCl:LA promoted stronger

lignin solubilization and higher lignin recovery, while ChCl:Gly:$FeCl_3$ enhanced hemicellulose removal and enzymatic digestibility through Lewis acid-assisted deconstruction. The highest enzymatic hydrolysis yields reached 75.8% for ChCl:LA and 93.8% for ChCl:Gly:$FeCl_3$. On a 100 g raw OPEFB basis, ChCl:LA pretreatment at 140 °C for 6 h produced 21.6 g glucose and 24.7 g recovered lignin, whereas ChCl:Gly:$FeCl_3$ pretreatment at 140 °C for 3 h produced 21.7 g glucose and 23.1 g recovered lignin. The recovered DES lignins showed high purity and were successfully incorporated into CMC-based films. ChCl:LA lignin improved water resistance and reduced WVTR, while ChCl:Gly:$FeCl_3$ lignin provided stronger antioxidant activity and tensile reinforcement. These findings demonstrate that DES pretreatment enables the dual valorization of OPEFB into fermentable glucose and functional lignin-derived packaging materials, supporting a multiproduct biorefinery pathway for sustainable biomass utilization.

Author keywords

CMC-lignin film; Deep eutectic solvent; Enzymatic hydrolysis; Fractionation; Modified severity factor; Oil palm empty fruit bunch

Indexed keywords

Engineering controlled terms

Cellulose; Chlorine compounds; Composite films; Delignification; Enhanced recovery; Eutectics; Fruits; Glucose; Iron compounds; Lactic acid; Lignin; Recovery; Solubility; Solvents

Engineering uncontrolled terms

Choline chloride; CMC-lignin film; Deep eutectic solvents; Empty fruit bunches; Glucose production; Modified severity factor; Oil palm; Oil palm empty fruit bunch; Solvent pretreatment; Valorisation

Engineering main heading

Enzymatic hydrolysis; Fractionation

Funding details

Details about financial support for research, including funding sources and grant numbers as provided in academic publications.

Funding sponsor	Funding number	Acronym
Lembaga Pengelola Dana Pendidikan See opportunities by LPDP	4299/B3/ DT . 03 . 08 /2025	LPDP

Funding text

This research is funded by the Indonesian Endowment Fund for Education (LPDP) under the EQUITY Program (Contract No. 4299/B3/DT.03.08/2025)

Corresponding authors

Corresponding author	A. Widjaja
Affiliation	Department of Chemical Engineering, Institut Teknologi Sepuluh Nopember, Kampus ITS Sukolilo, Surabaya, 60111, Indonesia
Email address	arief.widjaja@its.ac.id

About Scopus

Privacy matters

Language

日本語版を表示する

查看简体中文版本

查看繁體中文版本

Просмотр версии на русском языке

Customer Service

Help

Tutorials

Contact us

ELSEVIER